



Cite this: *Chem. Soc. Rev.*, 2024, 53, 7875

## One-pot chemo- and photo-enzymatic linear cascade processes

J. M. Carceller,  K. S. Arias,  M. J. Climent,  S. Iborra \* and A. Corma \*

The combination of chemo- and photocatalyses with biocatalysis, which couples the flexible reactivity of the photo- and chemocatalysts with the highly selective and environmentally friendly nature of enzymes in one-pot linear cascades, represents a powerful tool in organic synthesis. However, the combination of photo-, chemo- and biocatalysts in one-pot is challenging because the optimal operating conditions of the involved catalyst types may be rather different, and the different stabilities of catalysts and their mutual deactivation are additional problems often encountered in one-pot cascade processes. This review explores a large number of transformations and approaches adopted for combining enzymes and chemo- and photocatalytic processes in a successful way to achieve valuable chemicals and valorisation of biomass. Moreover, the strategies for solving incompatibility issues in chemo-enzymatic reactions are analysed, introducing recent examples of the application of non-conventional solvents, enzyme–metal hybrid catalysts, and spatial compartmentalization strategies to implement chemo-enzymatic cascade processes.

Received 29th November 2023

DOI: 10.1039/d3cs00595j

[rsc.li/chem-soc-rev](https://rsc.li/chem-soc-rev)

*Instituto de Tecnología Química (Universitat Politècnica de València-Agencia Estatal Consejo Superior de Investigaciones Científicas), Avda dels Tarongers s/n, 46022, Valencia, Spain. E-mail: [acorma@itq.upv.es](mailto:acorma@itq.upv.es), [siborra@itq.upv.es](mailto:siborra@itq.upv.es); Fax: +34 963877809*

### 1. Introduction

Nature has developed over the years the most complex and optimized multistep catalytic processes in the form of cascade reactions catalysed by enzymes, which are involved in the



**J. M. Carceller**

*Jose M. Carceller was born in Valencia, Spain, in 1991. He studied Chemistry at the Universidad de Valencia and completed his PhD in the research group of Prof. Avelino Corma under the supervision of Prof S. Iborra and Prof. M. José Climent at the Institute of Chemical Technology at the Universitat Politècnica de València (UPV-CSIC). Then he received the Margarita Salas grant and carried out his postdoctoral studies with Prof. Todd Hyster at the Department of Chemistry at Princeton University. Then, he came back to Spain and continued his postdoctoral studies at the Institute of Chemical Technology (UPV-CSIC) in the research group of Prof. Corma. His research interests include the development of chemo-enzymatic processes using heterogeneous catalysts and immobilized enzymes for the synthesis of fine chemicals and biologically active compounds, and the development of new enzyme activities using directed evolution and photocatalysis.*



**K. S. Arias**

*Karen S. Arias received her BS in Chemistry from the University of Quindío (Colombia) and her MS in Sustainable Chemistry from the Polytechnique University of Valencia (UPV) (Spain). After completing her PhD study in 2016 under the supervision of Prof. Maria J. Climent at the Institute of Chemical Technology (ITQ, UPV), she joined the group of Prof. Avelino Corma at the ITQ as a researcher associate. Since then, her research has mainly focused on converting biomass-derived platform molecules into high valued chemicals and fuels through enzymatic and heterogeneous catalyses.*



metabolic networks needed for life.<sup>1</sup> The ingenious strategies and highly efficient cascade reactions in the microenvironment of a cell, basically in a one-pot system, have inspired scientists to perform organic synthesis through cascade reactions using mono- or multifunctional catalytic systems. A cascade reaction can be defined as the reaction with at least two consecutive events, where the product of the first step serves as the substrate for the subsequent step. It can be performed in a sequential mode or in a concurrent (or simultaneous) mode. While in the concurrent mode all the catalysts and reactants are present from the beginning and the reaction conditions are unchanged, in the sequential mode (also called relay or temporal compartmentalization), only after the completion of the first step, an additional component (catalyst, co-factor, solvent, *etc.*) is added, and supplementary operations (changes in temperature, concentration, pH, *etc.*) can also be performed.



**M. J. Climent**

*Maria Jose Climent Olmedo was born in Alginet (Spain). She is a Full Professor at the Chemistry Department of the Technical University of Valencia. She obtained her PhD in 1991 from the University of Valencia and in 1993 she became a member of the Institute of Chemical Technology (ITQ) at the Technical University of Valencia working in the group of Prof. Avelino Corma. Her main research focuses on the application of heterogeneous catalysts*

*and enzymes to the synthesis of fine chemicals and valorization of biomass-derived platform molecules into chemicals and biofuels through one-pot cascade strategies.*



**S. Iborra**

*Sara Iborra (Carlet, Valencia) is a Full Professor at the Chemistry Department of the Polytechnical University of Valencia (UPV). She received her PhD in 1987 from the Universidad de Valencia and in the same year she joined the Chemistry Department of the UPV as an Assistant Professor. She has been a member of the Institute of Chemical Technology (ITQ) at the UPV since 1991, where she works in the research group of Prof. Avelino Corma. The*

*main focus of her current research involves the application of heterogeneous catalysts (acid-base and redox) to the synthesis of fine chemicals and valorization of biomass.*

Cascade processes in a one-pot mode offer a variety of advantages over the conventional step-by-step approach, such as the avoidance of purification of intermediates, reducing therefore the operation time, waste production and cost of the process. Additionally, atom economy, stereochemical control and substrate scope can be improved, while the cooperative effect between the different catalytic sites can increase reactivity and selectivity by allowing equilibrium reaction steps to proceed to practically full conversion. Therefore, process intensification through cascade catalysed processes is currently an area of increasing interest.<sup>2-5</sup>

On the other hand, biocatalysis has generated even more interest in industry and academia over the past few years and has emerged as a sustainable and economically viable approach to produce chemicals that require high chemo-, regio- and stereo-selectivities. The combination of chemocatalysis with biocatalysis, which couples the flexible reactivity of the chemocatalysts with the highly selective and environmentally friendly nature of biocatalysts, is, therefore, of most interest. Traditionally the chemo-enzymatic processes have been carried out as multi-pot multi-step processes, where an intermediate separation/isolation stage after each reaction step is required.<sup>6</sup> However, the design of chemo-enzymatic cascade processes in a one-pot mode, mimicking the nature, which occur in a concurrent or sequential mode, is a research area of increasing interest.

While multi-enzymatic cascade reactions are often successfully achieved as they take place under similar reaction conditions,<sup>7</sup> the combination of chemo- and biocatalysts in one-pot is challenging because the optimal operating conditions of both catalysts may be rather different. In fact, the majority of chemocatalysts are active under relatively severe reaction conditions (temperature, pH, organic solvents, *etc.*) that are not compatible with enzymes, which usually operate under very mild reaction conditions (room temperature, neutral pH, aqueous solutions, *etc.*).<sup>8,9</sup> Furthermore, the different catalyst stabilities and the mutual deactivation of the chemo- and/or biocatalysts are additional problems often



**A. Corma**

*Avelino Corma is a Professor and founder of the Instituto de Tecnología Química (CSIC-UPV) in Valencia (Spain). He has been carrying out research on heterogeneous catalysis in academia and in collaboration with companies. He has worked on fundamental aspects of acid-base and redox catalyses with the aim of understanding the nature of the active sites and reaction mechanisms. With this basis, he has developed catalysts that are being used commercially in several*

*industrial processes. He is an internationally recognized expert in solid acid and bifunctional catalysts for oil refining, petrochemistry and chemical processes. He has published more than 1000 research papers and is an inventor of more than 130 patents.*



encountered in one-pot processes. A typical example is the inactivation or inhibition of enzymes by metal ions.<sup>10</sup> Thus, the search for a compatibility window in which both catalysts coexist and operate with reasonable activity is key for the success of a chemo-enzymatic one-pot process. It is not surprising that the number of examples where both classes of catalysts work concurrently in an efficient way is limited when compared with processes performed in a sequential mode, where there is more freedom to operate. Therefore, there are no standard procedures for the development and optimization of chemo-enzymatic cascades. As a result, researchers have developed ingenious strategies to overcome the barriers between both catalytic toolboxes such as the use of bio-conjugated nanohybrids or spatial compartmentalization, which includes use of biphasic systems, membrane filtration, catalyst encapsulation, and performing reactions in a flow mode.<sup>11,12</sup>

The potential of chemo-enzymatic processes was first highlighted in the early 1980s by the van Bakkum group for the production of mannitol from glucose. The authors combined an enzyme (glucose isomerase) with a heterogeneous metal catalyst (Pt/C). In this process glucose is first *in situ* transformed into fructose using an immobilized glucose isomerase, which is subsequently hydrogenated to mannitol in the presence of Pt supported on carbon.<sup>13</sup> Further works addressing catalyst and process development were performed by both the Steward and van Bakkum groups.<sup>14,15</sup>

However, after these pioneering studies of combining metals and biocatalysts, there was for more than a decade a lack of significant studies on chemo-enzymatic reactions up to the pioneering contributions on dynamic kinetic resolutions (DKRs). These processes are mainly applied to the preparation of enantiomerically pure amines and alcohols from racemic mixtures, which combine chemocatalytic racemization and hydrolase-catalyzed resolution in water<sup>16–19</sup> or lipase-catalyzed resolution in organic solvents.<sup>20–23</sup> In fact, in the last 30 years, most of the chemo-enzymatic processes that have been reported correspond to just two groups: dynamic kinetic resolutions and enzymatic processes with concomitant regeneration of co-factors.<sup>5,24,25</sup>

As DKR has been extensively reviewed,<sup>26–30</sup> recent reviews on chemo-enzymatic cascade processes have focused on different particular aspects, such as the synthesis of chiral compounds by combining metal chemocatalysts with enzymes,<sup>31–33</sup> chemo-enzymatic cascades in aqueous media<sup>34</sup> and the prevailing methods to overcome compatibility issues.<sup>12,35,36</sup>

The aim of this review is to give the readers a wide overview of the variety of transformations and strategies adopted for combining enzymes and chemo- and photocatalytic processes in a successful way to achieve valuable chemicals and bring out the vast potential that the combination of both catalytic systems has for organic synthesis in the field of sustainable chemistry. Thus, we have focused on prominent and up-to-date examples of linear chemo-enzymatic cascades, where the starting substrate is first transformed by the chemocatalyst prior to the biocatalyzed reaction or *vice versa* in one-pot. In the first section a series of selected examples of chemo-

enzymatic cascades have been classified according to the type of compound synthesized and the different approaches adopted have been discussed. In the second section, different strategies for solving incompatibility issues in chemo-enzymatic reactions will be discussed, introducing recent examples of the application of enzyme–metal hybrid catalysts as well as examples of spatial compartmentalization strategies to implement chemo-enzymatic cascade processes. Finally, the combination of photocatalytic and biocatalytic transformations in linear cascades will also be discussed.

## 2. Synthesis of organic compounds through chemo-enzymatic cascade strategies

### 2.1. Synthesis of alcohols and amines

A variety of chemo-enzymatic approaches, particularly focused on the synthesis of chiral compounds, have been reported. In this section, we will discuss the different strategies adopted for the synthesis of these compounds.

**2.1.1. Synthesis of chiral secondary alcohols and amines by combining a prochiral ketone formation step with bioreduction and bioamination respectively.** Chiral secondary alcohols and amines are an important class of building blocks in the pharmaceutical, perfume and agrochemical industries.<sup>37–42</sup> Chiral alcohols are usually produced through deracemization protocols such as dynamic kinetic resolutions (DKRs)<sup>43,44</sup> or by coupling simple oxidation–reduction steps usually accomplished by multienzymatic combinations.<sup>45–47</sup> In the case of amines, the chiral resolution is still performed in most cases *via* diastereomeric salt formation with chiral carboxylic acids as resolving agents. However, this technique has an important drawback, since the maximum yield achieved for the desired chiral amine from the starting racemate product is 50%, while the other 50% usually is discarded. Alternative approaches are for instance the asymmetric hydrogenation of the corresponding imine or enamide employing transition metal catalysts, where the enantiopure amine is obtained with variable success.<sup>48</sup> However, it is also possible to achieve chiral secondary alcohols and amines starting from different substrates (racemic alcohols, alkenes, allyl alcohols and alkynes) *via* a chemocatalytic step (oxidation, hydration, and isomerization) that produces a prochiral ketone, which can be enantioselectively transformed by an enzyme into the desired chiral alcohol or amine.

Alcohol dehydrogenases (ADHs) (also termed ketoreductases, KREDs) are an important family of enzymes that are able to catalyse the complete reduction of carbonyl groups (aldehydes or ketones) to the respective chiral alcohols. These biocatalysts have been successfully used for the production of chiral alcohols, amino alcohols, *etc.*<sup>49,50</sup> Compared with hydrolytic enzymes, ADHs have been much less used for the production of optically pure alcohols since ADHs require stoichiometric amounts, with respect to the substrate, of co-factors such as nicotinamide adenine dinucleotide (NADH) or nicotinamide



adenine dinucleotide phosphate (NADPH). However, recently, the development of highly efficient methods for the regeneration of the co-factors, such as the use of formate dehydrogenase or isopropanol as a co-substrate of ADH, has allowed the use of catalytic amounts of co-factors efficiently.<sup>51–53</sup>

In the case of amines, enzymes such as  $\omega$ -transaminases ( $\omega$ -TAs) have emerged as powerful alternatives to hydrolases and proteases for chiral amine preparation.<sup>54</sup>

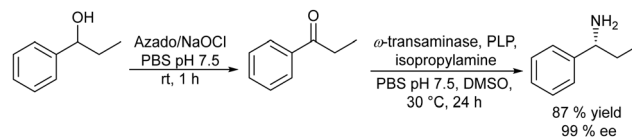
Transaminases catalyse the transfer of an amino group from an amino donor on a carbonyl group in the presence of the co-factor, pyridoxal-5'-phosphate (PLP). Thus, the increased accessibility of  $\omega$ -TAs and the development of engineered enzymes have converted the biotransamination process into a viable and attractive production route for enantiopure amines in the pharmaceutical industry.<sup>55</sup>

In this section, we will discuss several chemo-enzymatic strategies for the synthesis of chiral alcohols and amines starting from different substrates that involve the formation of a prochiral ketone as the first step.

Based on the chemo-enzymatic oxidation of racemic alcohols combined with the bioreduction approach, Lavandera *et al.*<sup>56</sup> developed an efficient one-pot process in a sequential mode for deracemization of secondary alcohols (Scheme 1). The authors combined a TEMPO (2,2,6,6-tetramethylpiperidin-1-oxyl) based oxidation system with alcohol dehydrogenase (ADH) catalyzed enantioselective bioreduction. A key point for this study was the optimization of the oxidative step in a buffer medium, which is necessary for the ADH-catalyzed reduction.

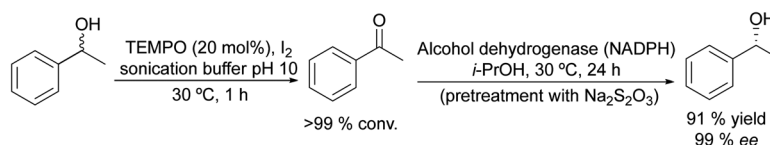
Selecting as a model reaction the oxidation of (*rac*)-phenylethanol to acetophenone, TEMPO combined with different oxidants (that allow the reoxidation of TEMPO) was tested. The study of the compatibility of the ADH in the presence of the different oxidation systems showed that TEMPO combined with I<sub>2</sub> was the most effective. Moreover, it was fully compatible with the ADH-catalyzed bioreduction of the resulting ketones when the excess of iodine (that affects the labile co-factor (NADPH) and the enzyme) is quenched with an aqueous Na<sub>2</sub>S<sub>2</sub>O<sub>3</sub> solution. The protocol was applied to a wide variety of secondary alcohols using Prelog and antiPrelog alcohol dehydrogenases achieving enantiopure (*S*)- and (*R*)-alcohols with conversions over 90%.

Following the same strategy González-Sabín *et al.*<sup>57</sup> reported the chemo-enzymatic deracemization of secondary alcohols using the organic radical 2-azaadamantane *N*-oxyl (AZADO)/sodium hypochlorite as the oxidation system combined with ketoreductases in a sequential mode. It was shown that the presence of AZADO did not affect the enzyme activity, but the excess NaClO used in the first step is detrimental for the



Scheme 2 Synthesis of chiral amines from racemic alcohols by combining chemocatalyzed oxidation and bioamination.

subsequent biotransformation. In this case, the problem was easily solved because the isopropyl alcohol used in excess as the hydrogen donor in the enzymatic step quenches the remaining NaOCl in the reaction medium. Following this protocol, a variety of racemic secondary alcohols were converted into enantiomerically pure alcohols in overall yields of up to 98%. Moreover, the strategy was also applied efficiently to the conversion of *rac*/mesodiols into only one enantiomer. This strategy has advantages over the multienzymatic deracemization, providing higher enantiomeric excess of the chiral alcohol and working at higher concentrations of substrates. The authors applied this approach to the synthesis of chiral amines by coupling the oxidation step with the bioamination of the intermediate prochiral ketone catalyzed by  $\omega$ -transaminases ( $\omega$ -TA)<sup>58</sup> (Scheme 2). To combine both steps, first, the authors focused on the exploration of an efficient method to perform the oxidation step in aqueous media, compatible with transaminases. It was shown that 2-azaadamantano-*N*-oxyl (AZADO) combined with NaOCl resulted in an excellent oxidation system able to work in aqueous media at basic pH to perform the oxidation of a wide variety of secondary alcohols into the corresponding prochiral ketones. Then, the amination process of the different prochiral ketones was optimized by screening the activity of a variety of commercial  $\omega$ -transaminases at basic pH. Optimization of the bioamination step leads to the formation of a variety of valuable chiral amines with high diastereo- and enantioselectivities. The possibility of coupling both steps in a concurrent mode was studied using 1-phenylpropanol as a model substrate. However, several important incompatibilities exist, such as the deactivation of the co-factor of the  $\omega$ -TA, pyridoxal-5'-phosphate (PLP), in the medium, the inhibition of AZADO by DMSO, the co-solvent required for the bioamination, and the inhibition of alcohol oxidation at the low concentration typically required for  $\omega$ -TAs (10–20 mM), precluding the concurrent mode. However, the cascade process was successfully achieved in a sequential mode by performing the alcohol oxidation first at the required concentration (250 mM) in an alkaline buffer solution. Once the oxidation was completed, the reaction mixture was diluted to 10 mM with an alkaline buffer solution containing the (*R*) or (*S*)  $\omega$ -transaminase,



Scheme 1 Synthesis of chiral alcohols from racemic mixtures by combining chemocatalyzed oxidation and bioreduction.

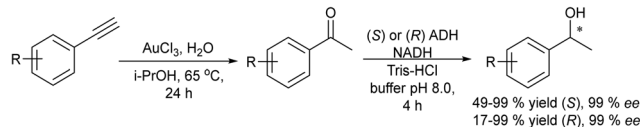


isopropylamine (as the amino group donor), PLP (co-factor), and DMSO as a co-solvent. The corresponding chiral amine, 1-phenylpropanamine, was obtained in 87% yield and with >99% ee (Scheme 2). The method showed broad substrate scope and was successfully applied to a variety of substrates including sterically hindered  $\beta$ -substituted cycloalkanol, giving excellent results in terms of conversion (up to 97%) and stereoselectivity.

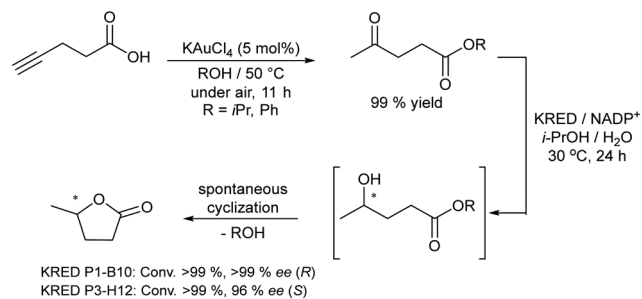
On the other hand, the synthesis of chiral secondary aromatic alcohols at laboratory and industrial scales is an important topic in chemistry. The alcohols are usually achieved by the asymmetric reduction of the corresponding aryl ketones (obtained through a Friedel–Crafts acylation) or through enzymatic kinetic resolutions.<sup>59,60</sup> However, non-activated alkenes, such as styrene, could also be a source of chiral secondary alcohols through a direct asymmetric hydration process of the C=C bond, although efficient methodologies have not been sufficiently developed.<sup>61</sup> Therefore, Gröger *et al.*<sup>62</sup> developed a chemo-enzymatic process in a sequential mode to produce chiral secondary benzylic alcohols from styrene derivatives. This formal hydration process is based on the Wacker–Tsuji oxidation of the alkene (catalyzed by PdCl<sub>2</sub> in the presence of benzoquinone) into a ketone intermediate, which is subsequently reduced to the chiral alcohol in the presence of an alcohol dehydrogenase (ADH) (Scheme 3). Using styrene as a model substrate, the authors showed that Pd species formed during the Wacker–Tsuji oxidation step have a strong inhibitory effect on the ADH activity, leading to a very low yield of the target chiral alcohol (14%). Then, the strategy used to suppress the inhibitory effect of Pd(II) species was the addition of different Pd(II) complexing agents such as thiourea, EDTA, or 2,2'-bipyridine after the oxidation step. Using this protocol, high yield of the corresponding chiral benzyl alcohol could be obtained and the process was extended to a variety of styrene derivatives with good success. Therefore, considering the lack of a generally applicable and efficient chiral catalyst suitable for the direct transformation of non-activated alkenes into chiral aromatic alcohols this chemo-enzymatic process represents an important tool to synthesize these types of compounds.

Chiral amines were also successfully obtained using a similar strategy. For instance, Gröger *et al.*<sup>63</sup> combined the Wacker oxidation of non-activated alkenes using PdCl<sub>2</sub>/CuCl as the catalyst with transamination using transaminases<sup>64</sup> or reductive amination using an amine dehydrogenase enzyme that uses ammonia as a nitrogen source. In both cases, excellent results in terms of yield and enantioselectivity were obtained in these one-pot two-step processes.

Gotor-Fernández *et al.*<sup>65</sup> synthesized enantiopure 1-arylpropan-2-amines through the Wacker oxidation of allylbenzene derivatives catalysed by palladium(II) Pd(TFA)<sub>2</sub> and iron(III) as the



Scheme 4 Synthesis of chiral alcohols from alkynes by combining alkyne hydration and bioreduction.



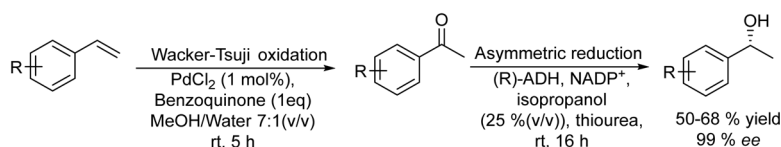
Scheme 5 Synthesis of chiral lactones by combining chemocatalyzed hydration of alkynes and bioreduction.

oxidant, followed by biotransamination. The authors showed for the first time the possibility to combine Pd(II)/Fe(III) (chemo-oxidative system) with an enzyme catalysed step without affecting the enzymatic activity. The target chiral amines were obtained in 72–92% yield with 99% ee.

Besides alkenes, alkynes can be also used as starting substrates for the synthesis of prochiral ketones by means of the acid catalysed nucleophilic water addition to the alkyne. The use of gold salts as catalysts for alkyne hydration represents a more environmentally friendly method compared with the traditional oxymercuration or the use of large amounts of mineral acids.<sup>66,67</sup>

The synthesis of chiral alcohols from alkynes was reported by Mihovilovic *et al.*<sup>68</sup> The chemo-enzymatic method involves the Au-catalyzed (AuCl<sub>3</sub>) alkyne hydration followed by ADH-catalyzed bioreduction in a sequential mode, where the solvent used for the chemocatalyzed step (isopropanol) is used as the secondary substrate for co-factor regeneration in the biocatalyzed step. A variety of *S*- and *R*-chiral alcohols were successfully obtained using alcohol dehydrogenases derived from *Rhodococcus ruber* and *Lactobacillus kefir* respectively (Scheme 4).

A related transformation was reported by González-Sabín *et al.*<sup>69</sup> by using KAuCl<sub>4</sub> as the catalyst and pentynoic acid as the substrate. Thus, the alkyne was first hydrated into a keto group, which was subsequently reduced by a ketoreductase into the corresponding alcohol, which cyclized spontaneously to the chiral lactone (Scheme 5).



Scheme 3 Synthesis of chiral aromatic alcohols from non-activated alkenes by combining oxidation and bioreduction.



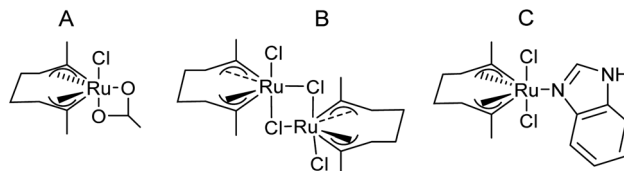
A similar strategy involving gold-catalyzed alkyne hydration and transamination of the intermediate ketone with transaminases was employed by Rueping *et al.*<sup>70</sup> for the synthesis of chiral amines with excellent success.

Recently, Gotor-Fernandez *et al.*<sup>71</sup> reported a chemo-enzymatic process by combining a gold(i) catalyst and enzymes to transform propargylic derivatives into a variety of nor(pseudo)ephedrine derivatives in a regio- and stereoselective way. Ephedrine-type alkaloids are an important family of nitrogen-containing compounds with multiple applications in medicinal chemistry as mimics of adrenaline. Due to the presence of two stereogenic centers, highly stereoselective multienzymatic processes are the preferred synthetic methods.<sup>72–74</sup>

The chemo-enzymatic cascade process involves as the first step the highly regioselective hydration of racemic or enantiopure propargyl esters or amides into the corresponding ketone ester or keto amide intermediates catalyzed by a gold(i) N-heterocyclic carbene (NHC) complex (IPrAuNTF<sub>2</sub>) followed by (dynamic) asymmetric biotransamination or bioreduction of the corresponding keto ester or keto amide intermediate (Scheme 6). Under optimized reaction conditions, a series of protected diamine, diol, amino-alcohol derivatives were obtained from propargyl esters or amines in variable yields (57–86% isolated yield), while the (stereo)selectivity of the overall cascade process was determined by the type of biocatalyst, achieving diastereomeric excess and enantiomeric excess in the range of 70–99% and >98% respectively. The advantage of the strategy is that it allows access to a variety of nor(pseudo)ephedrine derivatives and analogues bearing two chiral centers in a direct manner, avoiding multienzymatic methods that usually require low substrate concentration and suffer from mutual deactivation of enzymes.

Another class of substrates that allow access to prochiral ketones are allylic alcohols, which can be isomerized to ketones using transition metal complexes (Ru, Rh, and Ni) as catalysts.<sup>75,76</sup>

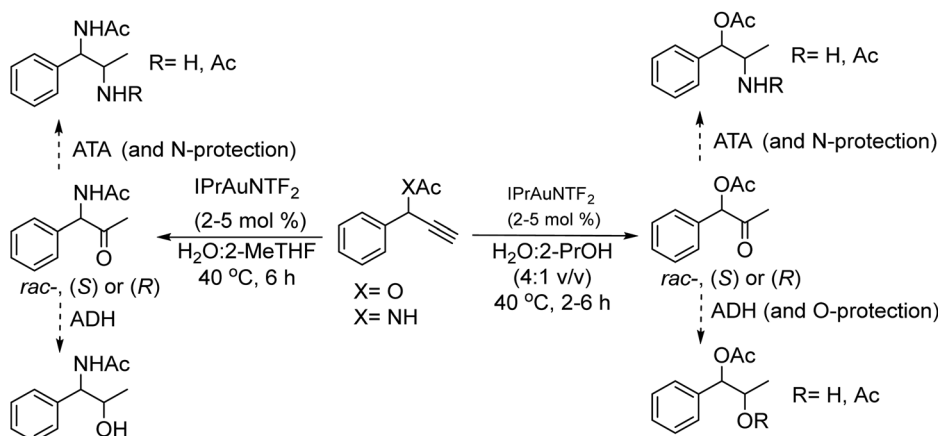
González-Sabín *et al.*<sup>77</sup> coupled, for the first time, the ruthenium-catalysed isomerisation of allylic alcohols with asymmetric bioamination catalyzed by ω-transaminases in an aqueous medium in a sequential mode. The authors evaluated three



Scheme 7 Ru based chemocatalyst complexes.

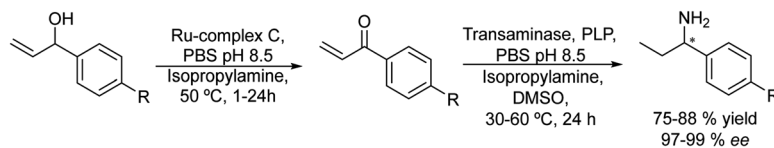
highly efficient ruthenium(IV) catalysts (A–C) (see Scheme 7) in the allylic isomerization of α-vinylbenzyl alcohol, using the reaction conditions required for the enzymatic step, *i.e.* a phosphate buffer solution containing isopropyl amine as the amino donor. Interestingly, while most of the Ru catalysts previously reported did not show activity for the isomerisation reaction when working in pure water as a solvent and below 80–100 °C, the three complexes were active and selective catalysts for obtaining the desired ketones, working at 50 °C, with complex C being the most efficient catalyst. The authors tried to perform the cascade process in a concurrent mode; however, the deactivation of the Ru catalyst by both the enzyme and pyridoxal-5'-phosphate (co-factor) was observed. Therefore, the cascade reaction was performed in a sequential mode by adding the enzyme and co-factor after the first step before diluting the reaction media to the required concentration of ketone. The cascade process was applied to the synthesis of a variety of chiral amines with high yields and enantiomeric excesses (Scheme 8).

Applying a similar protocol and using a ketoreductase in the enzymatic step, the same authors also synthesized chiral alcohols from racemic allylic alcohols.<sup>78</sup> The study of compatibility of the Ru-catalysts (A, B and C) with the enzyme and the required additives (NADPH and the co-factor regenerating agent isopropanol) showed that the Ru-complex B could maintain its activity in the presence of the additives. Then, with optimum concentrations of the different components and temperature, the reaction could be performed in a concurrent mode achieving yields of the desired chiral alcohols between 60 and 86% and ee >99%, (Scheme 9). This case constitutes the first example of a concurrent metal-catalyzed and biocatalyzed reaction in water.

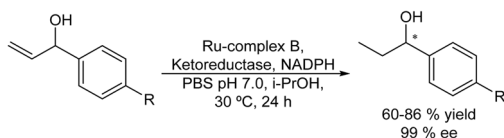


Scheme 6 Gold(i)-catalyzed hydration of propargylic ester and amide and subsequent asymmetric enzymatic reactions.



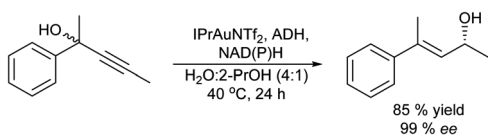


**Scheme 8** Synthesis of chiral amines from allylic alcohols in a sequential mode by combining chemocatalyzed isomerization and bioamination.



**Scheme 9** Synthesis of chiral amines from allylic alcohols in a concurrent mode by combining chemocatalyzed isomerization and bioreduction.

Another type of isomerization that gives access to prochiral ketones is for instance the Meyer-Schuster rearrangement of propargylic alcohols. The process comprises the metal catalysed (Cu, Ag, Au, In...) transformation of propargylic (acetylated) alcohols into the corresponding  $\alpha,\beta$ -unsaturated carbonyl compounds, which occurs *via* a formal 1,3-hydroxyl shift and tautomerisation usually under harsh reaction conditions. The chemo-enzymatic approach combining the Meyer-Schuster rearrangement with enantioselective ketone bioreduction was reported for the first time by Gotor-Fernández *et al.*<sup>79</sup> to obtain chiral  $\beta,\beta$ -disubstituted allylic alcohols. These compounds are important synthetic intermediates and have been used for instance as precursors of aroma compounds.<sup>80</sup> The process combines in a concurrent mode the rearrangement of propargylic alcohols catalysed by a gold carbene complex and bioreduction with ADH of the produced ketone to afford the desired chiral allylic alcohol. Therefore, the authors performed an exhaustive optimization of the reaction conditions of the gold catalyst, to find a compatible reaction window where the gold catalyst and enzyme (ADH) can work in an aqueous medium. Thus, the combination of an active carbene gold(I) catalyst [1,3-bis(2,6-diisopropylphenyl)imidazol-2-ylidene][bis(trifluoromethanesulfonyl)-imide]gold(I) (IPrAuNTf<sub>2</sub>) with alcohol dehydrogenases (ADHs derived from *Rhodococcus ruber*) allowed the synthesis of a broad panel of optically active (*E*)-4-arylpen-3-en-2-ols in good isolated yields (65–86%) (Scheme 10). The chemo-enzymatic cascade was also effectively expanded to a variety of 2-hetarylpen-3-yn-2-ol, hexynol and butynol derivatives. Moreover, the use of alcohol dehydrogenases of opposite enantioselectivity allowed the direct synthesis of both allyl alcohol enantiomers (93–>99% ee) under very mild reaction conditions. Using a similar strategy, the authors

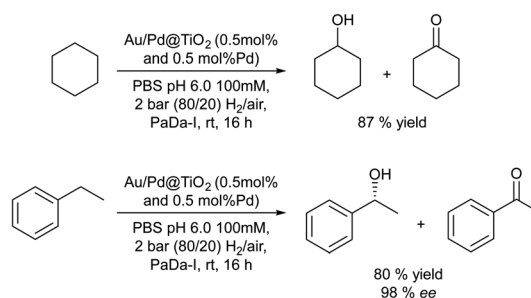


**Scheme 10** Synthesis of chiral  $\beta,\beta$ -disubstituted allylic alcohols from propargylic alcohols in a concurrent mode by combining a metal catalyzed Meyer-Schuster rearrangement with bioreduction.

combined the Meyer-Schuster rearrangement of propargylic alcohols catalysed by IPrAuNTf<sub>2</sub> with transaminases in aqueous media. In this case, in order to avoid the deactivation of the gold catalyst in the presence of the nucleophilic amine derivatives, the reaction was performed in a sequential mode, achieving the corresponding chiral allylic amines in good conversion (67–95%) and excellent selectivities (>97% ee).<sup>81</sup>

Finally, the selective C–H oxidation of saturated hydrocarbons is another route to obtain alcohols and ketones. However, this type of oxidation is highly challenging, since many catalysts are less selective and overoxidation of products is usually observed. Hutchings *et al.*<sup>82</sup> presented an elegant chemo-enzymatic process to produce alcohols (including chiral alcohols) from hydrocarbons, which involves the *in situ* generation of H<sub>2</sub>O<sub>2</sub> *via* oxygen reduction catalyzed by gold-palladium nanoparticles supported on TiO<sub>2</sub> combined with an unspecific peroxygenase PaDa-I that allows the efficient and selective oxidation of C–H bonds. The authors selected the oxidation of cyclohexane to cyclohexanol as the model reaction and after an exhaustive optimization of the reaction parameters the one-pot chemo-enzymatic process could be achieved in a concurrent mode (Scheme 11). Thus, the substrate, the heterogeneous catalyst (0.5 mol% Au and 0.5 mol% Pd@TiO<sub>2</sub>) and the biocatalyst were added in a batch reactor under 2 bar (80/20 H<sub>2</sub>/air), which generates H<sub>2</sub>O<sub>2</sub> at a concentration of 10–20 ppm. Working at room temperature and after 16 h, 87% yield of the desired cyclohexanol with a negligible amount of cyclohexanone was obtained. Under the optimized conditions the authors studied the formation of the chiral R-1 phenylethanol and excellent results in terms of yield and enantioselectivity were obtained (78% yield, 98% ee).

**2.1.2. Synthesis of chiral alcohols and amines by combining a C–C bond forming step with bioreduction and bioamination respectively.** Combination of C–C bond forming reactions with enantioselective biocatalytic transformations represents a powerful tool in organic chemistry to construct a specific carbon



**Scheme 11** Synthesis of alcohols by the oxidation of saturated hydrocarbons in a concurrent mode.

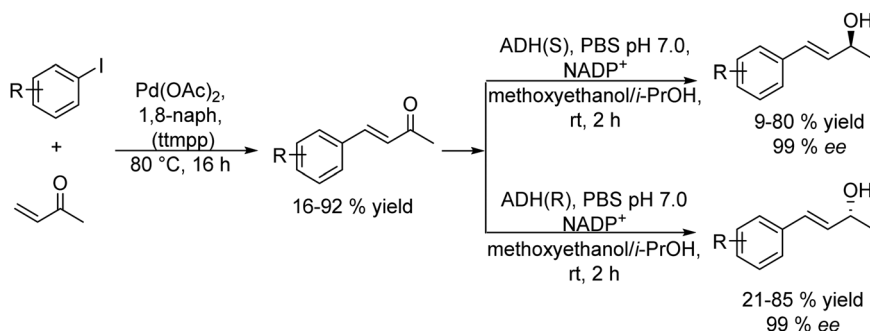


structure. Therefore, metal catalyzed cross-coupling reactions, such as Heck and Suzuki reactions, and aldol condensation have been effectively combined with biotransformations to produce valuable chiral alcohols and amines.

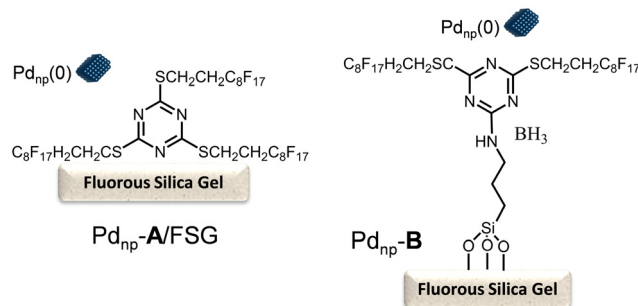
The Heck reaction is a C–C cross-coupling process between aryl halides or vinyl halides and activated alkenes catalyzed by palladium catalysts in the presence of a base. By combining the Heck cross-coupling reaction with bioreduction, enantiomerically pure allylic alcohols have been efficiently obtained. These compounds are useful building blocks in organic synthesis for the preparation of a variety of biologically active molecules.<sup>83–85</sup>

The most practical procedures to produce chiral allylic alcohols are based on kinetic resolution *via* asymmetric enzymatic acylation and on dynamic kinetic resolution methods of racemic allylic alcohols.<sup>86–90</sup> While these procedures are based on the conversion of the preformed carbon structure into the desired chiral allylic alcohol, the chemo-enzymatic strategies allow constructing directly chiral allylic alcohols with a desired carbon structure. Cacchi *et al.*<sup>91</sup> developed for the first time a sequential chemo-enzymatic process for the preparation of chiral allylic alcohols by combining the Heck reaction of aryl iodide derivatives with butenone in the presence of palladium acetoacetate ( $\text{Pd}(\text{OAc})_2$ ) as the catalyst with the enantioselective reduction of the  $\alpha,\beta$ -unsaturated ketone intermediate using an alcohol dehydrogenase (ADH). The Heck reaction conducted selectively with the  $\alpha,\beta$ -unsaturated ketone intermediate was performed by a method developed by the authors under solvent-free conditions in the presence of a high affinity proton acceptor (proton sponge) (1,8-bis(dimethylamino)naphthalene (1,8-BDAN) and 2,4,6-trimethoxyphenyl)phosphine (tmpp) and using an excess of butenone. After reaction completion, the excess of butanone was removed by evaporation, and the ADH and the required additives (see Scheme 12) were added to the reaction mixture. Following the optimized protocol, a series of aryl iodides provided the corresponding (*R*)- (with LB-ADH) and (*S*)- (with TADH) allylic alcohols in general in excellent isolated yields and >99% ee. Interestingly, no enzyme inhibition was observed in the biocatalytic step due to the presence of Pd or other reactants in the reaction medium. The method proved to be superior in terms of yield and enantioselectivity respect to conventional dynamic kinetic resolution methods.<sup>16,92,93</sup>

Based on the combination of Heck reaction and bioreduction, the same authors performed the synthesis of *R*-(-)-rhododendrol.<sup>94</sup>



Scheme 12 Synthesis of chiral allylic alcohols by combining a metal catalyzed Heck reaction with bioreduction.



Scheme 13 Perfluoro-tagged palladium nanoparticles immobilized on a fluorosilica gel through fluorosilica–fluorosilica interaction ( $\text{Pd}_{\text{np}}\text{-A/FSG}$ ) and covalent bonding ( $\text{Pd}_{\text{np}}\text{-B}$ ).

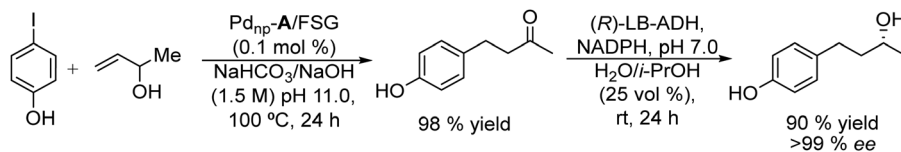
This compound is an aglycone intermediate used for the synthesis of rhododendrin,<sup>95–97</sup> a natural product widely used for its analgesic and anti-inflammatory properties.<sup>98,99</sup>

In this study, the authors prepared two different Pd chemo-catalysts immobilized on a fluorosilica gel, both through fluorosilica–fluorosilica interactions ( $\text{Pd}_{\text{np}}\text{-A/FSG}$ ) and covalent bonding ( $\text{Pd}_{\text{np}}\text{-B}$ ) (Scheme 13), which were tested in the Heck reaction in aqueous media. After optimizing the buffer solution and pH, the Pd catalysts were successfully applied to the Heck reaction of a variety of aryl iodides with 3-buten-2-ol, showing the high stability of the Pd catalysts that could be recycled several times retaining their activity and selectivity. Then, synthesis of (*R*)-(-)-rhododendrol was selected as a probe for evaluating the feasibility of the chemo-enzymatic process. For doing that, the Heck reaction between 4-iodophenol and 3-buten-2-ol was performed under optimized conditions (see Scheme 14). Then, after cooling, alcohol dehydrogenase [(*R*)-ADH], the co-factor (NADPH), and isopropanol (as the co-factor regenerating agent) were added to the reaction mixture, and the enzymatic step was completed at room temperature in 24 h. After that, (*R*)-(-)-rhododendrol was isolated in 90% yield and >99% ee (Scheme 14).

The process was satisfactorily extended to prepare a variety of other chiral alcohols and represents an alternative to the use of air-sensitive phosphine Pd complexes.

Metal catalyzed Suzuki–Miyaura cross-coupling between aryl halides and phenyl boronic acid derivatives is another C–C bond forming reaction that has been successfully combined





Scheme 14 Synthesis of (*R*)-(-)-rhododendrol by combining a Pd catalyzed Heck reaction with bioreduction.

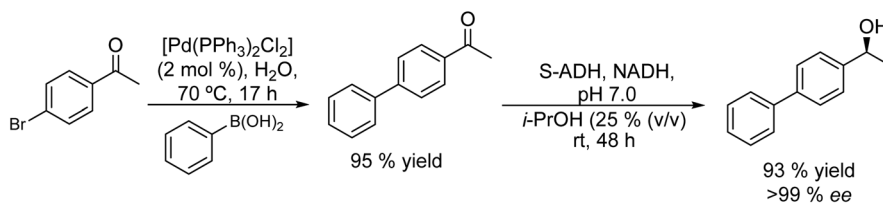
with ketoreductases and transaminases to obtain chiral biaryl alcohols and amines in high enantioselectivity.

Thus, chiral biaryl alcohols, which are of great interest in the synthesis of polymers, fluorescent brighteners and chiral ligands<sup>100</sup> were prepared by Gröger *et al.*<sup>101</sup> for the first time through a one-pot process by combining a Suzuki cross-coupling reaction catalyzed by a Pd complex with a subsequent asymmetric enzymatic reduction in the presence of the enzyme ADH in aqueous reaction media (Scheme 15).

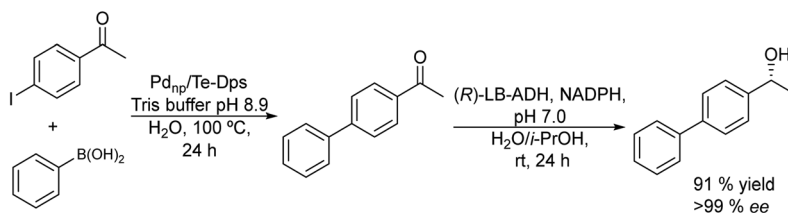
Taking as a model the reaction between 4-bromoacetophenone and the boronic acid, the authors studied the possible incompatibilities between the chemical and enzymatic steps. They found that while the Pd complex had a minor negative impact on the enzyme activity, an excess of boronic acid and the use of triphenylphosphine as a base in the Suzuki step strongly inhibited the ADH activity. Then, triphenyl phosphine was substituted by sodium carbonate, and boronic acid was added in stoichiometric amounts. Under these reaction conditions the cascade process was performed in a sequential mode and then to

achieve the Suzuki reaction towards practical completion (>95%), the pH was adjusted (pH 7) and the ADH, the corresponding co-factor and isopropanol as the co-factor regenerating agent were added to the reaction media. The corresponding chiral biaryl alcohol was achieved in excellent yield (91%) and >99% ee. The process was applied to a variety of substituted bromoacetophenones and boronic acids, affording the corresponding chiral biaryl alcohols in excellent yields. Based on this pioneering work and to avoid the use of air-sensitive phosphine ligands, Cacchi *et al.*<sup>102</sup> prepared water-soluble palladium nanoparticles, stabilized primarily within a protein cavity (Pd<sub>np</sub>/Te-Dps), to synthesize chiral biaryl alcohols in aqueous media using the same strategy. Thus, the Suzuki–Miyaura cross-coupling step followed by the asymmetric enzymatic reduction catalysed by an alcohol dehydrogenase derived from *Lactobacillus brevis* was performed efficiently. However, it was not possible to reuse the aqueous solution containing the catalyst system (Scheme 16).

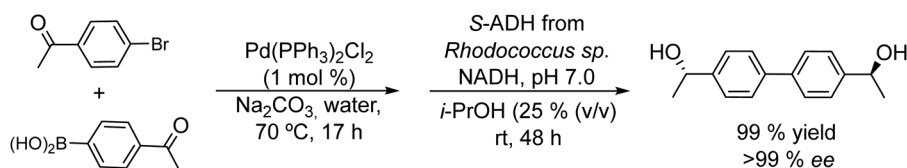
Symmetrical chiral biaryl diols (Scheme 17) were also synthesized by Gröger *et al.*<sup>103</sup> following a similar strategy.



Scheme 15 Synthesis of chiral biaryl alcohols by combining a Pd catalysed Suzuki cross-coupling and bioreduction.

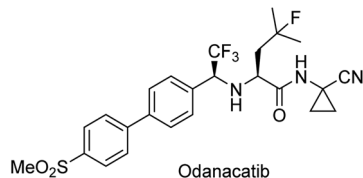


Scheme 16 Synthesis of chiral biaryl alcohols by combining Pd catalysed Suzuki cross-coupling and bioreduction.



Scheme 17 Synthesis of symmetrical chiral biaryl alcohols by combining Pd catalyzed Suzuki cross-coupling and bioreduction.





Scheme 18 Odanacatib used for treatment of the osteoporosis disease.

Symmetrical chiral diols are of interest as chiral ligands in asymmetric synthesis and also as monomers for the synthesis of enantiomerically pure polymers,<sup>104</sup> such as polyesters.

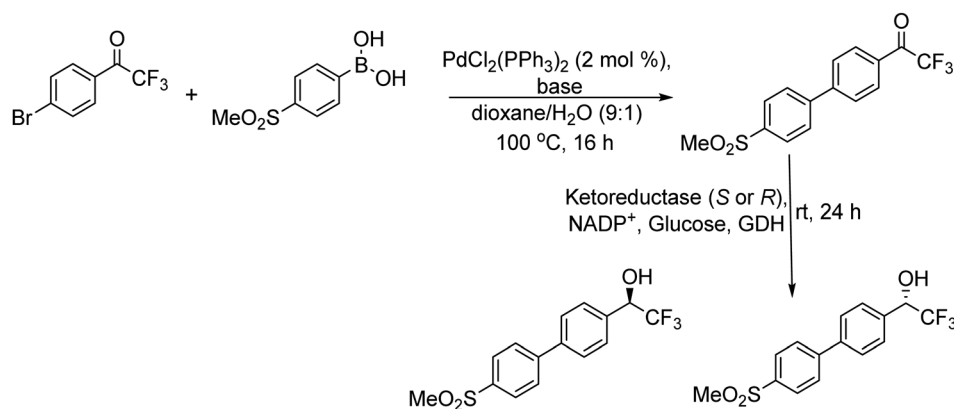
The authors performed the Suzuki cross-coupling reaction between the halogenated ketone and the phenylboronic substituted ketone, using a triphenylphosphine Pd complex [Pd(PPh<sub>3</sub>)<sub>2</sub>Cl<sub>2</sub>] under aqueous conditions at moderate temperatures (70 °C). Excellent results were obtained in terms of yields of the desired ketones (92–99%) in moderate time (17 h). After pH adjustment to 7 the enzyme ADH derived from *Rhodococcus* sp. and the required additives (isopropanol and NADP<sup>+</sup>) were added to the reaction medium. Under these conditions excellent yields and enantioselectivities of the desired biaryl diols were obtained (yield > 99% and ee > 99%) (Scheme 17).

Gotor-Fernández *et al.*<sup>105</sup> applied this strategy to synthesize a chiral building block of the drug odanacatib (Scheme 18), which is used in the treatment of osteoporosis. The desired chiral intermediate was obtained with excellent yield (97%) and enantioselectivity (99%) (Scheme 19).

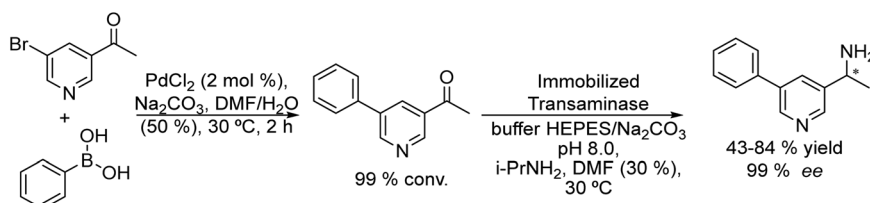
These strategies have important advantages with respect to conventional synthesis of biaryl alcohols, which requires

stoichiometric amounts of a chiral auxiliary for the reduction of the intermediate ketone or is based on enzymatic resolutions,<sup>106,107</sup> which in general give poor yields of the target chiral alcohol.

An example of the combination of the Suzuki–Miyaura cross-coupling reaction with a biocatalyzed transamination step to produce chiral biaryl amines was reported by Bornscheuer *et al.*<sup>108</sup> The authors performed the Suzuki–Miyaura coupling reaction of aryl bromides such as 5-bromo-3-acetyl-pyridine with boronic acid in the presence of PdCl<sub>2</sub>/Na<sub>2</sub>CO<sub>3</sub> as a catalytic system, dissolved in a 50% aqueous solution of *N,N*-dimethylformamide (DMF). When the corresponding biaryl ketone was formed in quantitative yield, an engineered transaminase derived from *Aspergillus fumigatus* along with the different required additives was added to the reaction media (see Scheme 20). Interestingly, a conveniently modified transaminase showed excellent compatibility with the reaction conditions of the Suzuki–Miyaura step, achieving an 84% yield of the chiral biaryl amine with 99% ee. The robust feature of the enzyme, allowed the design of a transamination step in a flow reactor using the transaminase immobilized on resins (EziG<sup>TM</sup> carriers). Thus, after the Suzuki–Miyaura step, the resulting reaction medium was directly used as feed of the continuous flow reactor after adjusting the different required additives for the transamination; however, the yield of the target biaryl amine was moderate (43%). This approach has an important advantage with respect to methods that require amine group protection strategies since free amines are known to be Pd-chelating functional groups. Moreover, it is known that the efficiency of the Suzuki–Miyaura reaction is low when *N*-protected substrates are involved.<sup>109</sup>

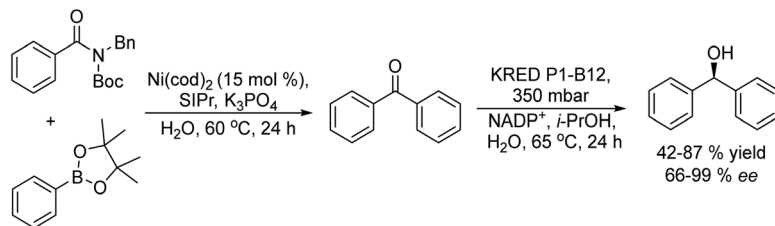


Scheme 19 Synthesis of the chiral building block of odanacatib by combining Suzuki cross-coupling and bioreduction.



Scheme 20 Synthesis of chiral biaryl amines by combining a Suzuki cross-coupling reaction in a batch mode with bioamination in a flow reactor.





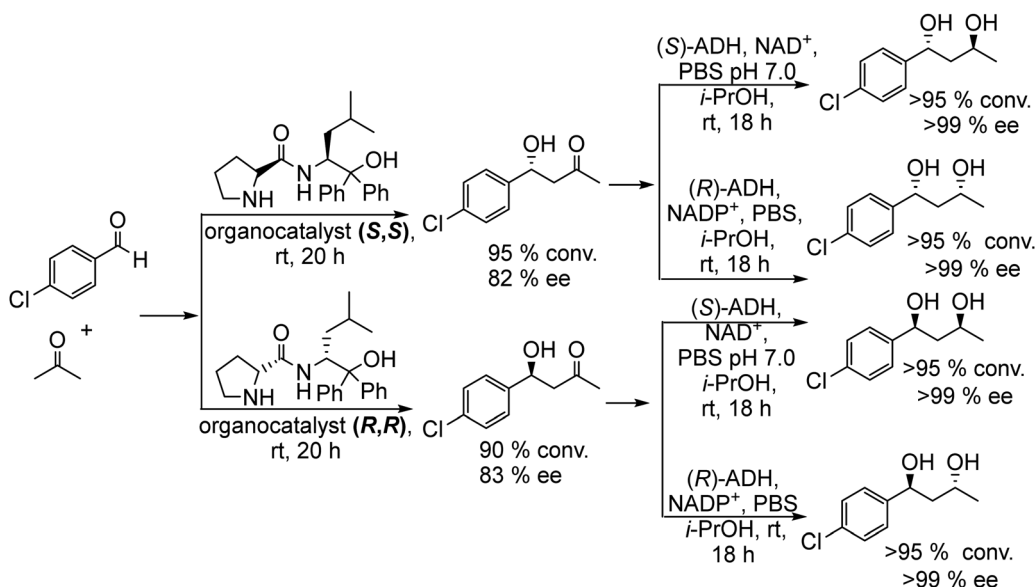
Scheme 21 Synthesis of chiral diarylmethanols by combining a Suzuki cross-coupling reaction with bioreduction (SIPr: 1,3-bis(2,6-diisopropylphenyl)imidazolidine).

Chiral diarylmethanols useful as intermediates for the synthesis of antihistaminics such as (*R*)-orphenadrine, were synthesized by Garg *et al.*<sup>110</sup> The process combines a Suzuki–Miyaura coupling reaction of arylamides with phenylboronic acid pinacol ester derivatives catalysed by nickel and an asymmetric reduction catalysed by an engineered ketoreductase (KRED P1-B12) (Scheme 21). The process was performed in a sequential mode in water, and the elimination of the acetone produced during the enzymatic step allowed driving the reaction to completion. An important finding for the success of the process was that the Suzuki–Miyaura coupling can be successfully performed in aqueous medium and that the engineered KRED P1-B12 can work in the stereoselective reduction step using *i*-PrOH–NADPH as the co-factor recycling system.

On the other hand, recent developments in asymmetric organocatalysis in homogeneous media have established that these catalysts are broadly applicable and constitute efficient synthetic tools for the preparation of many types of enantiomerically enriched and enantiomerically pure molecules.<sup>111–113</sup> Considering that the reaction diversity of asymmetric organo- and biocatalysis is complementary, the combination of both catalysts in chemo-enzymatic one-pot processes can enable a wide range of exclusive synthetic cascades. The potential of such chiral organocatalysts to form C–C bonds through an aldol condensation when combined with enzymes was demonstrated

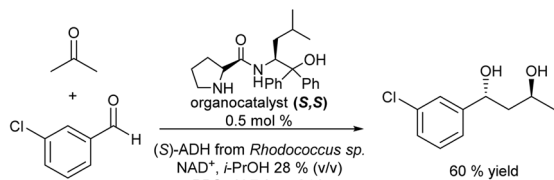
by Gröger *et al.*<sup>114,115</sup> for the synthesis of valuable 1,3-diols with two stereogenic centers. The chemo-enzymatic process couples the sequential stereoselective formation of both stereogenic centers by combining, in a sequential mode, an asymmetric aldol condensation using a chiral organocatalyst and a bioreduction using an alcohol dehydrogenase (ADH).

As a model reaction of the chemo-enzymatic process, the authors performed the enantioselective aldol condensation reaction of *p*-chlorobenzaldehyde and acetone in the presence of a proline derived asymmetric organocatalyst (*S,S* or *R,R*, Scheme 22), obtaining the corresponding enantiomerically enriched (*R*) or (*S*)  $\beta$ -hydroxyketones respectively. Then, bioreduction employing (*R* or *S*) ADH was performed at room temperature by addition of a phosphate buffer solution containing the co-factor (NAD<sup>+</sup> and NADP<sup>+</sup>) and 2-propanol (as a co-factor regenerator), achieving successfully the corresponding stereoisomer with high ee (see Scheme 22). Interestingly, it was found that the generation of the second stereocenter was controlled only by the biocatalyst, while the undesired influence of the first generated stereogenic center in the aldol adduct was not observed. Then, it is possible to define the enantioselectivity of each stereocenter by modulating only the organo- and the biocatalyst. Furthermore, the authors expanded the chemo-enzymatic process to other substituted aldehydes and the aldol



Scheme 22 Synthesis of chiral 1,3-diols by combining organocatalyzed asymmetric aldol condensation with bioreduction.





**Scheme 23** Synthesis of chiral 1,3-diols in a concurrent mode by combining organocatalyzed asymmetric aldol condensation with bioreduction.

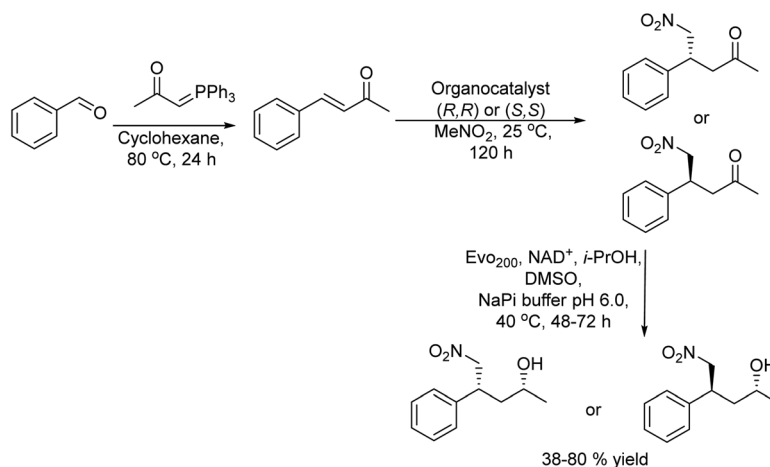
step was optimized in saturated aqueous NaCl solution.<sup>115</sup> The study showed that the organocatalyst concentration was key for controlling the enantioselectivity of the  $\beta$ -hydroxyketone intermediate. Thus, working in aqueous media and at low organocatalyst concentration (0.5 mol%), the aldol condensation yielded the chiral  $\beta$ -hydroxyketone with excellent success (99% ee), which was coupled with the enzymatic reduction. Following the same protocol, similar results in terms of yield and selectivity of chiral 1,3-diols were reported by Aoki *et al.*<sup>116</sup> by using chiral Zn<sup>+2</sup> complexes for the aldol reactions between acetone and substituted benzaldehydes followed by bioreduction of the  $\beta$ -hydroxyketone intermediate with ADH. Interestingly, Gröger *et al.*<sup>117</sup> developed later the chemo-enzymatic process in a spatial compartmentalized mode in a continuous flow system. As proof of principle, they performed the reaction between 3-chlorobenzaldehyde and acetone by combining two continuous flow reactors. In the first reactor containing the *S,S* organocatalyst immobilized over acrylic beads, the asymmetric aldol condensation was performed in organic media (cyclohexane) at 3 °C for 24 h, obtaining similar yields to those obtained with the free catalyst in aqueous media.<sup>115</sup> Then, after evaporation of the excess of acetone, the reaction mixture was used as a feed (along with isopropanol) of the second reactor, where ADH(*S*) and its co-factor NAD<sup>+</sup> were co-immobilized on the superabsorbent polymer Favor SXM 9155. The target chiral 1,3-diol was obtained in high conversion (89%) and excellent diastereo- and enantioselectivities (diastereomer ratio (dr) >35:1 and >99% ee) after 24 h at room temperature.

More recently, the authors reported the diastereoselective and enantioselective synthesis of 1,3-diols by combining the *S,S* organocatalyst and ADH (*S*) in aqueous media in a concurrent mode, where organo- and biocatalysts are introduced together at the beginning of the reaction.<sup>118</sup> First, the compatibility of the organocatalyst, the enzyme and the different required additives was shown. Then, a crucial task was to identify the appropriated reaction condition window under which both reaction steps could proceed efficiently, while side reactions (*e.g.*, reduction of the aldehyde used in the aldol step by the enzyme involved in the second step) were suppressed. Thus, by adjusting the reaction time and the amount of the different components (organo- and biocatalysts, aldehyde/acetone ratio and 2-propanol), 60% of the target chiral 1,3-diol was obtained (see Scheme 23). Interestingly, the process was further successfully implemented in a flow mode.<sup>119</sup>

Another example of combination of asymmetric organocatalysts with enzymes to generate two stereogenic centers was reported by Mangas-Sánchez and co-workers<sup>120</sup> for synthesizing chiral  $\gamma$ -nitroalcohols. Chiral  $\gamma$ -nitro alcohols (and ketones) are essential molecules in the synthesis of pharmaceutical compounds.<sup>121</sup> They can be produced *via* iminium-catalysed asymmetric Michael addition of nitromethane to  $\alpha,\beta$ -unsaturated carbonyl compounds.<sup>122,123</sup>

The authors<sup>120</sup> reported a three-step one-pot process to produce  $\gamma$ -chiral nitroalcohols starting from commercially available benzaldehyde derivatives by combining a Wittig reaction, chiral thiourea-mediated asymmetric conjugate addition of nitromethane, and bioreduction (Scheme 24).

Under optimized reaction conditions chiral  $\gamma$ -nitroalcohols were synthesized by reacting the benzaldehyde derivative with the preformed phosphonium ylide compound followed by the asymmetric 1,4-addition of nitromethane using cyclohexanediamine-based thiourea (*R,R*) or (*S,S*) as the asymmetric catalyst to form the intermediate chiral  $\gamma$ -nitro ketone in a one-pot sequential process. After reaction completion, the ketoreductase (Evo<sub>200</sub>) in a buffer solution and the co-factor and



**Scheme 24** Synthesis of  $\gamma$ -chiral nitro alcohols by combining a Wittig reaction, chiral-thiourea-mediated asymmetric conjugate addition of nitromethane, and bioreduction.



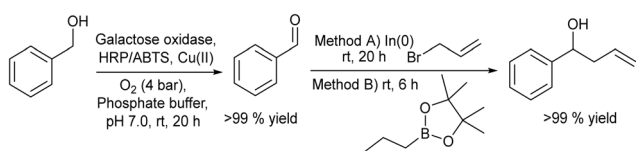
isopropanol as the co-factor regenerating agent were added (Scheme 24). Interestingly, the selection of a ketoreductase resistant to deactivation by nitromethane was a key point for the success of the process. Using this one-pot cascade process in a sequential mode and without significant adjustment of the reaction conditions, a variety of  $\gamma$ -nitro alcohols were obtained in 38–80% yield after three steps, while high diastereomeric and enantiomeric ratios were also obtained (up to  $\geq 97:3$  dr and er). The process represents the first case of the coupling of an asymmetric organocatalyzed step *via* iminium catalysis with a bioreduction step, in one-pot, to form two new stereogenic centers from a prochiral substrate.

### 2.1.3. Other chemo-enzymatic cascades leading to alcohols

**2.1.3.1. Synthesis of homoallylic alcohols.** Homoallylic alcohols are important building blocks, and are precursors, for instance, for the synthesis of chiral chromanes, lactones or urea derivatives.<sup>124–127</sup> Fuchs *et al.*<sup>128</sup> reported a chemo-enzymatic procedure for the synthesis of homoallylic alcohols, which involves the biooxidation of primary alcohols to the corresponding aldehydes in the presence of oxygen and the subsequent chemocatalyzed allylation to the target homoallylic alcohols (Scheme 25). Starting from phenylmethanol as the model substrate, the biooxidation was performed in phosphate buffer solution (PBS) using galactose oxidase, in the presence of a Cu(II) salt as a co-factor, and horseradish peroxidase (HRP) and 2,2'-azino-bis(3-ethylbenzothiazoline-6-sulfonic acid) (ABTS) for the removal hydrogen peroxide that was produced during the reaction. To achieve complete conversion to the benzaldehyde intermediate, optimization of the reaction conditions, such as oxygen pressure and concentrations of the Cu(II) salt and substrate, was carried out. The second step, the allylation process, was performed following two different methods: (A) a Barbier-type reaction that involves the nucleophilic addition between an alkyl halide and a carbonyl group catalysed by indium(0) and (B) metal-free addition of allylboronic esters.<sup>129,130</sup> It was shown that the combination of both steps in a concurrent mode was not possible because the biooxidation was completely inhibited in the presence of the allylating reagents (route A or B), due to the allylation of the active sites of the enzyme.

However, the cascade process could be successfully achieved when In(0) and allyl bromide or the allylboronic ester were added to the reaction medium after the completion of biooxidation.

The process was extended to a variety of benzylic alcohols that were transformed into the corresponding homoallylic alcohols with good to excellent conversion. A remarkable feature of the process is the functional group tolerance, which



**Scheme 25** Synthesis of homoallylic alcohols from benzylic alcohols by combining bio-oxidation with chemocatalyzed C–C coupling.

includes unprotected phenolic hydroxyl groups and basic heteroaromatic moieties.

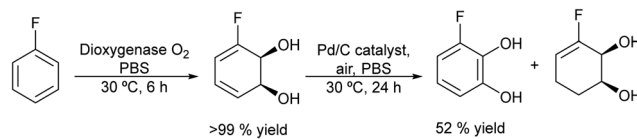
**2.1.3.2. Synthesis of catechols.** Catechols (1,2-dihydroxybenzenes) are widespread in nature and are widely used in the pharmaceutical and chemical industries. For instance, catechols and their derivatives are used in a variety of processes, such as the manufacture of inks, insecticides, plastics, photographic developers, rubber, *etc.*<sup>131</sup> Moreover, in cells, catechols work as antioxidants, preventing diseases produced by free radicals, such as heart disease, cancer and immune system decline. The synthesis of catechol derivatives is usually difficult and sometimes requires harsh reaction conditions, leading to the formation of isomeric mixtures of 3- and 4-catechols in low yields.<sup>132</sup>

The potential of combining a dioxygenase-catalysed *cis*-dihydroxylation of monosubstituted benzenes with a dehydrogenation step catalysed by Pd/C in a one-pot process to obtain catechols in aqueous media was reported by Hardacre *et al.*<sup>133</sup> As an example (Scheme 26) fluorobenzene is transformed into the corresponding *cis*-diol using the enzyme dioxygenase present in whole cells of *P. putida*. Subsequently, the *cis*-diol is transformed into the desired catechol (3-fluorocatechol) using Pd/C as the heterogeneous catalyst.

Optimization of the dehydrogenation step was performed initially using the Pd/C catalyst under different reaction conditions in order to minimize the formation of the *cis*-dihydrodiol byproduct. Starting from different monosubstituted aromatics, yields between 40 and 66% at 100% conversion were achieved. Moreover, the Pd/C catalyst was found to be stable and could be reused for 4 cycles without loss of activity and selectivity.

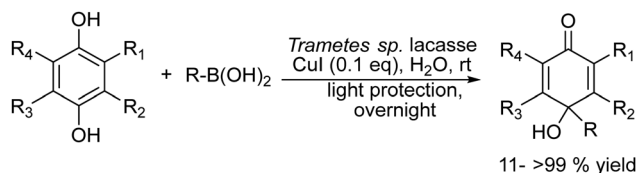
Finally, the one-pot process starting from fluorobenzene in aqueous phosphate buffer could be achieved by performing the biotransformation using a large volume of culture medium. Then, after concentration of the reaction mixture containing the target *cis*-diol and bacterial cells, the former is dehydrogenated in the presence of the Pd/C catalyst under an air atmosphere, achieving 52% yield of 3-fluorocatechol. In addition, the chemo-enzymatic process was compared with a biocatalyzed cascade method using whole cells of *P. putida* for *cis*-dihydroxylation combined with *E. coli nar B* for dehydrogenation, achieving similar yields of the target catechol.

**2.1.3.3. Synthesis of para-quinols.** The *p*-quinol is a key structural moiety found in numerous natural products,<sup>134</sup> pharmaceuticals,<sup>135</sup> and synthetic building blocks.<sup>136,137</sup> The main synthetic methods of quinols involve the oxidation of 4-alkylphenols and the direct alkylation of quinones using alkyl-lithium and Grignard reagents. These procedures require



**Scheme 26** Synthesis of 3-substituted catechols from monosubstituted aromatics by combining *cis*-hydroxylation with a Pd catalyzed dehydrogenation step.





**Scheme 27** Synthesis of *p*-quinols by combining laccase-catalyzed *in situ* oxidation of hydroquinones with the corresponding quinones.

corrosive, harsh and water-free conditions or the utilization of toxic transition metal catalysts, achieving in most cases modest yield of quinol.<sup>138–140</sup> Recently, Koszelewski *et al.*<sup>141</sup> reported the synthesis of *p*-quinols through the copper catalysed addition of boronic acid to quinone under aqueous conditions. However, the method suffers from a low atom economy and is limited to benzoquinone derivatives. To overcome these drawbacks, the authors envisioned<sup>142</sup> a chemo-enzymatic approach that combines laccase-catalysed *in situ* oxidation of hydroquinones to the corresponding quinones with subsequent CuI-catalysed C–C coupling with arylboronic acids in a concurrent mode (Scheme 27). After optimization of the reaction conditions, the synthetic applicability was shown for a wide spectrum of *p*-quinol derivatives that were obtained in yields higher than or similar to those obtained from quinones. Interestingly, the authors found that the enzyme not only participates in the oxidation reaction of the hydroquinone, but also increases the activity of the copper catalyst in the carbon–carbon bond formation of the second step by forming Cu complexes with the enzyme without key changes in the geometry of the active sites of the biocatalyst. The wide applicability of this chemo-enzymatic cascade strategy allows access to quinol structures difficult to obtain by traditional methods, representing an efficient synthetic alternative to existing procedures.

**2.1.3.4. Synthesis of chiral vicinal diols.** Enantioenriched vicinal diols are important intermediates in the pharmaceutical industry.<sup>143</sup> Monti *et al.*<sup>144</sup> developed for the first time a chemo-enzymatic one-pot two-step sequential procedure to obtain highly enantioenriched limonene 1,2-diols by combining the epoxidation of (+)- and (–)-limonene in the presence of heterogeneous titanium-grafted silica catalysts with a biocatalyzed hydrolytic epoxide ring-opening in the presence of limonene-1,2-epoxide hydrolase derived from *Rhodococcus erythropolis*. For the first step an excess of *tert*-butyl hydroperoxide (TBHP) in the presence of a titanium on silica catalyst was selected since it

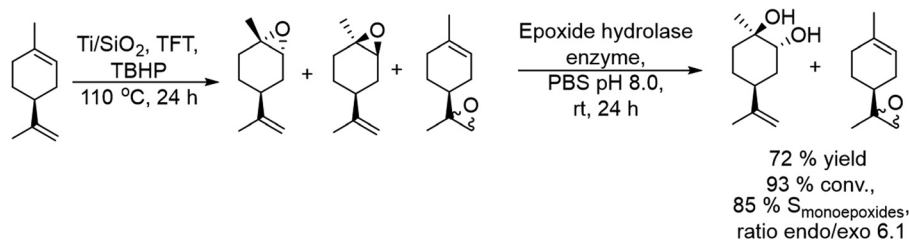
directs the epoxidation preferentially towards the endocyclic double bond of limonene (C1–C2).<sup>145</sup>

For instance, using (–)-limonene as the substrate and Ti/SiO<sub>2</sub> as the catalyst (Scheme 28), excellent selectivity of monoepoxides (85% at 93% conversion), as a mixture of *cis*-endo, *trans*-endo, and *exo* isomers (an endo/*exo* ratio of 6:1), was obtained after 24 h at reflux temperature with trifluorotoluene (TFT) as a solvent. For the hydrolysis step, the hydrolase in a buffer solution was added to the reaction mixture and the reaction proceeded in the biphasic TFT–water medium at room temperature for 24 h. Under these conditions, both endo-epoxides were completely hydrolyzed and an overall yield of 72% of the enantiomerically and diastereomerically enriched (*R,R,S*)-diol was achieved by this simple and straightforward procedure, while the *exo*-epoxides were not hydrolyzed. Interestingly the enzymatic activity was not influenced by the presence of the titanium catalyst and the residual amounts of TBHP oxidant.

In summary, chemo-enzymatic cascade processes can allow access to a variety of valuable chiral alcohols and amines. In general, main advantages of these cascade processes compared with conventional methods, involving kinetic resolutions or asymmetric catalysis, are associated with the possibility to start from very structurally different substrates, while higher yields and enantioselectivities of the desired product can be achieved under mild reaction conditions in aqueous media. In addition, the combination of chemocatalyzed C–C-bond forming reactions with enzymes allows access to a variety of more complex chiral structures, difficult to achieve by conventional asymmetric methods, including the easy generation of various stereogenic centers with high stereoselectivity by combining asymmetric organocatalysts with biocatalysts.

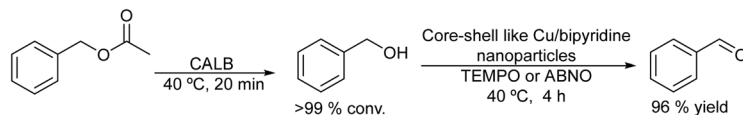
## 2.2. Synthesis of aldehydes

The selective synthesis of aldehydes by the partial reduction of esters is an important reaction in organic chemistry.<sup>146</sup> However, the reaction is usually performed through non-environmentally friendly protocols that require special reducing agents such as sodium diisobutyl-*t*-butoxyaluminum hydride and very low reaction temperature (between 0 °C and –78 °C) and that, in general, lead to a low yield of the corresponding aldehyde.<sup>147</sup> Recently, an environmentally friendly chemo-enzymatic method has been reported by Weberskirch *et al.*<sup>148</sup>, which involves the lipase catalyzed hydrolysis of the ester followed by the selective oxidation of the intermediate alcohol into the aldehyde in aqueous medium.



**Scheme 28** Synthesis of chiral vicinal diols by combining a chemocatalyzed epoxidation reaction with biocatalyzed epoxide hydrolysis.





Scheme 29 Synthesis of aldehydes from esters by combining enzymatic hydrolysis with oxidation.

A highly active and selective Cu(I)/bipyridine/*N*-oxyl catalytic system, which can operate under mild reaction conditions, was selected for the aerobic oxidation of the alcohol intermediate into the aldehyde.<sup>149</sup> However, an important drawback of the Cu(I)/bipyridine catalyst is its water-sensitive character. Therefore, to produce a water-resistant Cu(I)/bipyridine catalyst a core-crosslinked nanoparticle with a hydrophilic shell and a hydrophobic core was prepared by a microemulsion process using hexanediol dimethacrylate as a cross-linking monomer. The polymeric nanoparticles that provide a hydrophobic nano-environment for the Cu/bipyridine system were highly active and stable catalysts for performing the oxidation of a variety of aromatic and allylic alcohols in aqueous media using TEMPO or ABNO (9-azabicyclo[3.3.1]nonane *N*-oxyl) as the *N*-oxyl source. Interestingly, the polymeric shell of the nanoparticles also avoids the interaction of the chemocatalyst with the enzyme, preventing their mutual inhibition. Thus, the chemo-enzymatic process was efficiently performed in a sequential mode, where the total hydrolysis of the acetyl ester was first achieved in the presence of the enzyme CAL-B at 40 °C for 20 min. Then, after neutralization of the acetic acid produced during the hydrolysis, the Cu/bipyridine catalyst was added to the reaction media to perform the aerobic oxidation of the produced alcohol intermediates. The corresponding aldehydes were obtained in high yields (73–93%) (Scheme 29).

This chemo-enzymatic process represents a direct and eco-friendly route for the synthesis of aldehydes with high selectivity from the corresponding esters, avoiding conventional methodologies that use metal hydride salts involving high generation of wastes.

Another synthetic strategy to obtain chiral aldehydes, which can be used as fragrances and flavors, has been studied by Rudroff *et al.*<sup>150</sup> The authors described a chemo-enzymatic cascade process that involves as the first step the palladium-catalyzed Heck-coupling between aryl trifluoroborate derivatives and acrylic acids giving cinnamic acid derivatives, followed by two biocatalysed reduction steps where the acid group is first reduced to the corresponding alpha-unsaturated aldehyde (catalyzed by *Carboxylate Reductase* (NcCAR) whole cell) and finally, the C=C bond is asymmetrically reduced to the

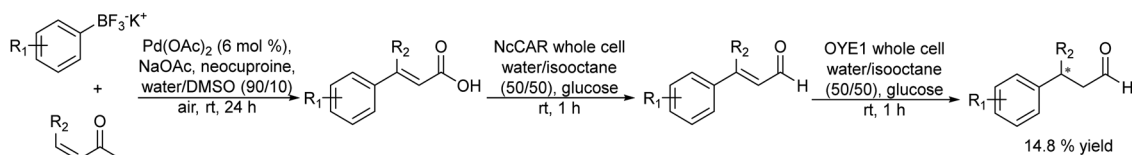
final chiral aldehyde by an enereductase (OYE1 whole cell) (Scheme 30).

A key point of this study was to find an enzyme with high activity to perform the selective bioreduction of the carboxylic acid into the aldehyde while avoiding the over-reduction of the aldehyde to the undesired alcohol. For this, the authors combined the random mutagenesis biotechnological strategy<sup>151</sup> with an *in situ* product removal (ISPR) strategy by working in a biphasic system (isooctane–water, 50/50 v/v), where the aldehyde is extracted from the aqueous phase, achieving complete conversion to the desired unsaturated aldehyde. The fusion of the two proteins necessary for the two biocatalysed steps, the NcCAR and OYE1, combined with the biphasic strategy, enabled both biocatalysed steps to occur simultaneously, affording the chiral aldehyde in excellent yield (80%) when starting from the pure carboxylic acid derivative.

However, when the whole chemo-enzymatic cascade process was performed in a concurrent mode the yield of the desired chiral aldehyde was only 14.8% due to the incompatibility between the CAR enzyme and the acrylic acid substrate necessary for the Heck reaction.

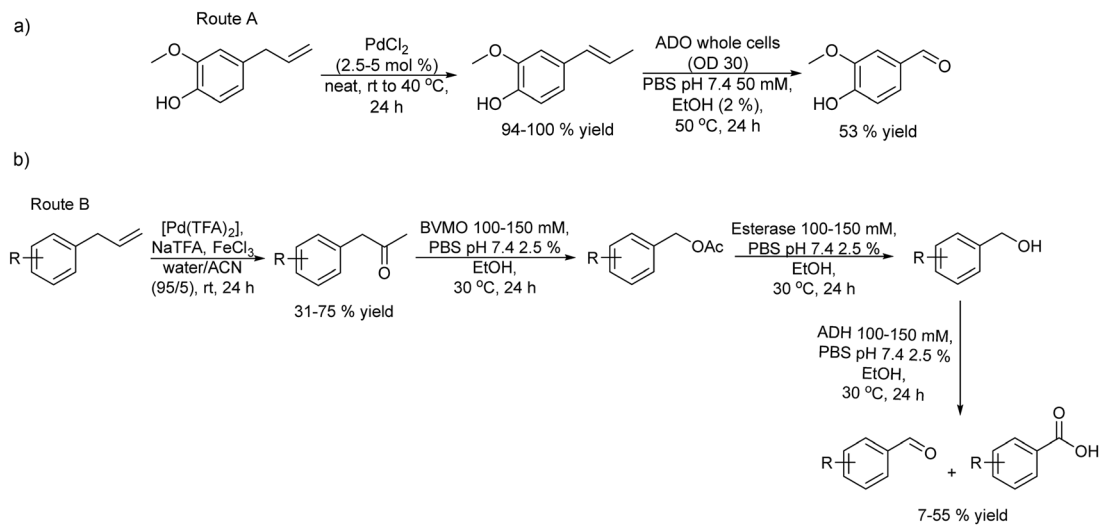
With interest in synthesizing fragrant aldehydes the same authors proposed two different catalytic routes starting from substituted phenyl propenes.<sup>152</sup> Route A (Scheme 31(a)) involves catalytic isomerization of the allylic alkene group followed by the alkene group cleavage performed using an aromatic dioxygenase enzyme (ADO). Route A was performed in a sequential mode by using PdCl<sub>2</sub> as the isomerization catalyst, followed by the addition of ADO (whole cells) after dilution of the reaction media with phosphate buffer and EtOH. However, due to the substrate specificity of the ADO enzyme, the chemo-enzymatic process only worked with substrates bearing a hydroxy group at the para position of the aromatic ring. Vanillin could be obtained through this approach in 53% yield (Scheme 31(a)).

Therefore, the authors explored another route (route B) in a sequential mode where the initial step is Wacker oxidation of the phenylpropene substrate to the ketone followed by three biocatalysed steps that involve *Baeyer–Villiger monoxygenase* oxidation of the ketone to the ester, hydrolysis of the ester performed by an esterase giving an alcohol that is finally biooxidized to the



Scheme 30 Synthesis of chiral aldehydes in a concurrent mode by combining C–C Heck coupling with biocatalysed carboxylic acid reduction into the aldehyde and asymmetric alkene reduction.





**Scheme 31** Synthesis of aldehydes from aryl propenes. Route (A): palladium-catalyzed isomerization followed by alkene cleavage. Route (B): Wacker oxidation followed by three consecutive bioreactions involving Baeyer–Villiger oxidation, ester hydrolysis, and oxidation.

aldehyde (Scheme 31(b)). An extensive study of a series of potential enzymes for this cascade process showed that *phenylacetone monooxygenase* (PAMO) as *Baeyer–Villiger–monooxygenase*, AlkJ derived from *Pseudomonas putida* as alcohol dehydrogenase and an esterase derived from *Pseudomonas fluorescens* (PfeI) were the optimum enzymes. The authors formed a mixed-culture with the three biocatalysts and studied the conversion of the ketone to the desired aldehyde. A crucial point in this study was to avoid the over-oxidation of the desired aldehyde into the undesired acid in the reaction. It was shown that the control of the buffer concentration and the addition of a small amount of EtOH in the reaction medium were key to achieving this goal. Thus, in the chemo-enzymatic process, the Wacker oxidation step was performed using palladium(II) trifluoroacetate [Pd(TFA)<sub>2</sub>] and iron(III) in water/acetonitrile (95/5% v/v). Then the reaction mixture was diluted with phosphate buffer, the pH was adjusted to 7.4 and the mixed-culture with the three biocatalysts was added. Moderate yields (7–55%) of the desired aldehydes were obtained after 24 h.

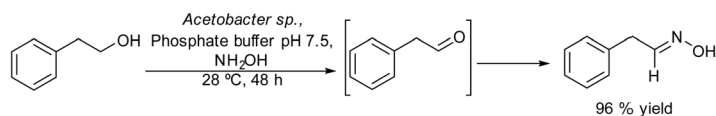
### 2.3. Synthesis of aldoximes

Aldoximes are important molecules with a wide range of applications in medicine, industry and analytical chemistry. In addition, they are very useful and versatile intermediates in synthetic organic chemistry to prepare oximes, nitriles, amides, etc.<sup>153</sup> Preparation of aldoximes by a one-pot process from primary alcohols is of special interest since habitually aldehydes exhibit low stability, making it challenging to prepare aldoximes in high yields. Molinari *et al.*<sup>154</sup> developed a chemo-enzymatic cascade process in a concurrent mode for the

synthesis of aldoximes from primary alcohols in aqueous media. The process combines the oxidation of primary alcohols by acetic acid bacteria dehydrogenases with the subsequent condensation of the aldehyde formed with hydroxylamine chlorohydrate (Scheme 32). In the enzymatic oxidation, the reaction kinetics has to be considered since the possible over oxidation of the aldehyde formed to the corresponding carboxylic acid can also occur. Using 2-phenylethanol as the model substrate three strains of acetic acid bacteria (*Acetobacter sp.* MIM 2000/61, *Gluconobacter oxydans* DSM 2343 and *Asaia bogorensis* SF2.1.) were tested in the oxidation step, showing that only *Gluconobacter oxydans* was mainly selective towards the corresponding aldehyde, while *Acetobacter sp.* and *Asia bogorensis* were fully selective towards the corresponding carboxylic acid. However, when the chemo-enzymatic process was performed in a concurrent mode (*i.e.* the biooxidation was performed in the presence of hydroxylamine) the three strains gave as the main product the aldoxime. These results suggest that the intermediate aldehyde (phenylacetaldehyde) reacts faster with the hydroxylamine than the oxidation to the acid form. It was found that high concentrations of hydroxylamine inhibit the enzymatic oxidation, therefore, by optimizing the reaction conditions, the chemo-enzymatic process could be applied to the synthesis of a variety of aldoximes from phenyl-alcohol derivatives in moderate to high yields (50–96%).

### 2.4. Synthesis of nitriles

Nitriles are important chemicals, and particularly, long-chain alkyl nitriles have attracted interest as solvents and as



**Scheme 32** Synthesis of aldoximes from alcohols by combining an enzymatic oxidation and a reaction with hydroxylamine in a concurrent mode.



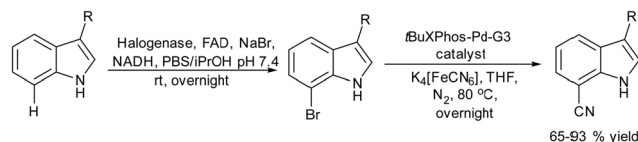
intermediates for amines in the surfactant field.<sup>155</sup> The conventional methods to synthesize nitriles are based on substitution or addition reactions with hydrogen cyanide or cyanides; however, an important drawback is the need for stoichiometric amounts of highly toxic cyanide.<sup>156</sup> Other alternative methods are based on ammoxidation<sup>157</sup> and dehydration of amides;<sup>155</sup> however, the main drawback of these processes is the high temperature required, which affects the selectivity of the process and economic cost.

Recently, Gröger *et al.*<sup>158</sup> developed an alternative chemo-enzymatic approach to produce nitriles by dehydration of aldoximes using aldoxime dehydratase. The starting aldehyde, nonanal, was first obtained through a hydroformylation step of octene in aqueous media using a rhodium complex as a catalyst. Then, the required amount of the aldehyde was taken from the formylation reactor and subsequently condensed with hydroxylamine in aqueous media to produce quantitatively the corresponding aldoxime. To avoid the inhibition effect of the residual hydroxylamine on the enzyme, the former was subjected to *in situ* thermal decomposition (100 °C, 16 h) and the recombinant whole-cell expressing aldoxime dehydratase was added to the reaction media (Scheme 33), achieving the corresponding nitrile in 67% yield.

A related chemo-enzymatic cascade process to synthesize aliphatic nitriles from alcohols was reported by the same group.<sup>159</sup> In this case, the aliphatic alcohol was converted into the aldehyde through a TEMPO-catalysed oxidation using hypochlorite as the oxidation agent and an aliphatic nitrile as an organic solvent. After oxidation completion, a hydroxylamine hydrochloride solution in water was added and stirred at room temperature up to the complete conversion of the aldehyde to the aldoxime. After phase separation, the organic phase bearing the aldoxime was directly used for the biocatalytic step using a supported aldoxime dehydratase, leading to the nitriles.

These chemo-enzymatic processes, which correspond to a formal hydrocyanation of alkenes, allow access to nitriles in moderate yields and avoid the use of harmful cyanide derivatives, while occurring under mild reaction conditions.

Halogenation of organic substrates using halogenases that use benign inorganic halide salts as the halogen sources represents an environmentally friendly alternative to conventional methods that often require the use of hazardous chemicals and harsh reaction conditions. Taking advantage of these

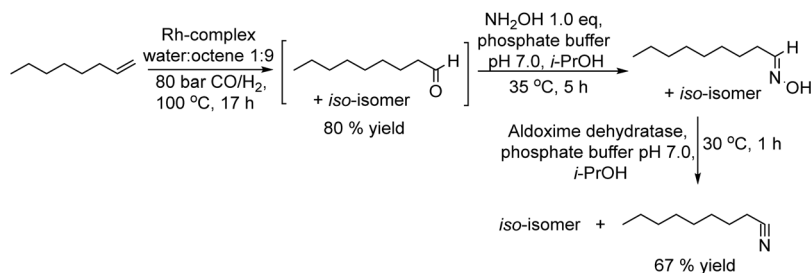


**Scheme 34** Synthesis of cyano-substituted indole derivatives by combining enzymatic halogenation and cyano group insertion.

enzymes, Micklefield *et al.*<sup>160,161</sup> developed a chemo-enzymatic method for the C–H functionalization of aromatic moieties of aryl and heteroaryl derivatives to nitrile groups, in a highly regioselective manner, by integrating a flavin adenine dinucleotide (FAD)-dependent halogenase (Fl-Hal) with Pd-catalysed cyanation. For instance, starting from indole scaffolds, the chemo-enzymatic cascade performed in a sequential mode involves as a first step the regioselective halogenation of the aromatic ring catalysed by the halogenase followed by palladium chemocatalyzed CN insertion using potassium ferrocyanide ( $K_4[Fe(CN)_6]$ ) as a non-toxic cyanide source (see Scheme 34). The enzyme was immobilized in the form of cross-linked enzyme aggregates (CLEAs) that showed higher halogenation efficacy, while improving biocatalyst stability and tolerance to higher substrate loadings. Moreover, enzyme directed evolution enabled the access to the C5, C6 and C7 positions of the indole scaffold regioselectively. Additionally, the encapsulation of the Fl-Hal–CLEA in a molecular weight cut-off (MWCO) membrane (12–14 kDa) enabled the easy separation of the enzyme from the reaction media before the addition of cyanation components and recycling the enzyme. Moreover, to take advantage of the versatility of the nitrile group, the cascade was extended to the synthesis of amides and carboxylic acids through the enzymatic hydration and hydrolysis of nitriles generated *in situ*, using nitrile hydratase and NITR enzymes within *E. coli* cells, respectively. This chemo-enzymatic process represents a valuable strategy to introduce nitrile groups in a regioselective manner, giving access through further transformation to a variety of important functionalities such as amines, oximes, amides, *etc.*

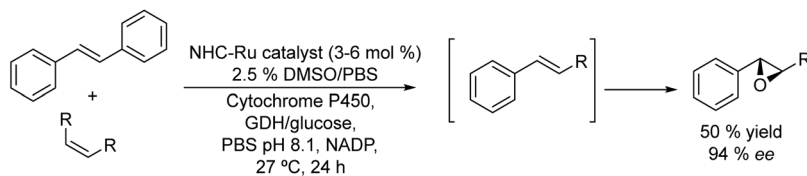
## 2.5. Synthesis of chiral epoxides

Epoxides are attractive synthons used in organic synthesis due to their chemical versatility.<sup>162</sup> Conventional methods for the synthesis of chiral epoxides are based on kinetic resolutions of racemic epoxides *via* epoxide-hydrolase catalysed enantioselective



**Scheme 33** Synthesis of nitriles from 1-alkenes by combining a hydroformylation step, a reaction with hydroxylamine and enzymatic dehydration of the aldoxime intermediate.





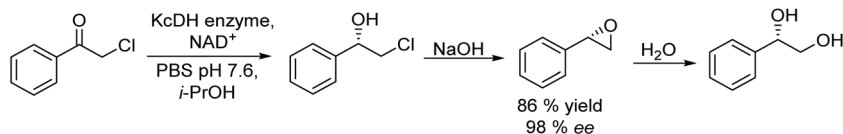
**Scheme 35** Synthesis of chiral aryl epoxides from alkenes in a concurrent mode by combining a metathesis reaction with biooxidation.

hydrolysis and chemical asymmetric epoxidation of alkenes, using the Sharpless, Jacobsen and Yian Shi methods.<sup>163</sup> However, these methods require expensive catalysts that work at low substrate/catalyst ratios, with limited efficiency and variable degrees of enantioselectivities. To overcome these drawbacks direct biocatalyzed stereospecific epoxidation of alkenes by monooxygenases (e.g., cytochrome P450s) represents an interesting alternative.<sup>164</sup> Taking advantage of monooxygenases, Zhao *et al.*<sup>165</sup> reported the synthesis of chiral aryl epoxides by combining Ru-complex catalyzed cross-alkene metathesis of stilbene and symmetric alkenes with biocatalyzed stereoselective epoxidation (see Scheme 35). Optimization of reaction conditions (Ru catalyst, substrate loading, organic cosolvent, reaction volume, buffer solution concentration, *etc.*) and enzyme engineering were required to perform the reaction in a concurrent mode in the aqueous phase to achieve moderate yield and high enantioselectivity of the aryl epoxide that can be regenerated by the glucose dehydrogenase (GDH)/glucose enzymatic system. In this study, the authors used a glucose dehydrogenase (GDH) to recycle NADPH continuously by reduction of NADP<sup>+</sup> with concomitant conversion of glucose to gluconic acid. The cascade process gives the E form of the corresponding epoxide with an enantiomeric excess of 94% and moderate yield (50%). The strategy allows constructing a variety of structurally different chiral epoxides in a direct way and under very mild reaction conditions.

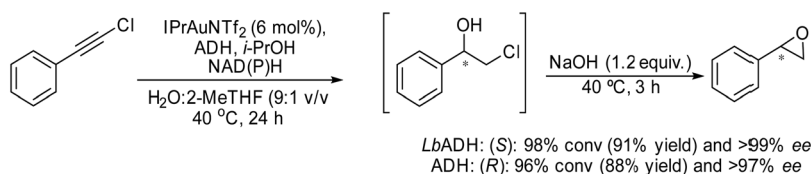
Another efficient chemo-enzymatic method for the synthesis of enantiopure epoxides starts from  $\alpha$ -chloroketones.<sup>166</sup> In this study, the bioreduction of  $\alpha$ -chloroketones using a newly developed ketoreductase (KcDH) (overexpressed in *Escherichia coli*) was combined with the base catalysed ring

closure of the intermediate halohydrin (see Scheme 36). After the biocatalyzed reduction of chloroacetophenone and chloro-1-phenoxy-2-propanone into the enantiomerically pure halohydrin intermediates, the corresponding chiral epoxides were easily obtained by adding an excess of NaOH while maintaining their ee. For instance, the (*R*)-styrene oxide was obtained in nearly enantiopure form (98% ee) and 86% yield. As a byproduct, the corresponding vicinal diol resulting from the epoxide opening was obtained in yield lower than 20%.

Another efficient chemo-enzymatic method to produce chiral epoxides and a variety of versatile chiral halohydrins has been recently reported by Gotor-Fernandez *et al.*<sup>167</sup> Taking advantage of the recently reported compatibility of ADHs with the N-heterocyclic carbene gold(I) complex (1,3-bis(2,6-diisopropylphenyl)-imidazol-2-ylidene)[bis(trifluoromethanesulfonyl)imide]gold(I) (IPrAuNTf<sub>2</sub>),<sup>79</sup> the authors designed a cascade in a concurrent mode to synthesize chiral halohydrins, which involves the gold-catalyzed regioselective hydration of haloalkynes, followed by the stereoselective bioreduction of the corresponding  $\alpha$ -halomethyl ketone intermediates into chiral halohydrins using alcohol dehydrogenases (ADHs). The hydration step was thoroughly investigated in order to conduct the chemo-enzymatic process in a concurrent mode, and under optimized reaction conditions, a variety of chiral halohydrins in yields ranging from 65–86% (isolated yields) and >98% ee were obtained. The success of the process was due to the thermodynamically favored reduction of the  $\alpha$ -haloketone intermediate, and therefore a small excess of isopropanol (acting as a co-factor recycling agent and as a co-solvent) was required, thus limiting the formation of byproducts, which are produced when



**Scheme 36** Synthesis of chiral epoxides from  $\alpha$ -haloketones by combining bioreduction and ring closure.



**Scheme 37** Synthesis of chiral epoxides from haloalkynes by combining a chemocatalyzed hydration step and bioreduction in a concurrent mode followed by cyclization of the chiral halohydrins.



using larger quantities of isopropanol. Finally, the chemo-enzymatic synthesis of the chiral halohydrin was integrated with cyclization into a chiral styrene oxide that was successfully accomplished by the addition of NaOH to the reaction medium (Scheme 37).

## 2.6. Synthesis of carboxylic acids and esters

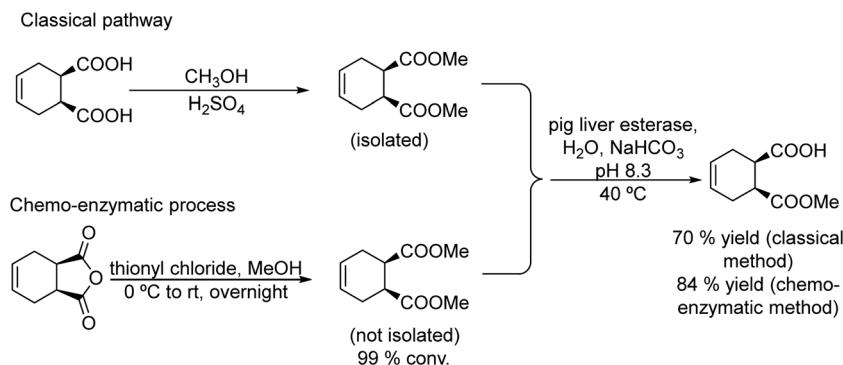
Carboxylic acids and their derivatives, particularly chiral compounds, are important scaffolds in organic synthesis for the preparation of a wide variety of pharmaceuticals, agrochemicals, flavors, *etc.* For instance, the chiral monoester, (1*S*,2*R*)-2-(methoxycarbonyl)-4-cyclohexenecarboxylic acid, is a strategic intermediate for the synthesis of drug candidates for the modulation of chemokine receptor activity.<sup>168,169</sup> Classically, the monoester is produced in two separate steps that involve first the esterification of (1*R*,2*S*)-4-cyclohexene-1,2-dicarboxylic acid (Scheme 38) with methanol in the presence of a strong acid as a catalyst. The dimethyl ester formed (*meso*-diester) is subsequently isolated and purified and then selectively hydrolysed by an esterase into the desired monoester in  $\geq 99.5\%$  enantiomeric excess.

An improved chemo-enzymatic process for the synthesis of this high value monoester was developed by Wardenga *et al.*<sup>170</sup> The method involves first a chemical esterification starting from *meso*-phthalic anhydride to produce the *meso*-diester followed by the selective enzymatic hydrolysis of one ester group catalyzed by a pig liver esterase. Optimization of the esterification step was performed, showing that the esterification of the *meso*-anhydride with methanol in the presence of thionyl chloride, instead of sulphuric acid, as the catalyst, was fully selective towards the *meso*-diester. Then, the reaction

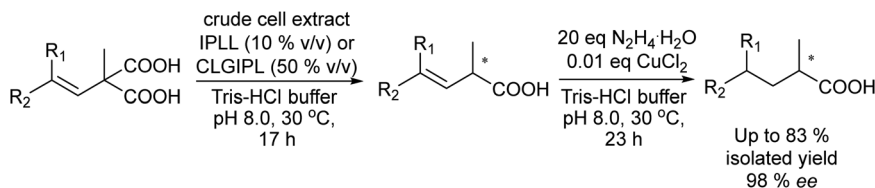
conditions were adjusted and esterase was added to perform the biocatalytic step (see Scheme 38). Under these conditions, the desired monoester was obtained in 84% yield (instead of 70% obtained using the classical procedure) and  $\geq 99.5\%$  ee. Several advantages are associated with the one-pot protocol, such as the use of the *meso*-anhydride as the starting reagent (cheaper than the diacid) and the overall yield improvement of the desired product, while the time-consuming workup steps and waste production can be reduced.

Enantiopure 2-methyl-substituted carboxylic acids are commonly used as pharmaceutical compounds, building blocks, flavors and fragrances.<sup>171,172</sup>

Recently, Kourist *et al.*<sup>173</sup> reported a chemo-enzymatic cascade synthesis to produce optically pure short-chain 2-methylalkanoic acids.<sup>171,172</sup> The chemo-enzymatic strategy combined the enzymatic asymmetric decarboxylation of methylvinylmalonic acid derivatives and the chemical reduction of the non-activated C=C double bond (Scheme 39). The decarboxylation step of methylvinylmalonic acid derivatives was performed using engineered arylmalonate decarboxylase (AMDase) variants IPLL and CLGIPL derived from *Bordetella bronchiseptica* as biocatalysts and tris-HCl buffer at 30 °C. After full substrate conversion into monoacids with high optical purities, the second step, the C=C double bond reduction, was performed through the *in situ* generated diimide. Diimide is a hydrogen donor that can selectively reduce non-activated unsaturated bonds by a concerted hydrogen transfer without producing racemization of the stereocenter. Due to its instability, the diimide has to be generated *in situ* from its precursor hydrazine by using an oxidation catalyst such a copper salt. The chemo-enzymatic sequential cascade using *R*- and *S*-selective AMDase variants produced



Scheme 38 Synthesis of (1*S*,2*R*)-2-(methoxycarbonyl)-4-cyclohexenecarboxylic acid through the classical and chemo-enzymatic processes.



Scheme 39 Synthesis of chiral 2-methyl substituted carboxylic acids from methylvinylmalonic acid derivatives by combining biodecarboxylation with C=C bond reduction.



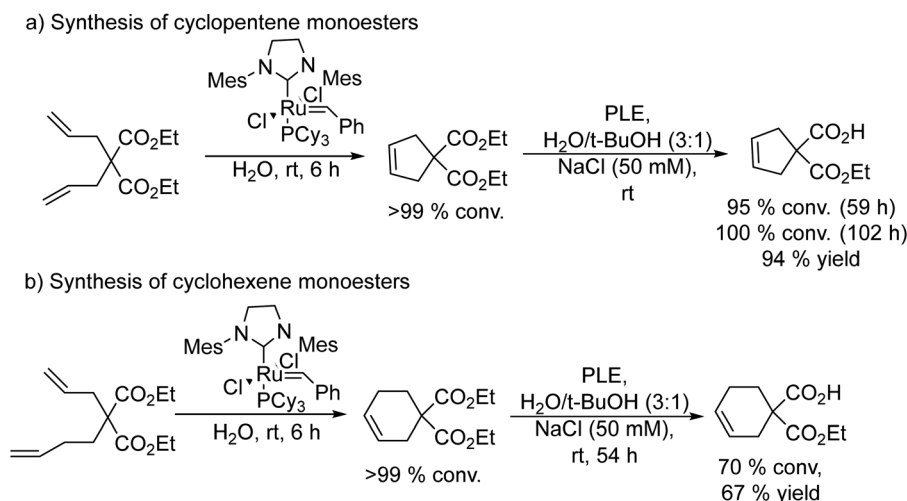
chiral short-chain 2-methylalkanoic acids in excellent yield and ee (up to 83% isolated yield and 98% ee).

This strategy represents an important advancement compared to the conventional methods to prepare these challenging compounds, which is mainly based on kinetic resolutions (inherently limited to 50% maximum yield) or asymmetric hydrogenation of  $\alpha,\beta$ -carboxylic acids, leading to moderate enantioselectivities and lower yields.<sup>174,175</sup> Interesting chemo-enzymatic processes performed by combining C–C bond forming reactions with enzymes have also been reported for the synthesis of carboxylic acids. Thus, Gröger *et al.*<sup>176</sup> reported a new synthetic process for the preparation of cyclic malonic acid monoesters, which are of interest as intermediates for the preparation of non-natural amino acids bearing a quaternary carbon center. The authors combined a metathesis reaction of unsaturated malonic acid ester derivatives with ester hydrolysis catalyzed by esterases in a cascade process in a sequential mode. Commercially available Ru carbene Grubbs' II metathesis catalyst, which is able to act efficiently in water,<sup>177</sup> was selected for the first step. For instance, excellent conversion of the substrate diethyl 2,2-diallylmalonate into the corresponding cyclopentene diester derivative was obtained under optimized reaction conditions in aqueous media (see Scheme 40). After completion of the metathesis step, the pig liver esterase (PLE) enzyme was added to the reaction media. Interestingly, it was found that

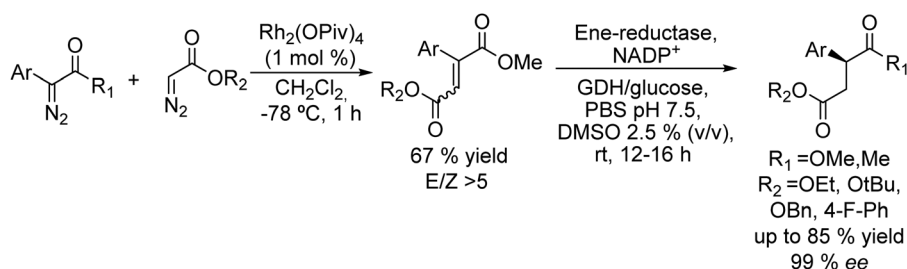
the enzyme was compatible with the metal catalyst, and the enzymatic hydrolysis proceeds with high conversion. However, the selectivity towards the desired monoester was moderate due to the subsequent decarboxylation of the monoester formed. Optimization of the solvent composition for the enzymatic step (*i.e.* using a mixture of water and *t*-butanol) allowed the suppression of the decarboxylation process, achieving high selectivity towards the monoester. The process was also successfully applied to the synthesis of cyclohexene monoester derivatives (see Scheme 40b).

The process constitutes an interesting straight-forward route to access these types of compounds, avoiding the conventional, multistep and low-selective route starting from dihalogenate alkenes and malonic acids.

Chiral unsymmetrical diesters such as 2-substituted succinate derivatives are important intermediates<sup>178–181</sup> in the synthesis of biologically active compounds such as  $\gamma$ -butyrolactone derivatives.<sup>182,183</sup> Zhao *et al.*<sup>184</sup> developed a one-pot chemo-enzymatic procedure in a sequential fashion to prepare chiral 2-substituted succinate derivatives. The process comprises rhodium-catalyzed heterocoupling of two diazoesters, which provides the alkene derivative, which is subsequently reduced by an ene-reductase (ER), which occurs with up to 99% enantiomeric excess (Scheme 41).



**Scheme 40** Synthesis of cyclic malonic acid monoesters from unsaturated malonic acid ester derivatives by combining a metathesis reaction with enzymatic hydrolysis.



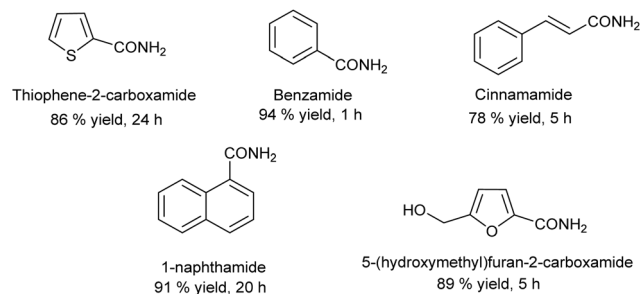
**Scheme 41** Synthesis of chiral 2-aryl substituted succinate derivatives from diazoesters by combining a diazocoupling reaction and bioreduction.



The authors selected dirhodium(II) tetrakis(pivaloate)  $[\text{Rh}_2(\text{O-Piv})_4]$  as the catalyst for the diazo coupling of aryldiazo compounds with diazoacetate derivatives, due to its demonstrated high chemo- and stereoselective activity for diazo coupling reactions,<sup>185</sup> promoting preferentially the formation of the *E*-alkene. On the other hand, ene-reductases (ERs) have been shown to be efficient and cost-effective catalysts for the enantioselective reduction of 2-substituted fumaric acid derivatives.<sup>186</sup> ERs containing flavin mononucleotides (FMN) require NADPH or NADH as a co-factor to catalyze asymmetric reduction. Interestingly, the enzymatic process only promotes the enantioselective reduction of (*E*)-2-aryl-substituted dicarbonyl alkenes among a mixture of the *E* and *Z* isomers, while occurring efficiently in the presence of the Rh-complex catalyst, being possible to couple both steps in one-pot. Thus, the diazo coupling step was carried out in the presence of  $[\text{Rh}_2(\text{OPiv})_4]$  at  $-78^\circ\text{C}$  using  $\text{CH}_2\text{Cl}_2$  as a solvent to give the corresponding *E,Z*-alkene. Then, after removing  $\text{CH}_2\text{Cl}_2$ , the enzymatic system in a buffer solution using DMSO as a co-solvent was added to the reaction mixture and the reduction proceeded at room temperature. Under these conditions, excellent results for the corresponding chiral 2-aryl-substituted succinate derivatives (up to 85% isolated yield and 99% ee) were achieved. The success of the process in terms of high yield and enantioselectivity is attributed to the preferential production of the (*E*)-alkene in the diazo coupling step along with the selective reduction promoted by the ER of the (*E*)-alkene in a mixture of (*E*) and (*Z*) isomers. Thus, the process allows access to chiral 2-substituted succinate derivatives in higher yields and enantioselectivities than other synthesis methods based on organocatalytic and transition metal-catalyzed asymmetric hydrogenation of prochiral aryl-substituted fumaric (*E*) acid derivatives.<sup>187,188</sup>

## 2.7. Synthesis of amides

Amides represent another class of important scaffolds in organic synthesis, and a variety of structurally different amides can be obtained through chemo-enzymatic processes. For instance, the preparation of primary amines from aldehydes was reported by Sugai *et al.*<sup>189</sup> (Scheme 42). In this process the authors combine in a sequential mode the conversion of aldehydes into nitriles following Fang's procedure<sup>190</sup> using  $\text{NH}_3$  (aq),  $\text{I}_2$  and DMSO as a solvent (step (i), Scheme 42) with biological action to hydrate the intermediate nitrile (step (ii), Scheme 42) catalyzed by whole cells of *Rhodococcus rhodochrous* IFO 15564. It is interesting to notice that the biocatalyst used possesses two different activities, the nitrile hydratase that catalyzes the hydration of nitriles into the corresponding amides and amidase that catalyzes the hydrolysis of amides into carboxylic acids. The authors showed that by using DMSO

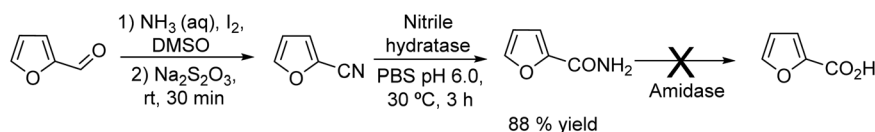


Scheme 43 Carboxamides obtained through the chemo-enzymatic process.

as solvent the amidase activity could be suppressed. Then, a variety of primary amides were obtained in excellent yields starting from the corresponding aldehydes (see Scheme 43) through a one-pot process involving 3 steps: (1) chemical reaction using Fang's procedure in DMSO; (2) neutralization of the excess of  $\text{I}_2$  by adding  $\text{Na}_2\text{S}_2\text{O}_3$  and adjusting to pH 8 and (3) adding the whole cells of harvested cells of *Rhodococcus* bacteria in phosphate buffer.

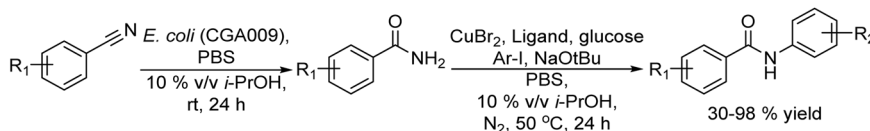
Very recently, Micklefield *et al.*<sup>161</sup> have developed a chemo-enzymatic method for the synthesis of amides starting from nitriles. The process involves as a first step the hydration of nitriles catalyzed by a nitrile hydratase followed by an Ullmann-type *N*-arylation with aryl iodide catalyzed by copper using *trans-N,N'*-dimethylcyclohexane-1,2-diamine as the ligand (Scheme 44).

The authors explored a wide range of reaction conditions and several parameters were optimized such as the enzyme, the form that the enzyme should be present (purified or directly inside the cells), ligand, temperature, amount of catalyst, *etc.* Under optimized reaction conditions (see Scheme 44) and working in a sequential mode in aqueous buffer supplemented with isopropanol, a variety of aromatic, heterocyclic and aliphatic amides (more than 50 examples), including drug molecules such as periciazine and probenecid, were obtained in good yields. Moreover, the authors showed that the integrated reactions are easily scalable, and the addition of a surfactant (TPGS-750-M), which provides micellar organo-compartments for the chemocatalyzed step, significantly increases the productivity of the process at very high substrate concentrations (up to 1200 mM), which are beyond of the scope of the enzyme. Compared with conventional amide synthesis, this integrated one-pot hydration/arylation cascade presents important advantages such as improvements in space-time yields, does not require protecting groups and circumvents harmful reagents.  $\beta$ -Hydroxyamides are an essential class of compounds in organic synthesis, specifically useful for the preparation of a variety of



Scheme 42 Synthesis of furan-2-carboxamide from furfural by combining the generation of a cyano group with biocatalyzed hydration.

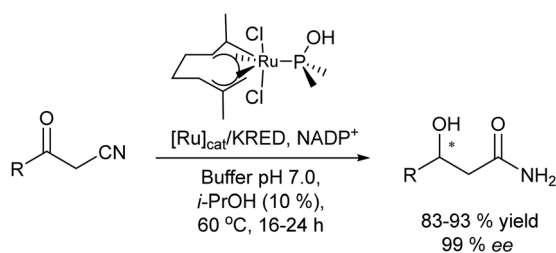




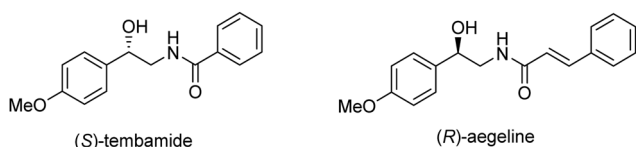
Scheme 44 Synthesis of amides by combining biocatalyzed hydration of nitriles with Ullman type arylation.

heterocycles such as oxazolidinones, azetidines, 1,4-diazepanes, or  $\beta$ -lactams,<sup>191</sup> and the access to these types of compounds is usually accomplished by hydration of the C $\equiv$ N bond of  $\beta$ -hydroxynitriles. The chemo-enzymatic synthesis of enantiopure  $\beta$ -hydroxyamides from  $\beta$ -ketonitriles was reported for the first time by González-Sabín *et al.*<sup>192</sup> through a hydration/bioreduction cascade process in aqueous medium occurring in a concurrent mode. The nitrile hydration performed using a commercially available Ru(IV) complex and the bioreduction of the keto group with a ketoreductase (KRED-P1-A0) took place simultaneously under mild reaction conditions, providing the corresponding (*R*)- $\beta$ -hydroxyamides in high yields and enantioselectivity (Scheme 45). The key to the success is attributed to the use of ruthenium(IV) catalysts, which exhibit higher compatibility with enzymes than ruthenium(II) complexes. Interestingly, the chemo-enzymatic process could be applied to prepare in very high yields the enantiopure alkaloids (*S*)-(+)-tembamide and (*R*)-(–)-aegeline through a simple synthetic sequence (Scheme 46). Interestingly, an alternative method to produce enantiopure  $\beta$ -hydroxyamides from  $\beta$ -ketonitriles is based on two-enzymatic steps catalyzed by a double enzymatic catalytic system composed of a ketoreductase (KRED) and a nitrile hydratase derived from whole cells of *R. rhodochrous*.<sup>193</sup> However, although the ee is very high (>99%) the final yield of the target compound is considerably lower than that achieved through the chemo-enzymatic process.

Cordova *et al.*<sup>194</sup> reported the integration of heterogeneous metal catalysis with heterogeneous enzymatic catalysis for the



Scheme 45 Synthesis of chiral  $\beta$ -hydroxyamides from  $\beta$ -ketonitriles in a concurrent mode by combining bioreduction with chemocatalyzed nitrile hydration.



Scheme 46 Enantiopure alkaloids obtained through the chemo-enzymatic process.

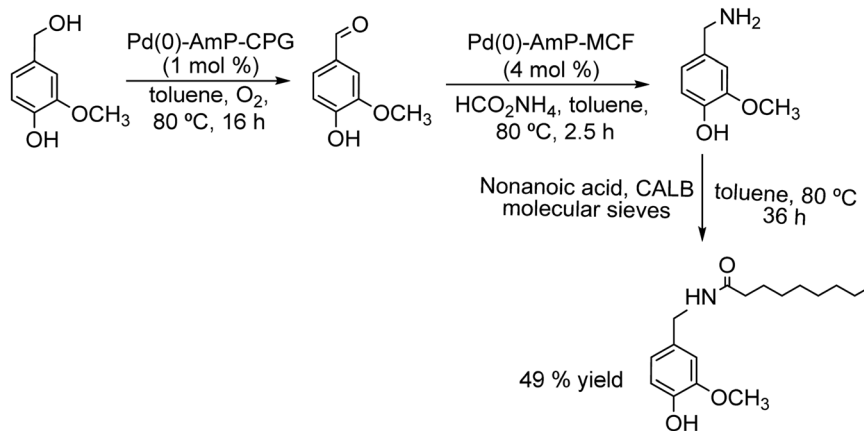
one-pot sequential synthesis of optically active and biologically important amines and amides (such as nonivamide and other capsaicinoid derivatives) starting from aldehydes, ketones or alcohols. An example of the chemo-enzymatic process for the synthesis of nonivamide (a food additive) is presented in Scheme 47. The process involves the Pd catalyzed oxidation of 4-(hydroxymethyl)-2-methoxyphenol into the aldehyde derivative followed by the reductive amination with ammonium formate affording a primary amine. In the last step, a lipase (CALB) catalyzes the coupling of the amine with the corresponding carboxylic acid into amide. Interestingly, all steps were performed in the same solvent (toluene) and at the same temperature (80 °C), taking advantage of the lipophilicity of the selected lipase. The authors developed two heterogeneous chemocatalysts based on Pd immobilized on aminopropyl-controlled pore glass (Pd<sup>0</sup>-AmP-CPG) and over aminopropyl-mesocellular foam (Pd<sup>0</sup>-AmP-MFC), which were highly selective for the alcohol oxidation and reductive amination respectively. Interestingly, the Pd catalyst accelerates the decomposition of formate/formic acid, which inhibits the catalytic activity of the lipase, offering the possibility to perform suitably the chemo-enzymatic process.

Combination of C–N bond forming reactions with enzymes to produce amides was reported by Reek *et al.*<sup>195</sup> The cascade process in a concurrent mode involves Pd catalyzed coupling between an aryl halide and an amine (Buchwald–Hartwig coupling) and lipase catalyzed amidation (Scheme 48).

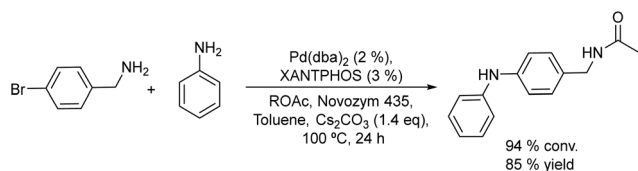
The authors showed that the amidation reaction of 4-bromobenzylamine with ethyl or methyl acetate as the acyl donor proceeded satisfactorily (100% conversion) using the resin bound lipase (Novozym 435<sup>®</sup>) as a catalyst in the presence of the reagents required for Pd-catalyzed coupling (Pd salts, phosphorus ligands, and Cs<sub>2</sub>CO<sub>3</sub> as a base) in toluene at 100 °C, giving the corresponding 4-bromobenzyl acetamide. Due to the robustness of the lipase under these reaction conditions, the cascade process could be optimized using different Pd ligands and acyl donors. It was found that using methyl acetate as the acyl donor and by performing the cascade process in a concurrent mode there was a synergistic effect between both catalytic processes, leading to higher performances than those achieved when the process was performed in separate steps. This behavior was explained by the presence of small amounts of CsOMe coming from the methanol released in the amidation step. The generation of the methoxide species, which are more basic and soluble in toluene than Cs<sub>2</sub>CO<sub>3</sub>, increases the amination rate, thus increasing the performance of the process.

Interestingly, the concept was extended to two other Pd-catalyzed coupling reactions such as the Suzuki–Miyaura (Scheme 49a) and Sonogashira (Scheme 49b) reactions. In both

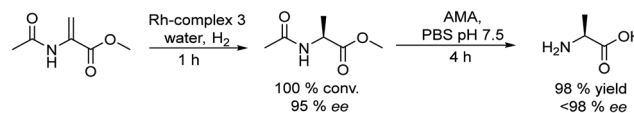




**Scheme 47** Synthesis of nonivamide by combining alcohol oxidation, reductive amination and bioamidation.



**Scheme 48** Synthesis of amides in a concurrent mode by combining a C–N bond forming reaction (Buchwald–Hartwig coupling) with bioamidation.



**Scheme 50** Synthesis of L-alanine from methyl 2-acetoamidoacrylate by combining organocatalyzed asymmetric hydrogenation with enzymatic hydrolysis.

cases the conversion of 4-bromobenzylamine was completed after 20 h, achieving high selectivity towards the final cascade products (70–89%).

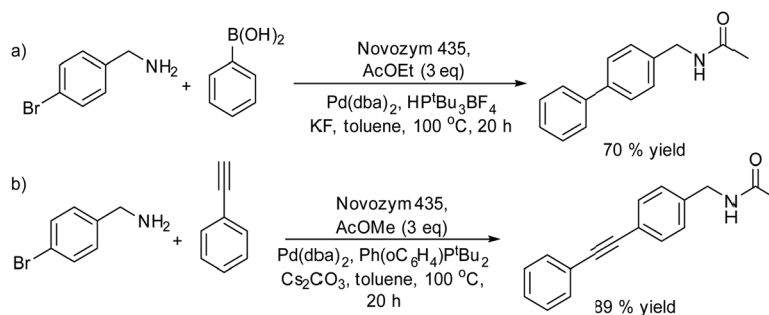
## 2.8. Synthesis of amino acids

The enantiopure amino acids (AAs) are useful intermediates in the synthesis of medicines, plant protection products and fine chemicals; for example, tryptophan is an essential chiral AA that plays a key role in the metabolic processes of the human body and can only be produced by microorganisms or plants.<sup>196,197</sup>

Enantiopure amino acids are generally produced using asymmetric reactions that produce high amounts of wastes. To overcome this drawback, Sheldon *et al.*<sup>198</sup> studied a chemo-enzymatic one-pot procedure taking as the model reaction the synthesis of

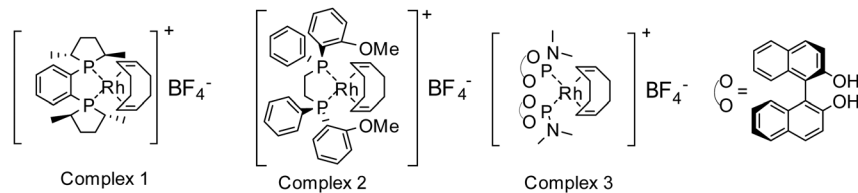
L-alanine, starting from methyl 2-acetamidoacrylate. The reaction involves the asymmetric hydrogenation of 2-acetamidoacrylate using an immobilised Rh-complex followed by hydrolysis of the chiral amidoester intermediate by using an aminoacylase (AMA) (Scheme 50).

The chemocatalyzed step was first optimized by testing different Rh-complexes anchored on a high area mesoporous aluminosilicate (ALTUD-1) under different reaction conditions and in different solvents. Results showed that the supported Rh-complex (3) (Scheme 51) was a very active, selective and stable chemocatalyst for the hydrogenation of 2-acetamidoacrylate in aqueous solution, achieving 100% conversion with 95% ee, after 1 h reaction time. The high stability against the leaching of the supported Rh-complex (3) in highly polar solvents such as water was attributed to the presence of more hydrophobic ligands compared with the Rh-complexes 1 and 2. For the biocatalyzed



**Scheme 49** Synthesis of amides by combining a Suzuki reaction (a) or a Sonogashira coupling reaction (b) with biocatalyzed amidation in a concurrent mode.



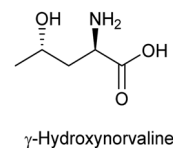


Scheme 51 Rh-complexes tested for reduction of methyl 2-acetamidoacrylate.

step two different acylases derived from *Aspergillus melleus* (AM) and the porcine kidney (PK) were selected. Both acylases are active for hydrolysing the amide group after the ester group is removed, since they require a terminal carboxylate group for binding with *N*-acyl-L-amino acids. Advantageously, both acylases were able to hydrolyse the ester group affording *N*-acetylalanine, which is subsequently converted into the desired L-alanine. In the chemo-enzymatic process, after hydrogenation completion, the acylase was added into a concentrated phosphate buffer solution and the reaction proceeded for 24 h. Interestingly, the acylase was highly active in the presence of the Rh-catalyst, while the presence of the chemocatalyst was detrimental for the PK acylase, and filtration of the chemocatalyst prior to the enzymatic process was required to maintain the enzyme activity. Additionally, the authors intended to perform the cascade process in a concurrent mode by adding all reactants and catalysts from the beginning; however, under these reaction conditions a strong inhibition of the process was observed mainly attributed to the detrimental influence of the buffer on the hydrogenation step and the adsorption of the enzyme on the chemocatalyst.

## 2.9. Synthesis of heterocyclic compounds

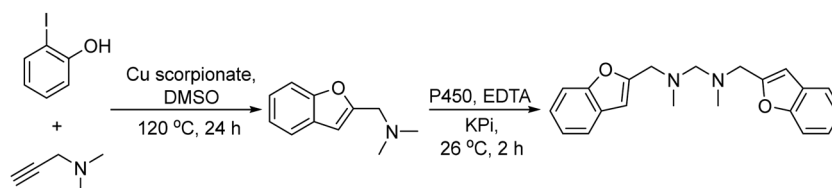
**2.9.1. Synthesis of benzofuran derivatives.** Benzofuran derivatives are pharmacologically active compounds, and particularly 2-substituted benzofurans with a secondary amine are intermediates for the synthesis of pharmaceuticals used in the treatment of infections caused by antimicrobial resistant bacteria (*e.g.* staphylococci).<sup>199</sup> General synthetic methods of 2-substituted benzofurans are based on the condensation reactions between ketones (or aldehydes) and a variety of different nucleophiles, under strong acidic or basic conditions that lead to limited yields of the target compound.<sup>200</sup> Therefore, chemo-enzymatic processes can be an interesting alternative for the synthesis of these compounds. As an example, Schwaneberg *et al.*<sup>201</sup> reported the synthesis of methylene-bridged bis(2-substituted benzofuran) through a one-pot sequential cascade reaction. In the first step, a palladium-free Sonogashira coupling between iodophenol and 3-dimethylamino-1-propyne

Scheme 53  $\gamma$ -Hydroxynorvaline.

catalyzed by the Cu complex, Cu-scorpionate, gives the benzofuran intermediate. In the subsequent step, after completion of the Sonogashira coupling, the monooxygenase P450 BM3 variant (A74S-F87V-L188Q) in phosphate buffer was added to reaction media and the formed 2-substituted benzofuran is hydroxylated and undergoes further formaldehyde elimination. The inhibitory effect of the remaining Cu catalyst on the enzymatic transformation was circumvented by the addition of EDTA, and an 84% yield of the target compound was obtained in 26 h (Scheme 52).

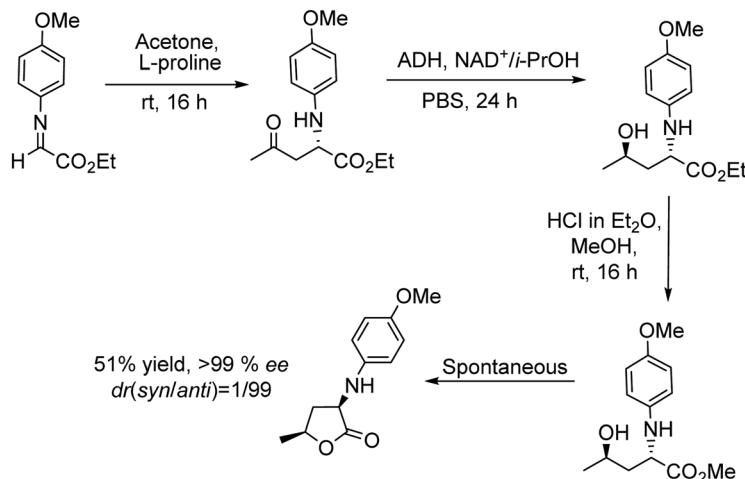
**2.9.2. Synthesis of chiral  $\alpha$ -amino- $\gamma$ -butyrolactones.** Chiral  $\alpha$ -amino- $\gamma$ -butyrolactones are common structural scaffolds in a variety of pharmaceuticals and natural products that display diverse biological activities. Moreover, the amino acid  $\gamma$ -hydroxynorvaline (Scheme 53), an open conformation structure, is an interesting compound that displays antidiabetic activity.<sup>202,203</sup>

Stereoselective syntheses of  $\alpha$ -amino- $\gamma$ -butyrolactones are mainly based on chemo-catalyzed processes,<sup>204</sup> which require auxiliary-assisted multiple steps and allow access to only one or two of four possible stereoisomers.<sup>205,206</sup> Faber *et al.*<sup>207</sup> developed a protocol that allows access to the four possible  $\gamma$ -butyrolactone diastereoisomers by sequential construction of the stereogenic centers. This was accomplished by combining an asymmetric Mannich-type reaction catalyzed by (*b*), or (*l*)-proline followed by a stereoselective biocatalytic reduction with (*S*, *R*) ADH (see Scheme 54). For instance, in the synthesis of the  $\alpha$ -amino- $\gamma$ -butyrolactone precursor of  $\gamma$ -hydroxynorvaline, the process involves as the first step the reaction between ethyl 2-oxoetanoate and 4-methoxyaniline to give the corresponding 4-methoxyphenyl (PMP) aldimine. The PMP-protected aldimine



Scheme 52 Synthesis of bis(2-substituted benzofuran) derivatives by combining Sonogashira coupling with bio oxidation.





**Scheme 54** Synthesis of the  $\alpha$ -amino- $\gamma$ -butyrolactone precursor of  $\gamma$ -hydroxynorvaline by combining an organocatalyzed asymmetric Mannich reaction with subsequent transesterification and bioreduction.

reacts with acetone (used also as a solvent) through a Mannich type reaction catalysed by (L)-proline giving the corresponding (S)-aminoketoester (ethyl (S)-2-amino-PMP-4-oxo-pentanoate) with 99% conversion and in optically pure form (ee 99%). After evaporation of acetone, the crude product was dissolved in buffer solution (PBS) and reduced by (S)-ADH in the presence of the co-factor  $\text{NAD}^+$  and isopropanol as the co-factor regenerating agent, giving the ethyl (2S,4R)-4-hydroxy-2-aminoester. Spontaneous lactonization of this compound was not complete, and in order to achieve the total lactonization of the 4-hydroxy-2-aminoester its transesterification with methanol was required. After this, the diastereomerically pure (3R,5S) amino lactone was obtained in 51% yield with an excellent diastereoselective yield (a dr of 99:1). Starting from this protected  $\gamma$ -butyrolactone, the  $\gamma$ -hydroxynorvaline was obtained in 58% yield after deprotection and lactone ring-opening (Scheme 54).

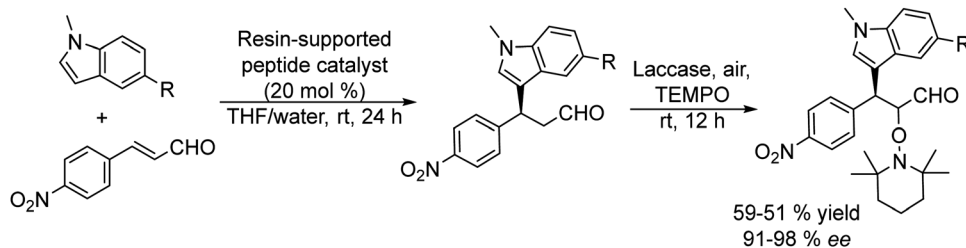
**2.9.3. Synthesis of chiral oxy-functionalized indole derivatives.** Indole derivatives represent an important class of biologically active compounds, and particularly, indoles with an oxygenated stereogenic carbon at the  $\beta$ -position of the ring, such as indolmycin<sup>208,209</sup> and diolmycin,<sup>210</sup> have attracted interest due to their antibiotic activity.

The framework of chiral oxy-functionalized indole derivatives can be built through the asymmetric Friedel-Crafts type conjugate addition of  $\alpha,\beta$ -unsaturated aldehydes to an indole followed by oxygenation at the  $\alpha$ -position of the carbonyl group. The synthesis

is usually performed through two separate steps, resulting in limited yields and enantioselectivities and generation of a high amount of wastes. To overcome these drawbacks Kudo *et al.*<sup>211</sup> developed for the first time the synthesis of oxy-functionalized indole derivatives through a one-pot chemo-enzymatic process. They combined the asymmetric Friedel-Crafts type alkylation of the indole with the bio-oxyamination at the  $\alpha$ -position of the aldehyde group of the adduct intermediate. The asymmetric Friedel-Crafts type reaction is performed using a resin supported peptide as a catalyst affording the chiral aldehyde intermediate (see Scheme 55). In the second step, the laccase enzyme was added for the  $\alpha$ -oxyamination with TEMPO ((2,2,6,6-tetramethylpiperidin-1-yl)oxyl). Both steps proceeded smoothly in aqueous media at room temperature and could be applied to the synthesis of several substituted indoles and pyrroles with high enantioselectivities.

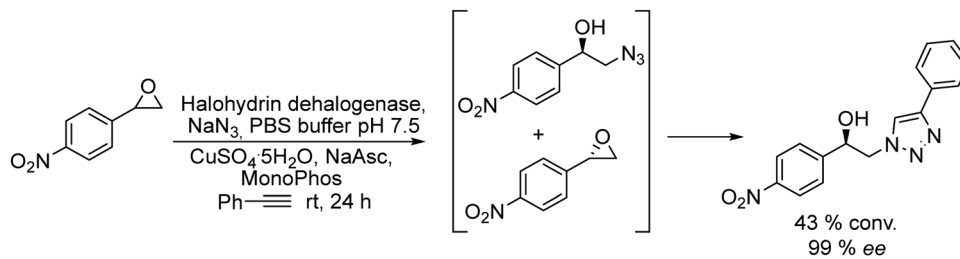
**2.9.4. Synthesis of 1,2,3-triazole derivatives.** The 1,3-dipolar cycloaddition of azides and alkynes to form 1,4-disubstituted triazole derivatives catalyzed by copper is considered as an important achievement in the 'click' chemistry finding applications in the drug discovery area, polymer chemistry and biological sciences, amongst others.<sup>212-220</sup> The optically pure triazoles are of particular interest as promising pharmacophores,  $\beta$ -adrenergic receptor blocker analogues and potential imaging agents.<sup>221</sup>

Chiral hydroxy triazoles have been synthesized by Feringa *et al.*<sup>222</sup> using a smart one-pot chemo-enzymatic process performed in a concurrent mode, where all additives and catalysts



**Scheme 55** Synthesis of chiral oxy-functionalized indole derivatives by combining symmetric Friedel-Crafts-type alkylation and bio- $\alpha$ -oxyamination.

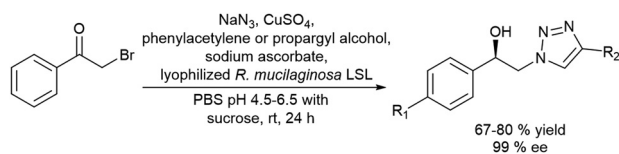




**Scheme 56** Synthesis of chiral  $\beta$ -hydroxytriazoles from aryl epoxides in a concurrent mode by combining enzymatic azidolysis with [3+2] cycloaddition of alkynes.

were added at the beginning of the reaction. The process involves as the first step the enantioselective azidolysis of aromatic epoxides to 1,2 azidoalcohols catalyzed by the enzyme halohydrin dehalogenase (developed by the authors)<sup>223</sup> followed by the [3+2] cycloaddition of the hydroxyazide intermediate to alkynes catalyzed by copper salts (Scheme 56). To develop the process in a concurrent mode the compatibility of the different additives required in both steps was thoroughly investigated. It was shown that the selectivity of the enzyme was preserved in the presence of the different additives required for the click reaction ( $\text{CuSO}_4$ , the reducing agent sodium ascorbate and the MonoPhos ligand), and the chemo-enzymatic process could be performed successfully under optimized conditions. For instance, 2-(4-nitrophenyl)oxirane was 43% converted after 24 h at room temperature into the corresponding triazole with 99% ee, along with the remaining epoxide with 75% ee (Scheme 56). However, the authors showed that the concentration of substrate and the structures of the epoxide and alkyne have a strong influence on the enzyme activity and selectivity.

Better results in the synthesis of chiral  $\beta$ -hydroxytriazoles through a different chemo-enzymatic cascade were achieved by Orden and coworkers.<sup>224</sup> In this case, the authors started from  $\alpha$ -haloketones, which underwent azidation and subsequent copper-catalyzed azide-alkyne cycloaddition with acetylene derivatives giving the corresponding  $\beta$ -ketotriazoles that are enantioselectively reduced by *Rhodotorula mucilaginosa* cells into the corresponding (*R*)- $\beta$ -hydroxytriazole (Scheme 57). The authors showed that starting from  $\alpha$ -chloroacetophenones, and working in a sequential mode, the isolated yields of (*R*)- $\beta$ -hydroxytriazoles were 55–65%. However, in a concurrent mode a competitive bioreduction of the starting  $\alpha$ -chloroacetophenone into the corresponding chlorohydrine was observed leading to low conversion of the target product. To overcome this drawback,  $\alpha$ -bromoketones, which are not prone to be



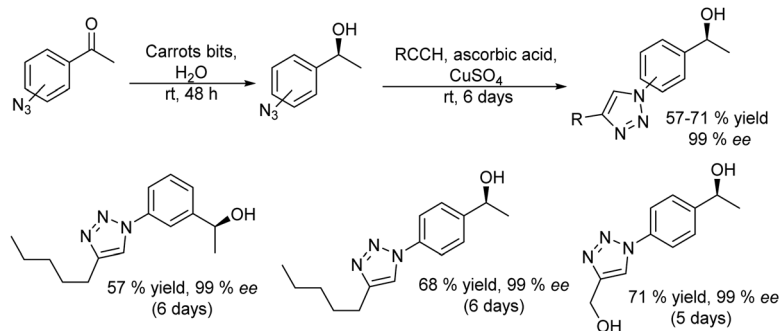
**Scheme 57** Synthesis of chiral  $\beta$ -hydroxytriazoles in a concurrent mode from  $\alpha$ -haloketones by combining azidation and subsequent copper-catalyzed azide-alkyne cycloaddition followed by bioreduction.

bioreduced into the bromohydrine, were selected as starting reagents. Thus, the cascade process could be effectively accomplished in a concurrent mode, achieving 67–80% isolated yields of the (*R*)- $\beta$ -hydroxytriazole derivatives. The fast and complete replacement of the bromine by the azide and the low capability of the enzyme to reduce bromoketones and azidoketones giving undesired products were the main factors responsible for the high yields of (*R*)- $\beta$ -hydroxytriazoles achieved.

Structurally different chiral hydroxytriazoles were synthesized by Omori *et al.*<sup>225</sup> following a chemo-enzymatic process in a sequential mode. In this case, the cascade process involves as the first step the enantioselective reduction of azidoacetophenone into the enantiomerically pure azidoalcohol intermediate that is subsequently coupled with alkynes through a click reaction catalyzed by copper salts. The authors performed the enantioselective reduction of azidoacetophenone using carrot bits as a biocatalyst, whose activity is attributed to the endophytic microorganism (*Daucus carota*) existing in the carrot roots and that previously had shown high levels of enantioselectivity for reducing a variety of prochiral ketones.<sup>225</sup> Thus, the reduction of azidoacetophenone was coupled with the click reaction using a variety of alkynes giving the target triazoles in moderate yields with an ee >99%; however, long reaction times were required (Scheme 58).

**2.9.5. Synthesis of iminocyclitols (polyhydroxylated pyrrolidines and piperidines).** The polyhydroxylated piperidines and pyrrolidines, known as iminocyclitols (Scheme 59), are strong glycosyltransferase and glycosidase inhibitors, owing to their resemblance of the transition state of the enzymatic reactions. Therefore, iminocyclitols are attractive as drug candidates for a number of diseases such as cancer, viral infections, lysosomal storage disorders, and diabetes.<sup>226–228</sup> Aldolases catalyze the reversible formation of C–C bonds with high enantioselectivities, providing rapid access to multiple scaffolds such as those leading to iminocyclitols.<sup>229</sup> In fact, most of the reported methods for the synthesis of iminocyclitols are based on chemo-enzymatic synthesis starting from dihydroxyacetone phosphate (DHAP) and using (DHAP)-dependent aldolases that catalyze the addition of DHAP to acceptor aldehydes containing azide groups. After removal of the phosphate group with phosphatase, reduction of the azide and subsequent intramolecular reductive amination give the iminocyclitol.<sup>230,231</sup> However, the necessity of a phosphatase to remove the phosphate ester intermediate and the impossibility to use





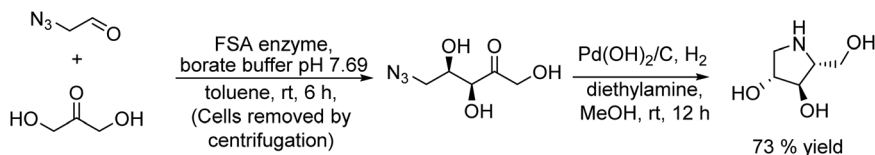
**Scheme 58** Synthesis of chiral hydroxytriazoles from azidoacetophenone by combining bioreduction with a click reaction.

nonphosphorylated dihydroxyacetone (DHA) make the process of limited applicability. To overcome these limitations, a highly improved chemo-enzymatic method for the synthesis of iminocyclitols was developed by Wong *et al.*<sup>232</sup> The authors selected fructose-6-phosphatealdolase (FSA) derived from *Escherichia coli*, due to its broad tolerance to donor and acceptor substrates, for the aldol condensation between dihydroxyacetone and azidoaldehyde derivatives and it was combined with reductive amination with a Pd supported catalyst in a sequential mode. As an example, the iminocyclitol, 1,4-dideoxy-1,4-imino-D-arabitol (Scheme 59), was obtained by reacting azidoacetaldehyde and dihydroxyacetone in the presence of FSA in a buffer solution giving the corresponding chiral aldol adduct intermediate. Then, after removing the cells, the Pd catalyst and the required additives in methanol as a solvent were added to the reaction media and pressurized with H<sub>2</sub>. After the reductive amination, the target iminocyclitol was obtained in 73% yield at room temperature after 12 h. The strategy was efficiently applied to the synthesis of different aminosugars in yields between 72 and 83%.

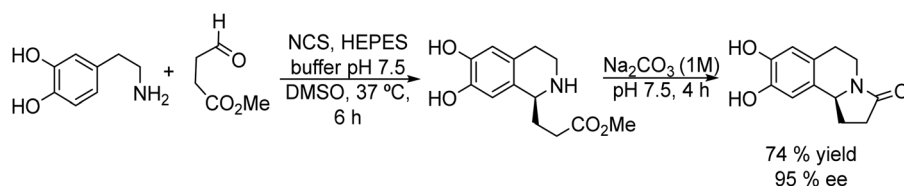
**2.9.6. Synthesis of tetrahydroisoquinoline and 2-quinolone derivatives.** Biocatalysts able to facilitate C–C bond formation are useful for the synthesis of products with pharmacological activities. For instance, the enzyme norcochlorine synthase

(NCS) is of significant interest for the synthesis of tetrahydroisoquinoline alkaloids (THIQs). These compounds are a large group of secondary metabolites with a variety of pharmacological activities including morphine (analgesic), magnoflorine (anti-hypertensive), and leucosine (anti-mycobacterial).<sup>233–235</sup> For instance, the alkaloid (*S*)-trolline, isolated from the flowers of *Trollius chinensis*, has shown antiviral and antibacterial activities against *Staphylococcus aureus*. However, the reported asymmetric chemical synthesis to obtain (*S*)-trolline is based on multistep asymmetric strategies needing the use of strong bases and toxic solvents and achieving limited yields (44–41%).<sup>236,237</sup>

Norcochlorine synthase (NCS) catalyzes the Pictet–Spengler reaction between 3-hydroxyphenethylamines (*e.g.* dopamine) and a carbonyl compound to form (1*S*)-THIQs with high stereoselectivity. Moreover, the enzyme has shown a remarkably wide carbonyl compound tolerance, accepting a variety of aldehydes and ketones.<sup>238,239</sup> Hailes *et al.*<sup>240</sup> developed a sustainable asymmetric route to produce tetrahydroisoquinoline alkaloids through a one-pot chemo-enzymatic process in a sequential mode, using the enzyme norcochlorine synthase (NCS), followed by a cyclisation process, to obtain alkaloids with two new heterocyclic rings (Scheme 60). The process combines the Pictet–Spengler reaction that involves a Schiff reaction between a linear methyl carboxylate bearing



**Scheme 59** Synthesis of iminocyclitols from azidoaldehyde derivatives and dihydroxyacetone by combining biocatalyzed aldol condensation with reductive amination.



**Scheme 60** Synthesis of the alkaloid *S*-trolline from dopamine by combining a biocatalyzed Pictet–Spengler reaction and cyclization.

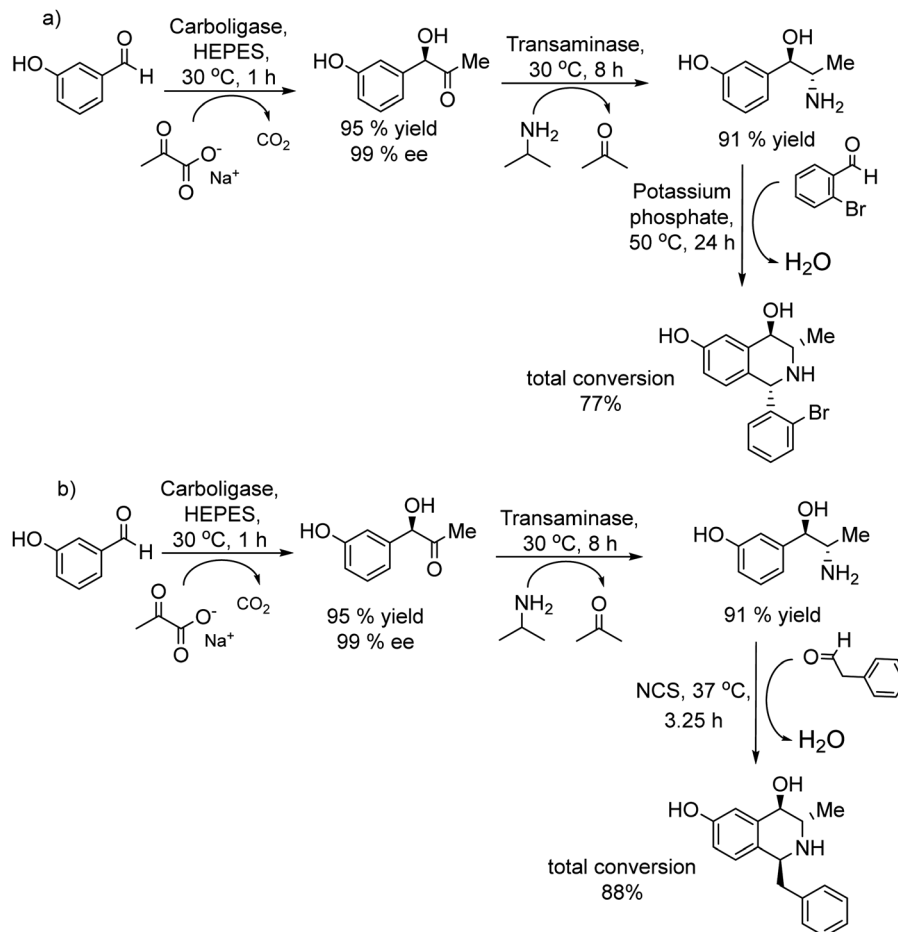


an aldehyde group and the amine group of the dopamine, followed by a Mannich-type reaction and an electrophilic aromatic substitution giving a tetrahydroisoquinoline intermediate, which after addition of  $\text{Na}_2\text{CO}_3$  is cyclized to the target compound. The authors showed that starting from dopamine and methyl 4-oxobutanoate, 74% yield and ee = 95% for (*S*)-trolline could be obtained in the chemo-enzymatic process. Moreover, the process was successfully extended to other dopamine derivatives and aldehyde derivatives with different chain lengths giving the corresponding THIQs.

Also, complex 1,3,4-trisubstituted tetrahydroisoquinolines (THIQs) with three chiral centers were synthesized in a selective manner without intermediate purification by Rother *et al.*<sup>241</sup> through a chemo-enzymatic sequential process in the aqueous phase. These compounds are interesting for the pharmaceutical industry due to the wide scope of activities, such as antitumoral,<sup>242</sup> antiparasitic,<sup>243</sup> and anticholinergic<sup>244</sup> properties. The cascade process involves two biocatalyzed steps combined with a chemocatalyzed path. In the first step the carboligation between 3-hydroxybenzaldehyde and sodium pyruvate in a buffer system was performed using the carboligase EcaHAS-1 derived from *Escherichia coli* (produced by the authors) as a biocatalyst (Scheme 61a). The produced chiral  $\alpha$ -hydroxy ketone intermediate was subjected in the second step to a transamination process with

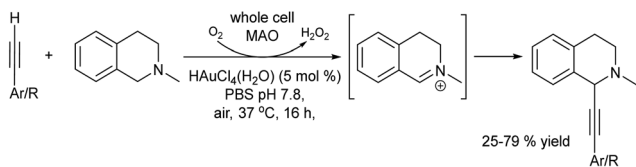
a transaminase (CV2025) (using isopropylamine as the amine donor and PLP as the enzyme co-factor) yielding 3-((1*R*,2*S*)-2-amino-1-hydroxypropyl)phenol. Then, after removing the enzymes by ultrafiltration, the 3-((1*R*,2*S*)-2-amino-1-hydroxypropyl)phenol is reacted with 2-Br-benzaldehyde through a chemocatalyzed Pictet–Spengler reaction catalyzed by potassium phosphate, yielding the 1,3,4-trisubstituted tetrahydroisoquinoline derivative with three chiral centers. To show the stereoselectivity of the phosphate-catalyzed Pictet–Spengler reaction, different aldehydes were screened, giving the corresponding chiral THIQs with variable success. Interestingly, when the Pictet–Spengler reaction step was performed using norcoclaurine synthase (NCS), instead of potassium phosphate, the THIQs obtained resulted in opposite stereoselectivities at the C1 position, providing access to both possible orientations of the C1 substituent of the THIQs (Scheme 61b).

An interesting chemo-enzymatic process giving access to C-1 alkynyl substituted *N*-alkyltetrahydroisoquinolines was developed by Turner *et al.*<sup>245</sup> by integrating in a concurrent mode biocatalytic oxidation of the *N*-alkyltetrahydroisoquinolines with gold catalyzed C–C coupling with acetylene derivatives in phosphate buffer. In this process, the enzyme monoamine oxidase (MAO) oxidizes the tetrahydroisoquinoline derivative, which



**Scheme 61** Synthesis of 1,3,4-trisubstituted tetrahydroisoquinolines (THIQs) with three chiral centers: (a) chemo-enzymatic and (b) three step biocatalyzed cascade.





**Scheme 62** Synthesis of alkynyl substituted tetrahydroisoquinoline from tetraisoquinolines and alkynes by combining biocatalytic oxidation and coupling with alkynes.

subsequently couples with the alkyne. Under optimized reaction conditions, a variety of alkynyl substituted tetrahydroisoquinoline derivatives were obtained in variable yields under very mild reaction conditions in aqueous media (Scheme 62).

Compared with multistep asymmetric strategies to synthesize THIQs, where lower yields are obtained and strong bases and toxic solvents are required,<sup>237,246,247</sup> the chemo-enzymatic processes described above represent much more efficient, sustainable and rapid routes to achieve these important compounds.

Other related important scaffolds present in many drugs are 2-quinolones. The challenge in the conventional synthetic methods of these N-heterocycles is their functionalization due to low reactivity of their  $\pi$ -electron deficient skeleton.<sup>248</sup> Recently, Castagnolo *et al.*<sup>249</sup> have reported for the first time the synthesis of 2-quinolones through a chemo-enzymatic process in a sequential mode. The process uses *N*-cyclopropyl-*N*-alkylaniline derivatives as starting compounds that are transformed in the first step into quinolinium ions through a cyclation/aromatization sequence biocatalyzed by horseradish peroxidase (HRP). The quinolinium ions are further carbonylated into 2-quinolone derivatives using  $K_3Fe(CN)_6$  in the second step (Scheme 63). A variety of 2-quinolone derivatives could be obtained in good isolated yields.

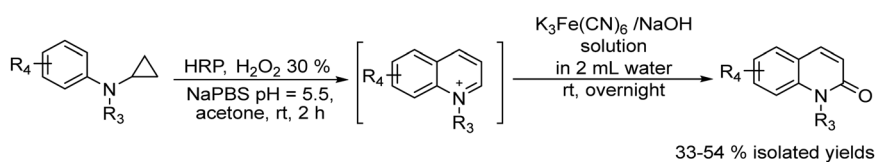
### 3. Chemo-enzymatic processes for biomass valorization

#### 3.1. Synthesis of HMF from glucose

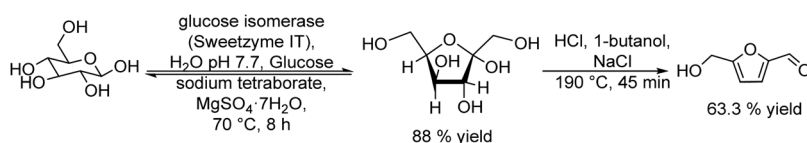
In the last few decades, the valorization of biomass resources into valuable chemicals has gained increased interest in

academic and industrial areas.<sup>250</sup> Chemo-enzymatic approaches have high potential to upgrade easily available and renewable bio-based compounds in a minimal number of steps in a selective and productive fashion. An interesting example of a chemo-enzymatic strategy for biomass valorization is the conversion of glucose into 5-hydroxymethylfurfural (HMF). This compound is a versatile platform molecule produced by dehydration of hexoses in acid media and can be converted into valuable derivatives such as 2,5-dimethylfuran (2,5-DMF), monomers like 2,5-furandicarboxylic acid (FDCA) and a variety of fine chemicals,<sup>251</sup> and biofuels.<sup>252–256</sup> The simplest and efficient way for producing HMF is by the acid-catalyzed dehydration of fructose. However, its production by isomerization of the most abundant and cheapest glucose is highly desired. However, the chemical or enzymatically catalyzed glucose–fructose isomerization is controlled by the thermodynamic equilibrium, which limits the conversion to almost isoquantities of both sugars. Therefore, a key issue in the synthesis of HMF from glucose is to shift the equilibrium from glucose to fructose. The strategy to shift the equilibrium towards the formation of fructose involves the use of sugar-complexing agents such as boronic acid derivatives, which exhibit higher affinity to fructose than to glucose allowing the shift of the equilibrium toward the fructose side.<sup>257</sup> Qi *et al.*<sup>258</sup> developed a sequential chemo-enzymatic process involving as the first step the borate-assisted isomerization of glucose into fructose catalyzed by a commercial immobilized glucose isomerase (Sweetzyme IT), which is a cross-linked enzyme with glutaraldehyde (CLEA) (Scheme 64). It was found that at a borate-to-glucose ratio of 0.5% the isomerization equilibrium of glucose to fructose shifted from 53% to 88% yield. After the isomerization step, the glucose isomerase was separated by vacuum filtration and the acid catalyst (HCl) and an organic solvent (1-butanol), along with NaCl to improve the partitioning of HMF into the organic phase, were added. The dehydration step of the resulting sugar mixtures was performed at 190 °C achieving 63.3% HMF yield.

Zhao *et al.*<sup>259</sup> combined a thermophilic glucose isomerase electrostatically immobilized on mesoporous silica functionalized with amino groups for glucose to fructose isomerization

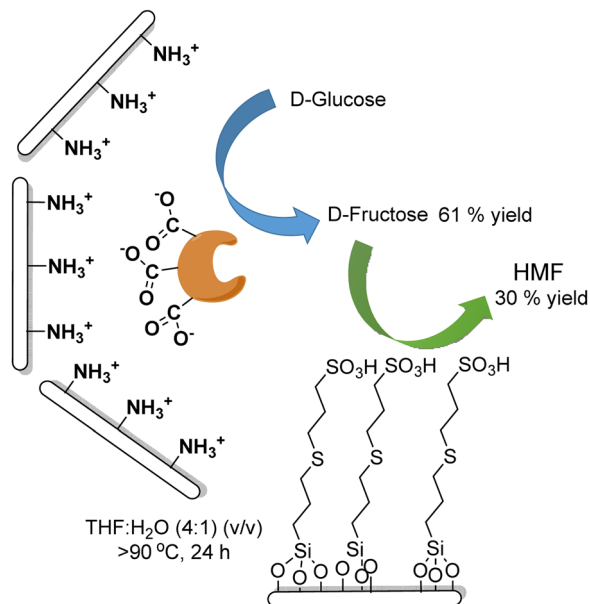


**Scheme 63** Synthesis of 2-quinolones starting from *N*-cyclopropyl-*N*-alkylaniline derivatives through a biocatalyzed cyclation/aromatization sequence followed by carbonylation.



**Scheme 64** Synthesis of HMF from glucose by combining biocatalyzed isomerization and chemical dehydration.





**Scheme 65** Biocatalyzed isomerization of glucose to fructose followed by chemical dehydration over heterogeneous catalysts to obtain HMF.

with mesoporous silica functionalized with sulfonic groups ( $-\text{SO}_3\text{H}$ ) for fructose dehydration (Scheme 65). A suitable monophasic reaction medium (THF:H<sub>2</sub>O) was chosen to accommodate both reactions in the tandem catalytic sequence in one pot using a combination of both heterogeneous catalysts under separately optimized conditions. Thus, by keeping the temperature first at 90 °C for 1 h the enzyme catalyzed glucose isomerization occurred, giving up to 61% fructose, and then the temperature was increased to 130 °C to accelerate fructose dehydration. Under these reaction conditions, 30% HMF with 64% of selectivity after 24 h was obtained. Unfortunately, the biocatalyst could not be recycled because of its short half-life ( $t_{1/2} = 15.8$  min) in the organic solvent. Moreover, it was observed that the efficiency of the tandem process is significantly limited by the large difference in rates for the two catalysts.

These chemo-enzymatic strategies allow access to HMF in moderate yields; however, it is interesting to notice that recently different heterogeneous chemocatalytic systems have been developed containing Lewis acid sites (for glucose isomerization) and Brønsted acid sites (for fructose dehydration) that allow obtaining HMF from glucose with similar HMF yields.<sup>260</sup> For instance, Davis *et al.*<sup>261</sup> combined HCl as the Brønsted acid and the Sn-beta catalyst bearing Lewis acid sites in a biphasic THF:water medium. The synergistic effects of this

catalytic system allowed obtaining 79% glucose conversion with 70% selectivity for HMF at 180 °C.

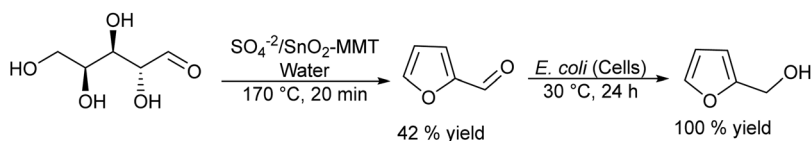
### 3.2. Synthesis of furfuryl alcohol and furfuryl amine from xylose

Furfuryl alcohol (FOL) is an important biomass derived alcohol used as an intermediate for the production of a variety of fine chemicals such as lysine amino acid, vitamin C, lubricants and fragrances.<sup>250,262–264</sup> Currently, FOL is produced at the industrial scale by liquid- or vapor-phase hydrogenation of furfural (FAL), which is obtained by the acid catalyzed dehydration of pentoses, such as xylose. However, for FAL hydrogenation, high pressure and/or noble metals along with high energy consumption are required.<sup>265,266</sup> Therefore bioreduction of FAL into FOL under mild reaction conditions represents an interesting alternative due to the product specificity and its high efficiency.<sup>267–269</sup> On the other hand, furfuryl amine (FLA) is an important platform molecule derived from furfural that is used for producing polymers, agrochemicals, additives, fragrances and pharmaceuticals.<sup>270–274</sup> Furfuryl amine is usually synthesized through the reductive amination of furfural with ammonia, using metal catalysts under harsh conditions.<sup>275,276</sup> Thus, bioamination of furfural represents an attractive alternative method to biosynthesize FLA under environmentally friendly reaction conditions.<sup>272</sup>

He *et al.* have performed extensive research on converting xylose and biomass-rich xylose into furfuryl alcohol and furfuryl amine through a sequential chemo-enzymatic process involving as a first step the acid catalyzed dehydration of xylose into furfural using tin-based heterogeneous catalysts. In the second step, bioreduction or bioamination is performed using recombinant *Escherichia coli* whole cells harboring reductase or  $\omega$ -transaminase.<sup>273,277–282</sup>

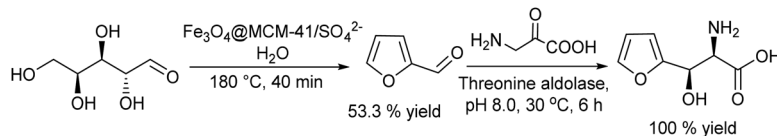
For instance, xylose dehydration was performed using an optimized heterogeneous acid catalyst based on a modified montmorillonite ( $\text{SO}_4^{2-}/\text{SnO}_2\text{-MMT}$ ), using water as a solvent at 170 °C, achieving 42% yield of furfural. After this, temperature was decreased to 30 °C, the recombinant *Escherichia coli* CCZU-K14 whole cells harboring a NADH-dependent reductase were added to the reaction media, pH was adjusted and the required co-factor (glucose) regenerating agent was added. The biocatalytic step yielded 100% FOL after 24 h reaction time (Scheme 66).<sup>278</sup>

The same chemo-enzymatic process was also performed using  $\text{SO}_4^{2-}/\text{SnO}_2\text{-attapulgite}$  as the acid catalyst for the dehydration of xylose-rich hydrolysate into furfural, while the recombinant *Escherichia coli* CCZU-A13 harboring a NADH-dependent reductase immobilized on carrageenan was used for the bioreduction to furfuryl alcohol. Similar results for the furfuryl alcohol production were obtained, but in this case the



**Scheme 66** Synthesis of furfuryl alcohol from xylose by combining chemical dehydration with bioreduction.





Scheme 67 Synthesis of  $\beta$ -(2-furyl) serine from xylose by combining dehydration with biocatalyzed aldol condensation.

carrageenan immobilized whole-cells and solid acid catalyst could be recycled up to 5 runs, retaining their activity.<sup>280</sup> More recently, and following the same protocol, the authors reported the direct conversion of the raw bamboo shoot shell and corncob into furfuryl alcohol or furfuryl amine.<sup>273,281,282</sup> In all cases, although the furfural yield (40–50% yield) was dependent on the type of solid tin-catalyst and the starting raw material, the selectivity towards the target product was 100%.

### 3.3. Synthesis of furan amino acid derivatives

**3.3.1. Synthesis of furan  $\alpha$ -amino acids from xylose.** Optically active noncanonical amino acids are of great interest as intermediates in pharmaceutical products, fine chemistry and food additives due to their various biological activities.<sup>283,284</sup> For instance,  $\beta$ -(2-furyl) serine, a heterocyclic  $\beta$ -hydroxy- $\alpha$ -amino acid, is a high added-value compound since it is a component of furan antibiotic derivatives as well as a precursor of the fine chemical 2-amino-1-(2-furyl) ethanol, an important chiral synthon in organic synthesis.

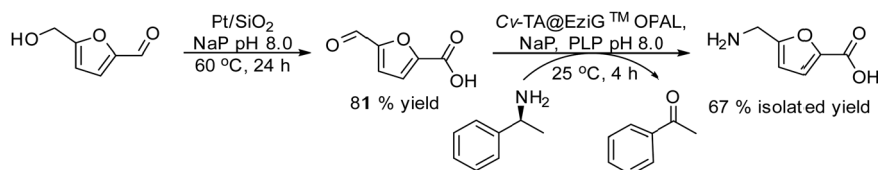
Ni and co-workers<sup>285</sup> reported the one-pot chemo-enzymatic synthesis of a chiral furan-based amino acid from corncob by integrating a magnetic core-shell solid acid catalyst,  $\text{Fe}_3\text{O}_4@\text{MCM-41}/\text{SO}_4^{2-}$ , with PLP-dependent threonine aldolase derived from *P. putida* (*PpThA*) (Scheme 67) to catalyze the aldol condensation between furfural and glycine. After process optimization, furfural was obtained from corncob in 63.6% yield using  $\text{Fe}_3\text{O}_4@\text{MCM-41}/\text{SO}_4^{2-}$  as a magnetic solid acid catalyst at 180 °C in 40 min. Subsequently, the biomass-derived furfural was freely transformed into the aldol-adduct  $\beta$ -(2-furyl)-L-serine in 73.6% yield, 99% ee, and 20% de using immobilized cells expressing *PpThA*, and without significantly reducing the product yields, the magnetic and biocatalysts could be efficiently recovered and reused for five cycles.

Compared with the conventional synthesis of  $\beta$ -(2-furyl)serine involving the chemocatalyzed aldol condensation between furfural and glycine, which leads to a racemic mixture, this chemo-enzymatic approach represents a straight-forward method to convert raw biomass into valuable chiral furyl amino acids.

**3.3.2. Synthesis of 5-aminomethyl-2-carboxylic acid from 5-hydroxymethyl furfural.** The amino acid 5-aminomethyl-2-carboxylic acid (AMFC) represents a very promising building block for polymer synthesis and can be used to produce unnatural peptides such as cyclopeptides.<sup>286</sup> The production of AMFC starting from HMF requires two consecutive steps: the first one is the oxidation of HMF to 5-formyl-2-furancarboxylic acid (AFCA), which can be performed using catalysts based on noble metals,<sup>287,288</sup> while the second step can be performed by the reductive amination of the formyl group with ammonia. However, this second step is difficult to achieve with high selectivity due to the instability of the furan ring under reductive conditions along with the tendency of furan aldehydes to form secondary and tertiary amines.<sup>289,290</sup> To overcome these drawbacks, recently, Heuson *et al.*<sup>291</sup> performed a chemo-enzymatic cascade process in a sequential mode starting from HMF, which involves as a first step the oxidation of HMF in 5-formyl-2-furancarboxylic acid using an optimized  $\text{Pt}/\text{SiO}_2$  catalyst, which was able to convert HMF into AFCA, with 81% yield in 24 h at 60 °C, in sodium phosphate buffer (pH 8). Then, the AFCA is converted in the amino acid AMFC, using a transaminase derived from *Chromobacterium violaceum* (*Cv-TA*) immobilized on the EziG support (Scheme 68). After 4 h at 20 °C, the AMFC could be obtained in 67% isolated yield, which represents the highest yield reported to date for this compound.

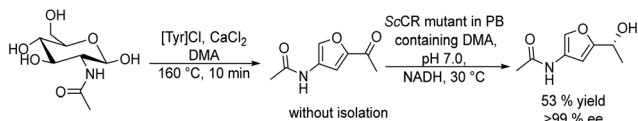
### 3.4. Synthesis of 3-acetamido-5(1-hydroxyethyl)furan from *N*-acetyl glucosamine

Besides lignocellulose, chitin is also a non-food type biomass, and after cellulose, it is the second most abundant biopolymer on earth. Chitin is widely found in the shells of crustaceans and insects and its annual production is about 100 billion tons.<sup>292</sup> It is constituted of units of *N*-acetyl glucosamine linked by  $\beta$  (1–4) linkages. The hydrolysis of chitin leads to *N*-acetyl glucosamine (NAG), which is a promising platform molecule to produce highly valuable N-containing chemicals. Thus, dehydration of NAG leads to 3-acetamido-5-acetylfuran (3A5AF), which is a versatile N-containing furan based building block. For instance,



Scheme 68 Synthesis of 5-aminomethyl-2-carboxylic acid from 5-hydroxymethyl furfural by combining oxidation with biocatalyzed reductive amination.





**Scheme 69** Synthesis of 3-acetamido-5-(1-hydroxyethyl)furan from *N*-acetyl glucosamine in a sequential mode by combining dehydration with biocatalyzed asymmetric reduction.

the asymmetric reduction of the keto group can afford the corresponding chiral furfuryl alcohol, (3-acetamido-5(1-hydroxyethyl)furan) (3A5HEF), which is a key intermediate for the synthesis of a variety of drugs.<sup>293–295</sup> Recently, Li *et al.* designed a chemo-enzymatic one-pot strategy to synthesize the chiral 3A5HEF starting from *N*-acetyl glucosamine in a sequential mode. The process involves as the first step the dehydration of NAG using tyrosine hydrochloride/CaCl<sub>2</sub> as an enzyme-friendly chemocatalyst in *N,N*-dimethylformamide (DMA) followed by the asymmetric reduction using a carbonyl reductase derived from *Streptomyces coelicolor* (ScCR) (see Scheme 69). To improve the reductase activity and stability the authors performed the structure-guided engineering of the enzyme, and two robust mutants were obtained, which showed 6-fold higher catalytic efficiency than the parent enzyme and improved thermal and organic solvent stability. Thus, 53% yield (99% ee) of the target chiral alcohol could be obtained in the one-pot chemo-enzymatic approach, which represents an important advantage compared with other reported methods where the isolation of the intermediate 3A5AF was required, which reduced the overall yield, while producing increased wastes.<sup>296</sup>

Considering that the main drawbacks encountered when dealing with biomass derived molecules are their poor stability under harsh reaction conditions and limited solubility in organic solvents, these examples show that chemo-enzymatic processes occurring in aqueous media and under mild reaction conditions can be an interesting alternative to transform biomass platform molecules into valuable compounds with high conversion and selectivity.

## 4. Reaction engineering strategies for solving incompatibility issues in chemo-enzymatic reactions

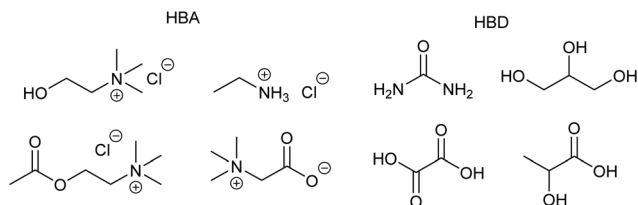
As we showed in the previous section, the synthesis of organic compounds through chemo-enzymatic cascade reactions suffers in general from a lack of compatibility between the chemo- and biocatalytic systems. Then most chemo-enzymatic methodologies are based on sequential processes where reaction conditions (catalysts, temperature, solvent, pH, substrate concentration, required additives) can be adjusted for each reaction step. However, researchers have developed different strategies to overcome these incompatibilities by performing, in many cases, the chemo-enzymatic processes in a concurrent mode. In this section, we will discuss the different approaches adopted for this purpose. In this way, adjusting the solvent

compatibility, for instance, increasing the solubility of organic compounds (including biomass raw materials), is an important approach, which can be achieved by using biocompatible neoteric solvents such as ionic liquids (ILs) and deep eutectic solvents (DESSs). Also, the mutual inactivation of the chemo- and biocatalysts is an important drawback, which can be particularly significant when metal-based catalysts and enzymes are involved in the cascade process. This has been solved by designing catalytic systems bearing spatial separation between the catalytic sites, such as the enzyme–metal hybrid catalysts, designed by co-immobilization of both catalysts on the same carrier or by bio-conjugation. Moreover, additional advantages of these systems can be their recyclability and the increase in activity by reducing the diffusion distance between catalytic sites of the involved intermediates. Particularly, they have been shown to be very effective in enzymatic oxidation where H<sub>2</sub>O<sub>2</sub> is released, and its accumulation results in strong inhibition of the enzymatic activity poisoning of the enzyme. Thus, the fast migration of H<sub>2</sub>O<sub>2</sub> toward the metal site nearby allows its rapid decomposition, preventing enzyme deactivation. As we will show, other strategies are based on spatial compartmentalization where enzymes, chemocatalysts, and required additives can be confined and can work effectively without interaction. Examples of these strategies are the use of porous hydrophobic membranes and biphasic and micellar systems (using biocompatible surfactants). They are of special interest for enzymes that do not work in organic media, while the solubility of organic substrates in the organic/lipophilic phase is increased. Encapsulation of enzymes and metal catalysts inside a cover has been particularly useful for organometallic complexes and represents another strategy to avoid mutual catalyst deactivation. Moreover, in some cases, the metal complexes are stabilized by encapsulation while increasing their water solubility and the turnover number of the metal catalyst. Finally, the combination of continuous flow reactors to perform compartmentalized chemo-enzymatic reactions will be discussed. This strategy, which requires the use of solid chemocatalysts and supported enzymes, represents a versatile approach where each catalytic system can efficiently work under very different reaction conditions, resulting in completely automated processes with high performances.

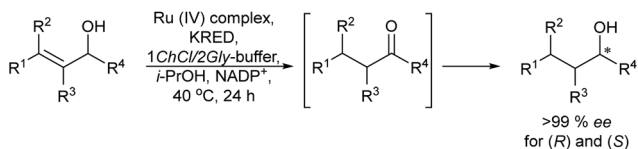
### 4.1. Chemo-enzymatic processes in non-conventional media

In the last few decades, neoteric solvents, such as ionic liquids (ILs) and deep eutectic solvents (DESSs), have emerged as environmentally friendly solvents, which are exciting alternatives to traditional solvents for chemo- and biocatalytic processes due to their wide range of physicochemical properties.<sup>297–306</sup> Deep eutectic solvents are formed by a mixture of salts, for instance quaternary ammonium salts, such as choline chloride, which act as hydrogen bond acceptors (HBAs), and uncharged hydrogen-bond donors (HBDs) (such as urea, carboxylic acids or polyols) (Scheme 70). The mixture forms a wide H-bond network that stabilizes liquid configurations and results in lower melting points than those of their individual components. DESSs are attractive because of their easy and inexpensive preparation, tunable properties, biodegradability,





**Scheme 70** Some examples of DESs possessing HBAs (quaternary ammonium salts) and HBDs (alcohols, carboxylic acids and amines).



**Scheme 71** Synthesis of optically active alcohols by combining Ru(IV)-catalyzed isomerization with enzymatic reduction in DES–buffer medium in a concurrent mode.

and non-volatility. Moreover, they are strongly water-miscible and hygroscopic.<sup>307</sup> Their lower cost and diminished environmental impact make them an effective alternative to ILs in multiple applications including organic synthesis.<sup>308</sup> Moreover, DESs have been applied as solvents in biocatalysis, where it has been shown that they can improve the efficiency of these reactions *via* increasing the substrate solubility and the activity and stability of enzymes.<sup>309–313</sup> The low solubility of most organic substrates in water limits the maximum substrate concentration; however, the unique properties of DESs allow reaching not only high substrate concentration, but also higher enantioselectivities than that can be achieved in water solutions in enzymatic processes.<sup>314,315</sup> These characteristics have stimulated their utilization in chemo-enzymatic cascades, although these systems also suffer from the typical drawbacks such as the incompatibility of the involved catalysts with reaction conditions or undesired catalyst cross-deactivation.

The first application of DESs in chemo-enzymatic cascade processes was reported by González-Sabin *et al.* in 2018.<sup>316</sup> The process was based on ruthenium-catalyzed isomerization of allylic alcohols to  $\alpha,\beta$ -saturated ketones followed by asymmetric

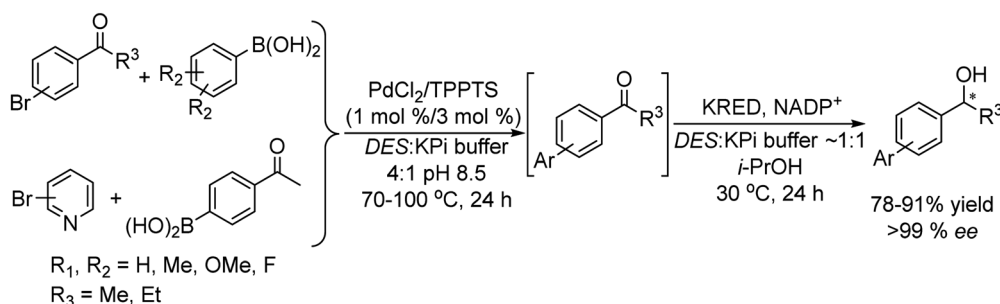
enzymatic reduction promoted by ketoreductases (KREDs) to produce chiral alcohols. (Scheme 71).

An optimization study of different DES systems for the bioreduction of prochiral aromatic ketones performed in DES–water mixtures showed that the DES based on sorbitol or glycerol as a HBD and choline chloride as a hydrogen bond acceptor (HBA) gave the best results at 50% w/w DES. Then, the cascade process was performed in a sequential mode, where metal-catalyzed isomerization of allylic alcohols was performed using a ruthenium(IV) complex as a catalyst. When the isomerization was complete, the KRED and co-factor were added and the reaction proceeded at 30 °C for 24 h. Thus, various chiral alcohols were obtained in isolated yields between 60 and 95% and ee (93–99%) using this protocol. The results showed that KRED was compatible with the reaction medium of the metal-catalyzed step, with the effect of the Ru(IV) catalyst on enzyme performance being insignificant. This behavior enabled the process to occur successfully in a concurrent mode, and a variety of allylic alcohols were transformed into the enantiopure saturated alcohols with good to excellent conversions (68–96%), improving previous results obtained in aqueous buffer media.<sup>317,318</sup>

In a parallel work, the same group<sup>319</sup> reported the use of mixtures of DES–buffer media in cascade reactions involving the palladium-catalyzed Suzuki cross-coupling followed by enzymatic reduction mediated by KRED to produce chiral biaryl alcohols (Scheme 72).

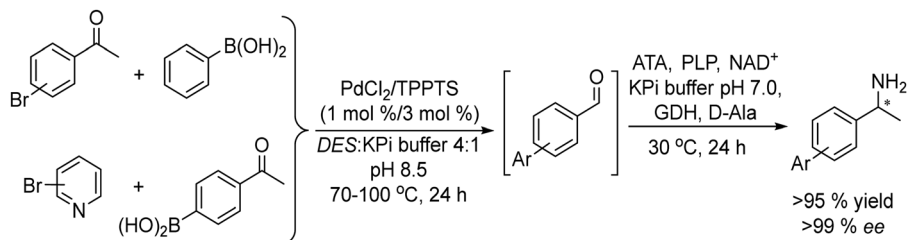
The optimization of the required parameters, such as the nature of the DES, DES–water ratio, temperature and substrate concentration, allowed the efficient coupling of both steps in a sequential mode, achieving the target chiral alcohols in 78–91% yield and >99% ee. Interestingly, the use of DES–water mixtures allowed increasing the substrate concentration up to 75 mM in the biocatalyzed step, which is considerably superior to those used in water solution (33–44 mM).

A similar protocol was applied to the synthesis of chiral biaryl amines,<sup>320</sup> by sequentially coupling a Suzuki reaction with asymmetric bioamination catalyzed by an amino transaminase (ATA) (Scheme 73). In this case, and owing to the limitations in the use of amine transaminases to convert bulky ketones, such as biaryl ketones, the authors used an (*R*)-selective amine transaminase derived from *Exophiala xenobiotica*, which was

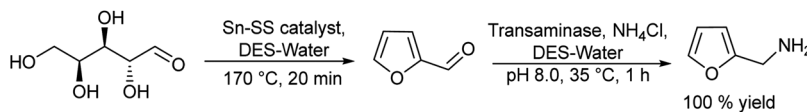


**Scheme 72** Synthesis of biaryl alcohols by combining palladium-catalyzed Suzuki cross-coupling with enzymatic reduction. TPPTS: triphenylphosphine trisulfonate; KPi: potassium phosphate.





Scheme 73 Synthesis of biaryl amines by combining palladium-catalyzed Suzuki cross-coupling with enzymatic transamination.



Scheme 74 Production of furfuryl amine (FLA) from xylose-rich biomass by combining xylose dehydration with enzymatic transamination.

identified, using data mining, as an efficient biocatalyst to convert biaryl ketones into the corresponding chiral amines with excellent enantioselectivity.<sup>321</sup> Optimization of the reaction conditions in both steps allowed finding a compatible window to perform the chemo-enzymatic process in a sequential mode. A critical point in the biotransformation step was to adjust the concentration of DES in the DES–buffer mixture, since the activity of the ATA was considerably reduced at DES concentrations higher than 15%. Therefore, after the Suzuki step (performed at 100 °C and 200 mM substrate concentration in a DES:water 4:1 mixture) the resultant reaction mixture was diluted to 25 mM (which results in a DES concentration of 10%) prior to the biotransformation step. The protocol was applied successfully to a variety of substrates, where the metal-catalyzed step proceeded quantitatively in all cases, and the resulting biaryl ketones were converted by the ATA quantitatively (>95%) into the corresponding (*R*)-biaryl amines with >99% ee.

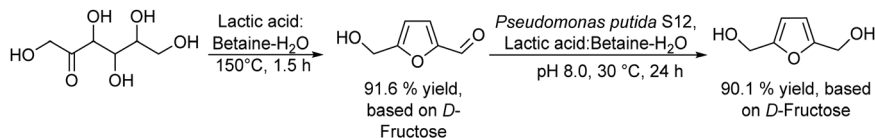
Very recently, He and co-workers have reported a series of studies on the valorization of biomass in DES–water systems. For instance, the production of furfuryl alcohol and furfuryl amine (FLA) from biomass rich-xylose<sup>322,323</sup> was achieved through a sequential chemo-enzymatic cascade reaction, by combining dehydration of xylose into furfural with enzyme catalyzed reduction or transamination. In the chemo-enzymatic process to produce furfuryl amine (Scheme 74) for the chemocatalyzed step, shrimp shell (SS) waste was used as the biobased support to prepare a sulfonated tin-based solid acid (Sn–SS) catalyst for converting sugarcane bagasse (SB) into furfural in DES–water (choline chloride/ethylene glycol–water). After optimization of reaction conditions (ChCl/EG loading, Sn–SS amount, temperature, and reaction time), it was possible to achieve 62.3% conversion of SB to furfural after 20 min of reaction time in ChCl/EG–water (20:80 v/v), which was 1.37 times greater than that of the aqueous system. As an explanation for this enhanced selectivity, the authors proposed that ChCl in the DES could increase proton reactivity and availability by influencing the stability of protons. The bioamination of furfural into furfuryl amine was carried out using newly formed

recombinant *Escherichia coli* pRSFDuet-CV-AlaDH cells expressing ω-transaminase and L-alanine dehydrogenase. The chemo-enzymatic cascade process was performed in a sequential mode, where first the SB was converted into furfural using the Sn–SS catalyst in ChCl/EG–water (20:80 v/v) at 170 °C for 20 min. After this, the solution was adjusted to pH 8.0 and diluted with a buffer solution and then pRSFDuet-CV-AlaDH whole-cells and NH<sub>4</sub>Cl as the amine donor were added. The transamination proceeded at 35 °C for 1 h and the SB-derived FAL could be entirely converted into FLA with a productivity of 0.458 g FLA per g xylan in SB. Similar results concerning FLA productivity (0.43 g per g xylan) were obtained when the process was performed starting from conorb in EaCl:Gy–water and using a sulfonated tin based hydroxyapatite combined with oxalic acid as the dehydrating agent.<sup>324</sup>

To increase thermostability and catalytic activity in the presence of high substrate concentration, the authors developed mutant transaminase strains using side-directed mutagenesis.<sup>325–327</sup> For instance, the authors showed that a triple mutant *Aspergillus terreus* ω-transaminase (HNILQE) could aminate furfural into furfuryl amine in high yield at 500 mM furfural concentration, which is considerably superior to the usual concentrations (100–300 mM) used for the wild-type strain transaminases. The chemo-enzymatic process proceeded in a three-component DES (choline chloride–malonic acid–lactic acid) that acted as a solvent and as an acid catalyst. Starting from D-xylose the dehydration step was performed at 190 °C for 45 min, giving furfural (70.6% yield), which was aminated by the enzyme mutant after adjusting the pH to 8 and the temperature (35 °C), affording the furfuryl amine in 97.6% yield after 24 h.<sup>325</sup>

Following a similar strategy, the authors developed chemo-enzymatic cascades in a DES–water system to produce efficiently furfuryl amine and furoic acid starting from different xylose sources such as corncob, bagasse, bamboo shoot shell, corn stalk, *etc.*<sup>328–330</sup> Tin based catalysts supported on biological macromolecules were used as chemocatalysts for the first step. By using a shrimp shell-supported solid acid catalyst (Sn–DAT–SS) in DES (ChCl:EG)–water (10:90, v/v) after 30 min at





Scheme 75 Synthesis of 2,5-bis(hydroxymethyl)furan (BHMF) from fructose by combining fructose dehydration with enzymatic reduction.

170 °C, corncob afforded the highest furfural yield (52.4%). The obtained furfural could be completely aminated to FLA by *E. coli* CCZU-XLS160 cells harboring  $\omega$ -transaminase after 24–72 h. On the other hand, furfural derived from different sources of biomass could be fully transformed into furoic acid using *Escherichia coli* HMFOMUT cells containing dehydrogenase.<sup>330</sup>

The authors also developed efficient chemo-enzymatic processes for the valorization of D-fructose and bread waste into 2,5-bis(hydroxymethyl)furan (BHMF) in acidic DES in a sequential mode.<sup>331,332</sup> Using lactic acid:betaine (LA:B)–water (15 : 85, v-v) as a solvent and acid catalysts, fructose was dehydrated into 5-hydroxymethylfurfural (HMF) in 92% yield at 150 °C in 1.5 h. HMF derived from fructose was then converted into BHMF (98.4% yield) using *Pseudomonas putida* S12 within 24 h at 30 °C and pH 8.0 (Scheme 75). Starting from bread waste, the HMF yield reached 44.2 mol% (based on the bread waste) and it could be transformed into 2,5-bis(hydroxymethyl) furan (using *E. Coli* HMFOMUT harbouring reductase activity) in 84.5% yield after 1 day at 37 °C, which represents a yield of 0.230 kg of BHMF per kg of bread.

Conversion of fructose and bread waste into 5-hydroxymethyl-2-furfurylamine has been recently developed in acidic DES using mutant biocatalysts.<sup>333–335</sup> For instance, in the valorization of bread waste, the cascade reaction was performed using betaine:malonic acid–water as the reaction medium. Starting from bread, in the first step, the DES catalyzed the hydrolysis, isomerization and dehydration steps achieving 30% yield of HMF at 190 °C in 45 min. Then HMF was subsequently aminated using *E. coli* cells expressing L-alanine dehydrogenase and the  $\omega$ -transaminase mutant as the biocatalyst and using D-alanine as the amino donor, achieving 92.1% yield of the amino-alcohol at 35 °C in 12 h. Interestingly, the use of the mutant biocatalyst not only reduced the amount of the amino donor but also allowed increasing the substrate tolerance (up to 500 mM HMF) of the whole cells, while enhancing the transamination activity of the enzyme.

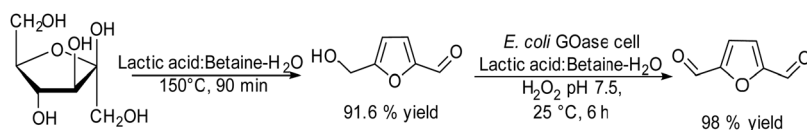
The authors also developed a chemo-enzymatic cascade to produce 2,5-diformylfuran (DFF), an important building block for furan-based chemicals, from fructose and from waste bread in the acidic lactic acid:betaine–water.<sup>336</sup> In this protocol, the fructose is efficiently dehydrated into HMF in the first step, and the HMF is biologically oxidized into DFF (Scheme 76) by *E. coli*

GOase. A productivity of 0.631 g DFF g<sup>-1</sup> fructose and 0.323 g DFF g<sup>-1</sup> bread could be respectively achieved.

#### 4.2. Enzyme–metal hybrid catalyst

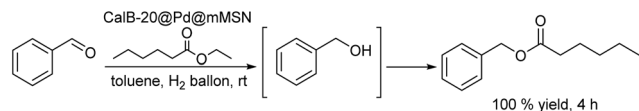
As shown for the different examples summarized in this work, the direct use of enzymes and metal catalysts in chemo-enzymatic one-pot reactions commonly leads to mutual inactivation of the catalysts. Therefore, the spatial separation of catalytic sites is a straightforward method to overcome incompatibility problems between catalytic species involved in chemo-enzymatic processes. An effective strategy is through the rational design of enzyme–metal hybrid catalysts.<sup>337</sup> The generation of incompatible metal and enzyme active sites on the same carrier not only provides catalyst stability, but moreover enzyme and metal active sites in close proximity exhibit improvement in activity (by reducing the diffusion distance of involved intermediates), which along with catalyst recyclability are important advantages of this strategy. The enzyme–metal hybrid catalysts can be synthesized through co-immobilization and bio-conjugation methods. In the following sections, relevant and updated examples of both strategies will be presented.

**4.2.1. Co-immobilized enzyme–metal hybrid catalysts.** A common approach to synthesize hybrid catalysts is by the immobilization of metals and enzymes on the same carrier. Mesoporous silicas and metal–organic frameworks (MOFs) have been the preferred materials to synthesize such nano-hybrids.<sup>338</sup> Mesoporous silicas with high surface area and large pore volume have been utilized as effective carriers for the co-immobilization of metals and enzymes. The first example was reported by Backvall in 2013, who co-immobilized Pd nanoparticles and lipase CALB on aminopropyl-functionalized siliceous mesocellular foams (AmP-MCF),<sup>339</sup> which permitted the two catalysts to catalyze the dynamic kinetic resolution (DKR) of a primary amine in a cooperative way enhancing yield and enantioselectivity. Concerning the application of these nano-hybrids in linear cascades, Wu *et al.*<sup>340</sup> designed a bifunctional catalyst where palladium nanoparticles (Pd NPs) and *Candida Antarctica lipase B* (CalB) were stepwise loaded into separate positions of a mesoporous silica. Before enzyme immobilization, the hybrid Pd–mesoporous particles were hydrophobized by surface alkylation, resulting in a tuned particle hydrophobicity, which allowed



Scheme 76 Synthesis of 2,5-diformylfuran (DFF) from fructose by combining fructose dehydration with enzymatic oxidation.





**Scheme 77** Cascade reaction in a concurrent mode involving benzaldehyde reduction followed by esterification using a co-immobilized CalB–Pd hybrid catalyst.

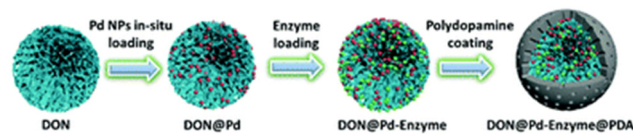
the dispersion of the catalyst in a variety of organic solvents. Thus, a cascade reaction in a concurrent mode involving benzaldehyde reduction followed by esterification with ethyl hexanoate was successfully performed in toluene giving the corresponding ester in 100% yield (Scheme 77). Additionally, the catalyst could be reused in several consecutive cycles maintaining high activity.

Prasad *et al.*<sup>341</sup> prepared a bifunctional catalyst combining gold nanoparticles and glucosidase. The as-synthesized Au NPs were coated with a silica shell using a sol–gel method, resulting in a core–shell architecture (Au@mSiO<sub>2</sub>). Then, the shell surface of Au@mSiO<sub>2</sub> was functionalized with epoxy groups, which were later used to attach the glucosidase through covalent binding. The resulting catalyst (Au@mSiO<sub>2</sub>@glucosidase) was used in a cascade reaction for converting 4-nitrophenyl-β-glucopyranoside into 4-aminophenol in a sequential mode. Thus, 4-nitrophenyl-β-glucopyranoside was first hydrolyzed by the enzyme into *p*-nitrophenol in aqueous solution up to completion. Then an excess of NaBH<sub>4</sub> was added to reduce the nitrophenol intermediate into aminophenol (Scheme 78). In this catalytic system, the presence of pores on the surface of silica lets both 4-nitrophenol and NaBH<sub>4</sub> to diffuse to the surface of the Au nanoparticles, where the reduction occurs.

However, the bifunctional catalyst becomes rapidly deactivated after consecutive reaction cycles, probably due to the denaturalization of the enzyme caused by the very high pH generated by the hydrolysis of NaBH<sub>4</sub>.

Recently, dendritic organosilica nanoparticles (DONs) have been used as excellent supports for co-immobilization of metals and enzymes, without extra hydrophobic modification.<sup>342</sup> DONs are a class of mesoporous materials with intrinsic hydrophobicity, bearing ordered center-radial mesoporous channels and high accessible internal surface areas.<sup>343</sup> The DONs were prepared by a continuous phase microemulsion method and were subsequently used to stepwise immobilize Pd nanoparticles and the enzyme. Finally, the DON@Pd–enzyme obtained was covered by a polydopamine shell (PDA) by self-polymerization of dopamine, thus obtaining the DON@Pd–Enzyme@PDA catalyst (Scheme 79).

The novel core–shell catalyst showed enhanced catalytic performance in chemo-enzymatic asymmetric synthesis of

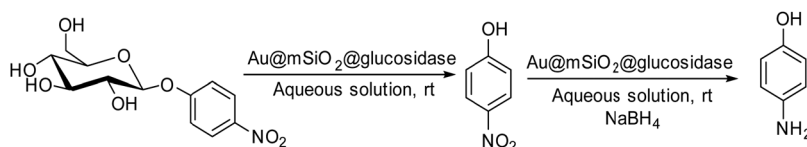


**Scheme 79** Formation mechanism and process of the amphiphilic chemo-enzymatic nanocatalyst. Reproduced with permission: Copyright 2020, The Royal Society of Chemistry (adapted from ref. 342).

chiral benzyl alcohols through a two-step concurrent cascade reaction. The process combines a Pd/Cu-catalyzed Liebeskind–Srogl (*L*–*S*) cross-coupling reaction between thioesters and boronic acids with asymmetric reduction catalyzed by alcohol dehydrogenase (ADH) derived from *Rhodococcus ruber* (Scheme 80). A variety of enantiomerically pure benzyl alcohol derivatives were obtained in high yields (60–86%). Additionally, the catalyst was also used for the DKR of racemic amines to obtain chiral amines in high yields. The authors showed that the hydrophobic microenvironment is responsible for increased stability, activity and cascade efficiency of the catalyst, while the hydrophilic PDA shell improves the dispersibility of the catalyst in water and acts as a protective barrier for the inner core. In fact, when the reaction was performed using DON@Pd–ADH without the PDA shell, an important decrease of the yield was observed because the exposed ADH was severely inactivated by copper ions and boronic acid.

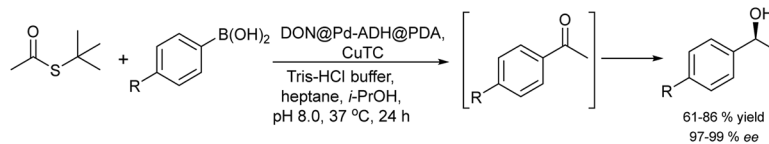
A core–shell structured magnetic wrinkled organosilica-based metal–enzyme integrated catalyst was developed by Jiang *et al.*<sup>344</sup> The wrinkled organosilica nanoparticles (WOS) were prepared starting from an optimized ratio of tetraethylorthosilicate (TEOS) as a silicon source, bis(triethoxysilyl)ethane, (BTSE) organosilica, Fe<sub>3</sub>O<sub>4</sub> nanoparticles, and urea. The urea was used to promote the hydrolysis and condensation of the silicon shell over the Fe<sub>3</sub>O<sub>4</sub> nanoparticles, and it was shown that the urea concentration had a significant influence on the wrinkled structures. Subsequent functionalization of the silica with amino groups allowed, on the one hand, the high dispersion of Pd ions (from a Pd salt), which were *in situ* reduced with NaBH<sub>4</sub>, and on the other hand, the amino groups serve as sites to anchor the enzymes through covalent bonds. The authors showed that by anchoring lipases the optimized hybrid catalyst was highly active in the dynamic kinetic resolution of chiral amines in an organic solvent. Moreover, by anchoring an alcohol dehydrogenase (ADH&Pd@WOS) chemo-enzymatic synthesis of chiral alcohols in water from α,β-unsaturated ketones could be performed in high yield and enantiomeric excess (Scheme 81).

Recently, Tyagi *et al.*<sup>345</sup> developed a biohybrid catalyst [Pd(0)–CALB@SiO<sub>2</sub>] by immobilizing *Candida Antarctica* lipaseB

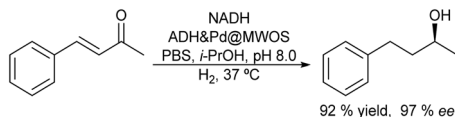


**Scheme 78** A cascade process involving hydrolysis and reduction sequences catalyzed by a co-immobilized Au–glucosidase hybrid catalyst.





**Scheme 80** Synthesis of chiral alcohols in a concurrent mode using metals and enzymes co-immobilized on dendritic organosilica nanoparticles (DON) as a hybrid catalyst. (CuTC: (copper(i) thiophene-2-carboxylate).



**Scheme 81** Synthesis of chiral alcohols from  $\alpha$ - $\beta$ -unsaturated ketones using a co-immobilized Pd@ADH hybrid catalyst.

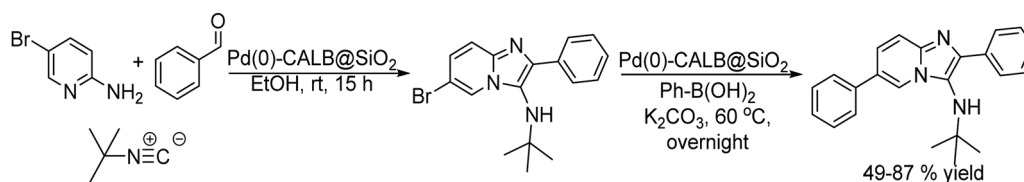
and Pd(PPh<sub>3</sub>)<sub>4</sub> within a silica framework. The hybrid catalyst was prepared starting from an emulsion of oleic acid in a mixture of EtOH:water, which acted as a template for the growth of spherical silica particles, while avoiding the contraction of the particles during drying. Then, after the addition of the lipase and Pd(PPh<sub>3</sub>)<sub>4</sub>, (3-aminopropyl)triethoxysilane (APTES) and tetraethylorthosilicate (TEOS) were added generating the biohybrid catalyst with a silica framework and amine functionality.

The [Pd(0)-CALB@SiO<sub>2</sub>] biohybrid was tested in a chemo-enzymatic cascade in a sequential mode involving as the first step the lipase catalyzed Groebke–Blackburn–Bienayme (GBB) multicomponent reaction, followed by the Pd catalyzed Suzuki–Miyaura coupling with boronic acids (Scheme 82). The process was exploited to produce a variety of clinically important imidazo[1,2-*a*]pyridine derivatives in isolated yields ranging from 49 to 87%. Interestingly, when Pd(PPh<sub>3</sub>)<sub>4</sub> and CALB-enzyme were used in the pure form as a catalyst in a one-pot process, the reaction afforded the target product only in trace amounts, suggesting the mutual deactivation of both catalysts. The biohybrid was not stable over several reuses and a decrease of activity was observed after the second run. This was attributed

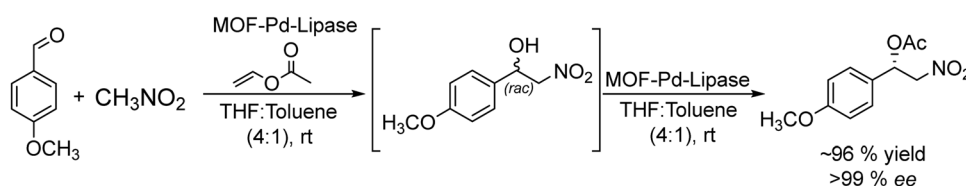
to the leaching of the enzyme and/or palladium from the catalysts.

Metal–organic frameworks (MOFs) are crystalline structures with high versatility for the design of pore geometries, porosity, and functionality since they can be finely adjusted by the rational design of the metallic centers and organic linkers or by post-synthetic methods.<sup>346–348</sup>

Preliminary studies performed by Chen *et al.*<sup>349</sup> showed that the specific interactions between the organic components of the MOFs and the supported enzyme prevent enzyme leaching and deactivation. Therefore, MOFs with large pores are considered to be promising candidates for the immobilization of enzymes. Recently, these features of MOFs have been successfully exploited for the preparation of enzyme–metal nanohybrids as catalysts for chemo-enzymatic cascades. For instance, Dutta *et al.*<sup>350</sup> performed the synthesis of a cobalt-based zeolitic imidazolate framework (ZIF67) in the presence of Pd nanoparticles and polyvinylpyrrolidone, to generate defect-rich Co(II) nodes and to produce large mesopores (~30 nm). This material, bearing stable Pd nanoparticles encapsulated inside the mesopores of the MOF, was incubated with *Candida antarctica* lipase A (CalA), which was also placed inside the mesopores, generating the multifunctional catalysts. The authors applied the hybrid catalysts in a cascade reaction that couples in a concurrent mode a nitroaldol condensation (catalyzed by Lewis acid sites, associated with Co(II) unsaturated nodes) with the Pd catalyzed racemization of the nitroaldol adduct intermediate, followed by their dynamic kinetic resolution catalyzed by the lipase (Scheme 83). The reactions performed in a mixture

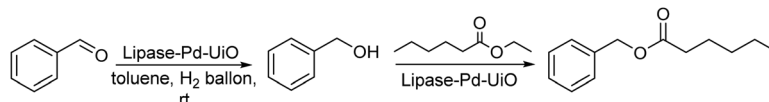


**Scheme 82** Chemo-enzymatic synthesis of aryl substituted imidazo[1,2-*a*]pyridines.



**Scheme 83** Combination of nitroalcohol condensation with DKR in a concurrent mode on a MOF-based Pd–lipase nanohybrid catalyst.



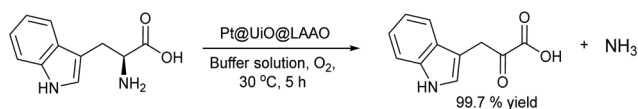


**Scheme 84** Combination of aldehyde reduction with transesterification on a MOF-based Pd-lipase nano hybrid catalyst.

of THF/toluene (4 : 1) at room temperature allowed a variety of chiral acetylated nitroalcohols to be obtained in high yields and  $ee > 99\%$ .

A zirconium-based UiO-66 MOF, bearing amino groups (UiO-66-NH<sub>2</sub>), was used as a carrier to confine Pd nanoparticles in the inner pores of the MOF, while a lipase CALB was physically adsorbed on the surface.<sup>351</sup> Moreover, after Pd immobilization, the hydrophobicity of the MOF could be tuned by ligand exchange reaction with lauric acid. The increase in hydrophobicity allowed enhancing the amount of immobilized enzyme and the dispersibility of the catalyst in organic solvents. The lipase-Pd-UiO catalyst was used in a chemo-enzymatic cascade to convert benzaldehyde into benzyl alcohol, which was subsequently esterified to benzyl hexanoate through a two-step sequential process (Scheme 84). Interestingly, the yield of the ester was higher with the hybrid catalysts than in a control experiment with a separate Pd-MOF and free-lipase, possibly due to the aggregation of free CalB in toluene. The reuse of the catalyst showed gradual deactivation, which was attributed to the denaturation of the lipase during the cascade process.

Biohybrids have been especially operative for enzymatic oxidation reactions, where H<sub>2</sub>O<sub>2</sub> is evolved, the accumulation of which in the reaction media not only deactivates the enzyme, but also generates byproducts. To overcome the negative effects of H<sub>2</sub>O<sub>2</sub>, the oxidation reactions are usually performed in the presence of catalase for H<sub>2</sub>O<sub>2</sub> decomposition. However, these multienzymatic approaches in general have limited stability, poor recyclability and high cost. To overcome these drawbacks Wu *et al.*<sup>352</sup> prepared a zirconium-based UiO-66 MOF with confined Pt nanoparticles inside the crystals and adsorbed L-amino acid oxidase (LAAO) on the external surface. The catalyst was applied to the synthesis of indole-3-pyruvic acid from L-tryptophan in buffer solution (see Scheme 85). In the biohybrid catalytic system based on UiO-66 MOF/Pt, the angstrom-scale pore size of UiO-66 MOF ensured the rapid diffusion of H<sub>2</sub>O<sub>2</sub> produced to Pt sites, where the fast decomposition suppressed enzyme deactivation and the decarboxylation of the target  $\alpha$ -keto acid into indole-3-acetic acid. Moreover, with this catalytic system, the deactivation of the enzyme observed when brought into direct contact with Pt nanoparticles was suppressed due to the spatial separation of the metal nanoparticles and the enzyme leading to a 99.7% yield of  $\alpha$ -keto acid, exceeding the yield of  $\alpha$ -keto acid achieved using the free enzyme (41.2%).



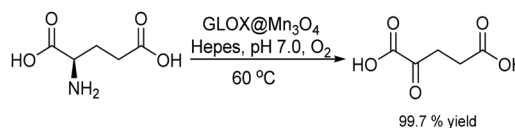
**Scheme 85** Chemo-enzymatic synthesis of indole-3-pyruvic acid from L-tryptophan on a MOF-based Pt-amino acid oxidase nano hybrid catalyst.

The same tandem reaction for the synthesis of indole-3-pyruvic acid from L-tryptophan was studied by Sun *et al.*<sup>353</sup> using as a bifunctional catalyst a nano hybrid of L-amino oxidase supported/encapsulated on cobalt phosphate nanocrystals (LAAO@CoPs). The catalyst was prepared by a one-pot bio-mimetic mineralization method under mild conditions, starting from Co salts and L-amino acid oxidase (LAAO). The nano hybrid exhibited a hierarchical nanoflower structure, where the enzyme was sporadically distributed in the inner part of the nanoflower. Thus, during the enzymatic oxidation of L-tryptophan, the nano-biohybrid structure maximizes the *in situ* decomposition of the H<sub>2</sub>O<sub>2</sub> intermediate through the channelling effect towards the Co sites, which are in direct contact with catalytic sites of LAAO, avoiding H<sub>2</sub>O<sub>2</sub> accumulation and by-product generation. The catalytic system achieved 100% conversion of L-tryptophan with the highest selectivity towards 3-indole-3-pyruvic acid reported up to now. Moreover, the catalyst was reused for several cycles maintaining 75% of its initial activity, while showing high stability against heat and proteolytic treatments.

Using a similar strategy, recently, Du *et al.*<sup>354</sup> reported a new bio-hybrid catalyst (GLOX@Mn<sub>3</sub>O<sub>4</sub>) by combining glutamate oxidase (GLOX) and trimanganese tetroxide (Mn<sub>3</sub>O<sub>4</sub>) nanocrystals through a one-step biomineralization method for chemo-enzymatic synthesis of  $\alpha$ -ketoglutaric acid from L-glutamate (Scheme 86).

The biohybrid catalyst maximizes the substrate channelling effects for *in situ* rapid decomposition of H<sub>2</sub>O<sub>2</sub>, formed during the enzymatic oxidation of sodium glutamate, diminishing the inhibition of GLOX by H<sub>2</sub>O<sub>2</sub> accumulation. The GLOX@Mn<sub>3</sub>O<sub>4</sub> catalyst exhibited excellent stability and reusability, and practically 100% yield of  $\alpha$ -ketoglutaric acid was achieved, which is 4.7 times higher than that obtained using the free GLOX system.

Another interesting example was reported by Sun *et al.*<sup>355</sup> for the production of gluconic acid from starch. In this case the authors immobilized Au nanoparticles onto sulfhydrylated mesoporous silica followed by the co-immobilization of glucoamylase (GA) and glucose oxidase (GOx). The biohybrid (GA&GOx@Au-SiO<sub>2</sub>) catalyst was highly efficient achieving a gluconic acid yield of 98% within 30 min, which is considerably superior than that obtained using the partly integrated system and free system. The high performance is attributed to the



**Scheme 86** Synthesis of  $\alpha$ -ketoglutaric acid from L-glutamate by combining glutamate oxidase (GLOX) and Mn<sub>3</sub>O<sub>4</sub> nanocrystals.

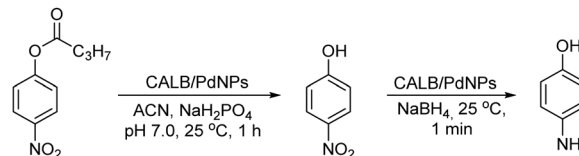


proximity effect of Au nanoparticles, GOx, and GA allowing the rapid transport of the reaction intermediates, glucose and H<sub>2</sub>O<sub>2</sub>, the latter being decomposed on the Au sites. Moreover, the GA&GOx@Au-SiO<sub>2</sub> catalyst conserved 84% of its initial activity after 10 consecutive runs, which was higher than that without immobilized Au nanoparticles. These examples show that these catalytic systems are interesting alternatives to the use of multienzymatic approaches in terms of performance and stability.

Carbon nitride (C<sub>3</sub>N<sub>4</sub>) was used for the first time as a support by Wu *et al.*<sup>356</sup> to construct a biohybrid catalyst through stepwise immobilizing Pd NPs and CalB. The 2D structure of C<sub>3</sub>N<sub>4</sub> providing an abundant amount of N atoms facilitated the immobilization of the Pd NPs. Then, CalB was covalently immobilized on the surface of C<sub>3</sub>N<sub>4</sub> using glutaraldehyde as the crosslinker. The bifunctional catalyst showed excellent activity in the hydrogenation of benzaldehyde with H<sub>2</sub> at room temperature, while the immobilized CalB showed higher activity in the esterification of the benzyl alcohol than the free enzyme. The cascade process for obtaining benzyl hexanoate from benzaldehyde and ethyl hexanoate was successfully achieved in toluene as solvent in a concurrent mode. The study of the recyclability of the catalyst showed that while the activity of the Pd in the reduction of benzaldehyde was maintained, a strong deactivation of the lipase was observed along consecutive reaction cycles.

**4.2.2. Bio-conjugated nanohybrids.** Bifunctional enzyme-metal catalysts can also be prepared in the absence of a support. This strategy takes advantage of the intrinsic functional groups (*e.g.*, -NH<sub>2</sub>, -SH, and -COOH) of the enzymes, which have a strong affinity for metal atoms, and the capacity of the enzymes to participate in the reduction of metal ions. The preparation strategy of these nanobiohybrids is very simple and direct and consists of the addition of a metal salt into an aqueous solution containing an enzyme at a particular temperature, generally from room temperature to 40 °C.<sup>357</sup> These bio-conjugated nanohybrids can have a crucial advantage over other systems in chemo-enzymatic reactions since they possess enzymatic and metallic activities in the same compartment.

Palomo *et al.*<sup>358,359</sup> reported the synthesis of novel nanobiohybrids based on enzyme-metal nanoparticles, which were generated *in situ* from an aqueous noble metal salt solution and a lipase (CALB). In this protocol, the enzyme acted at the same time as the supporting agent of metal ions and the reducing agent for metal nanoparticle formation, which in addition is stable against aggregation. Different Ag, Au, and Pd nanohybrids (CALB-PdNPs) composed of enzyme aggregates, where the metal nanoparticles are dispersed, were tested in typical metal catalysed reactions such as Heck and Suzuki-Miyaura cross coupling reactions. Taking advantage of the biocatalytic activity of the nanohybrid, which conserved its intrinsic enzymatic activity, and the stability of the metal nanoparticles in aqueous solutions, the authors applied the nanohybrid as a catalyst in a DKR process and in a chemo-enzymatic cascade model reaction. The cascade process, performed in a sequential mode, involves the enzymatic hydrolysis

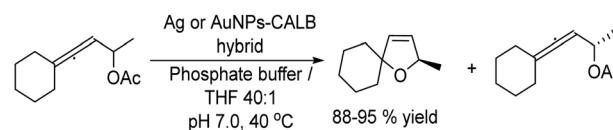


**Scheme 87** One-pot chemo-enzymatic reaction to obtain 4-aminophenol from 4-nitrophenylbutanoate combining ester hydrolysis with reduction on a lipase-Pd bioconjugated nanohybrid catalyst.

of 4-nitrophenylbutyrate to 4-nitrophenol, followed by the Pd catalyzed chemical reduction of the nitro group to 4-aminophenol using NaBH<sub>4</sub> as a reducing agent (Scheme 87). The process was successfully performed using these Pd-nanohybrids as chemo-enzymatic catalysts, and the TOF (defined as the moles of 4-aminophenol per mole of noble metal atoms in the nanocatalyst per minute) was in the range that was previously reported for the metal.

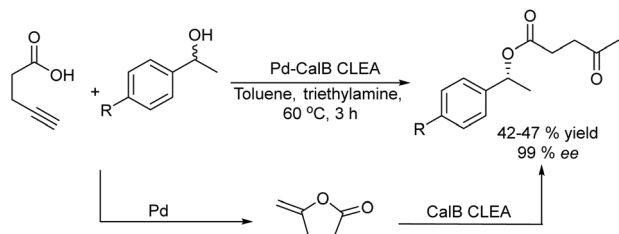
Porcine pancreatic lipase (PPL) encapsulated into a copper ion coordinated nucleotide composite (PPL@CuNC) was prepared through a simple *in situ* assembly approach followed by the metal reduction with NaBH<sub>4</sub>.<sup>360</sup> The biohybrid catalyst was tested in the same cascade reaction presented in Scheme 87 in a concurrent mode, achieving a 100% yield of 4-aminophenol. However, deactivation of the catalyst was observed, mainly due to the leaching of Cu metal nanoparticles, and after seven consecutive runs only 40% of its initial activity was retained. Recently, Palomo *et al.*<sup>361,362</sup> reported a novel strategy for the preparation of silver and gold nanoparticles-enzyme-polymer conjugate hybrids as bifunctional catalysts for cascade reactions. The authors prepared dextran-aspartic acid polymers that were used for encapsulating CALB through the ion exchange between the amino groups of the enzyme and the carboxylic groups of the polymer to obtain polymer-CALB conjugates, where Au and Ag ions were supported. It was observed that the enzyme-polymer conjugates directly caused the formation of smaller nanoparticles in both metal systems, without the necessity of an external reducing agent. The bifunctional catalyst was effectively applied in the stereoselective hydrolysis/cyclization cascade process starting from an allenic acetate to produce a 2,5-dihydrofuran in exceptional yield (88–95%) and enantiopurity (Scheme 88).

Interestingly, the authors also reported the synthesis of magnetic Fe nanoparticles-enzyme nanobiohybrids consisting of iron nanoparticles homogeneously dispersed in a lipase matrix that confers high stability against aggregation and oxidation of Fe. These novel magnetic nanostructures were used as heterogeneous catalysts for C-C coupling reactions, chemoselective hydrogenation and degradation of pollutants.<sup>363</sup>



**Scheme 88** Lipase-silver and gold bioconjugated nanohybrids as catalysts for the hydrolysis/cyclization of allenic acetate.





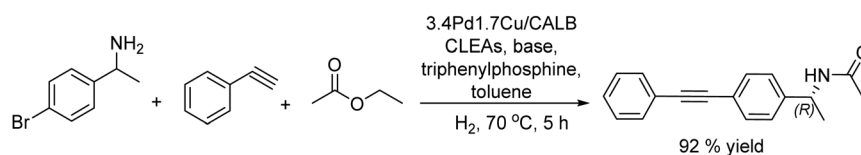
**Scheme 89** Kinetic resolution of benzyl alcohols using a the Pd-CALB-CLEA bioconjugated nanohybrid as the catalyst.

Bäckvall's group<sup>364</sup> developed a bifunctional catalyst based on cross-linked enzyme aggregates (CLEAs) of a lipase where Pd nanoparticles were introduced.

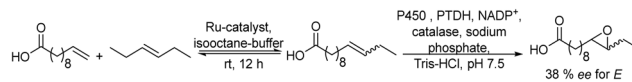
The CLEA was obtained by cross-linking with glutaraldehyde the lipase CALB and subsequently it was treated with palladium acetate that was reduced with Na(CN)BH<sub>3</sub> to generate the Pd(0)-CALB CLEA. The amorphous structure of the nanohybrid suggested that the Pd NPs were integrated and bound inside the CLEA matrix. These particles were used as catalysts in the Pd catalyzed cycloisomerization of 4-pentynoic acid to form a lactone that acted as an acyl donor for the lipase catalyzed kinetic resolution of a variety of benzyl alcohols (Scheme 89). Interestingly, the bifunctional catalyst was stable along six consecutive reaction cycles, retaining its activity and selectivity.

An advantage of the CLEA-metal catalytic system with respect to the biocatalyst supported on inert carriers is the increase of the catalytic activity per mass unit of the catalytic material. However, a drop in the CLEA enzymatic activity with respect to free enzymes is commonly observed.

In a similar way, Ge *et al.*<sup>365</sup> prepared an enzyme-bimetallic hybrid catalyst by *in situ* reduction of PdCu nanoclusters on cross-linked lipase aggregates (CALB CLEAs). The catalytic activity of PdCu/CALB CLEAs was evaluated in the chemo-enzymatic synthesis of (*R*)-*N*-[1-(4-(phenylethynyl)phenyl)ethyl]-acetamide (Scheme 90), which is an important building block of chiral compounds. In this one-pot cascade reaction that occurs in a concurrent mode, lipase catalyzes the acylation of the (*R*) enantiomer of amine and the bimetallic nanoclusters have two different functions: they catalyze the Sonogashira reaction and the racemization of the (*S*) enantiomer of amine, simultaneously (Scheme 90). The strong bimetallic synergistic effect existing between Pd and Cu within PdCu/CALB CLEAs provided excellent activity in the cascade process, achieving 90% yield with 99% ee of the target product. In addition, the catalyst retains 70% of its initial activity after ten consecutive runs.



**Scheme 90** Chemo-enzymatic synthesis of (*R*)-*N*-[1-(4-(phenylethynyl)phenyl)ethyl]-acetamide in a concurrent mode using the PdCu/CALB CLEA catalyst.



**Scheme 91** Chemo-enzymatic cross-metathesis/epoxidation in a biphasic system.

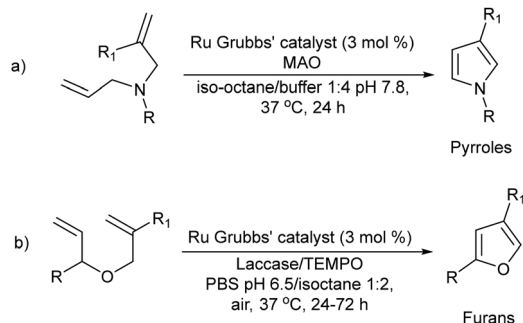
### 4.3. Spatial compartmentalization

The generation of different microenvironments in cellular processes enabling the compatibility of specific tasks in enzymatic reactions in a one-pot mode has inspired researchers to develop different strategies to combine chemo- and biocatalysts by compartmentalizing the catalytic systems. In this section, a variety of existing methods for spatial compartmentalization of chemo- and enzymatic catalysts applied to relevant chemo-enzymatic transformations will be discussed.

**4.3.1. Compartmentalization using biphasic systems.** One of the most simple and practical strategy to compartmentalize incompatible catalysts in chemo-enzymatic reactions is by using biphasic systems that usually combine an aqueous buffer solution and an organic solvent. In these systems, chemo- and biocatalysts can work effectively without interaction and can be successfully applied particularly to enzymes that do not work in organic media. Moreover, the solubility of the organic substrates can be considerably enhanced compared with single aqueous phase media, while in some cases, the phases containing chemocatalysts and enzyme can be separated and recycled. However, as the reaction medium has a strong influence on the activity and stability of the catalysts, an important task is to identify suitable biphasic systems to perform a given chemo-enzymatic process. In this section several relevant examples of chemo-enzymatic cascades performed in biphasic systems in concurrent and sequential modes will be presented.

The combination of cross-alkene metathesis with biocatalyzed stereoselective epoxidation in a concurrent mode was first reported by Hartwig *et al.*<sup>366</sup> using a Ru carbene catalyst and cytochrome P450 to perform the metathesis and epoxidation respectively in a biphasic system (Scheme 91). The cascade reaction that involves the metathesis between terminal unsaturated carboxylic acids and symmetrical alkenes followed by epoxidation with P450 was performed in a biphasic isooctane-buffer medium. An air and water stable second-generation Hoveyda-Grubbs' catalyst was selected for the metathesis step, while isooctane was selected as the organic phase due to its suitability as a solvent for olefin metathesis and compatibility with P450 enzymes. In this process, the equilibrium-controlled metathesis process that leads to a mixture of alkenes occurs in the organic phase, while the P450 enzyme in the aqueous phase



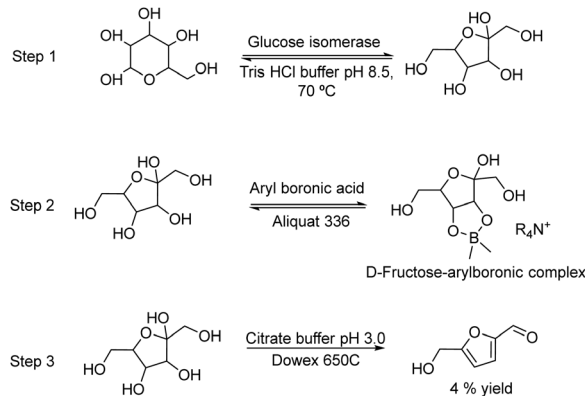


**Scheme 92** Chemo-enzymatic ring-closing metathesis/aromatization cascade in a biphasic system to obtain pyrroles from diallyl amines (a) and furans from diallyl ethers (b).

transforms selectively one alkene from the mixture of alkenes into epoxide. Owing to the irreversible enzymatic step that shifted the metathesis equilibrium, the target product could be obtained in higher yield than those achieved in a stepwise process.

Using a similar strategy, Castagnolo and co-workers reported the direct synthesis of pyrroles and furans from diallyl amines and diallyl ethers respectively in a biphasic iso-octane-buffer medium. Pyrroles were obtained through one-pot cascade ring-closing metathesis/aromatization by a combination of ruthenium Grubbs' catalyst and monoamine oxidase derived from *Aspergillus niger* (MAO-N) (Scheme 92a).<sup>367</sup> Furans were obtained by combining the ruthenium Grubbs'-catalyzed ring-closing metathesis of diallyl ethers and *Trametes versicolor* laccase/TEMPO for aromatization (Scheme 92b).<sup>368</sup> The strategy was effectively applied to synthesise a variety of pyrroles and furans in moderate to good yields.

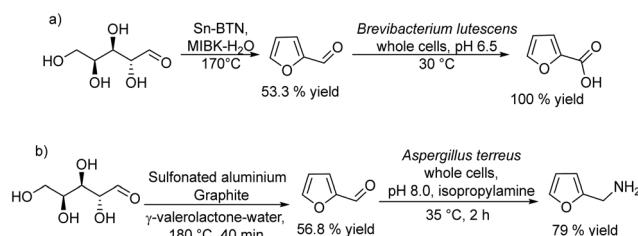
Chemo-enzymatic systems in biphasic media have also been utilized for valorization of biomass. For instance, and as discussed above, the integration of glucose to fructose isomerization and fructose dehydration into a one-pot system to produce HMF is of relevant importance. Dumeignil *et al.*<sup>369</sup> developed a strategy for the synthesis of HMF, combining the enzymatic isomerization of glucose into fructose using the glucose isomerase followed by the chemical dehydration of fructose. The strategy was based on the compartmentalization of both catalysts (the enzyme and the chemocatalyst) in two isolated aqueous phases separated by an organic-liquid interphase. Thus, glucose is first enzymatically isomerized to fructose in the aqueous phase. Fructose is then preferentially complexed with aryl boronic acid at the interphase of the organic phase, and the fructose complex is transported through the organic phase to the interphase of the second aqueous receiving phase containing citrate buffer (pH 3), where the complex is hydrolyzed and subsequently fructose dehydrates to HMF. The fructose transport allows overcoming the limitation of thermodynamic equilibrium of glucose-fructose isomerization, achieving 70% glucose conversion instead of 46% without fructose transport. However, the reversibility process between the two aqueous phases limited the final yield of HMF (4%), although selectivity was high (70%) (Scheme 93).



**Scheme 93** Steps for the synthesis of HMF from glucose in a biphasic system.

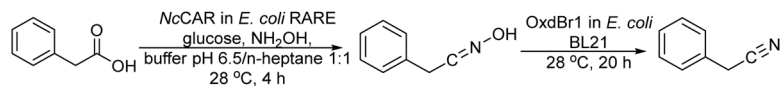
More recently, He and co-workers reported two chemo-enzymatic one-pot processes to valorize corncob into furfuryl amine and furoic acid<sup>370</sup> in a biphasic medium. In these processes, performed in a sequential mode, biomass is first converted to furfural in the presence of a heterogeneous acid catalyst and subsequently biotransformed into furoic acid or furfuryl amine. For instance, corncob was transformed into furfural using an optimized heterogeneous acid catalyst based on tin-based solid acid Sn-bentonite (Sn-BTN) and methyl isobutyl ketone (MIBK)-H<sub>2</sub>O as the optimized biphasic medium at 170 °C, yielding 53.3% furfural. After this, the temperature was decreased to 30 °C, pH was adjusted, and *Brevibacterium lutescens* whole cells were added to the reaction medium. The enzymatic step achieved 100% furoic acid within 18 h (Scheme 94a). In a similar way, for the production of furfuryl amine, corncob was converted into furfural using sulfonated aluminium-based alkaline-treated graphite (Al-AG) as a catalyst in a  $\gamma$ -valerolactone-water biphasic medium (1:4) at 180 °C, for 40 min, and a maximum furfural yield of 56.8% was obtained. Then, the enzymatic step was performed at 35 °C by adding *Aspergillus terreus* whole cells expressing  $\omega$ -transaminase and isopropyl amine as the amine donor. After 2 h, furfuryl amine was obtained in 79.0% yield (Scheme 94b). Recently these results were improved by using a robust mutant of *Aspergillus terreus* whole cells achieving 90–93% yield of furfuryl amine, at higher substrate concentration (500 mM).<sup>327,371</sup>

Recently, it has been reported that carboxylic acids, which are easily available from biomass resources, can be converted



**Scheme 94** Chemo-enzymatic one-pot processes to valorize corncob into (a) furoic acid and (b) furfuryl amine in a biphasic medium.





Scheme 95 Chemo-enzymatic conversion of carboxylic acids into nitriles in biphasic media.

into nitriles through a new chemo-enzymatic cascade process in a biphasic system.<sup>372</sup> The strategy combines the aldehyde synthesis from carboxylic acids using a carboxylic acid reductase (CAR) followed by chemical *in situ* aldoxime formation and its subsequent dehydration to nitrile catalyzed by an aldoxime dehydratase (Scheme 95). The process was performed in a biphasic buffer/heptane system in a sequential mode, where first CAR harbouring cells were incubated with hydroxylamine for 4 h. Then, aldoxime dehydratase (OxdBr1) harbouring cells were added and reaction proceeded for 24 h. The cytotoxic activity of the aldehyde intermediate on CAR was avoided by removing the aldehyde as aldoxime, while a key point was to select an aldoxime dehydratase able to work under the aerobic conditions required for the CAR enzyme. Interestingly the presence of the organic phase improved product recovery of aliphatic and volatile nitriles with respect to the single phase buffer media.

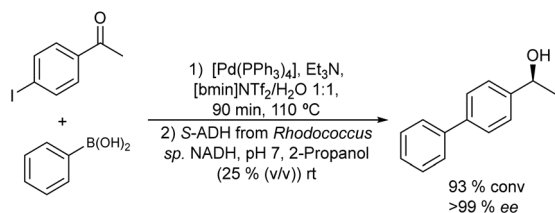
A biphasic system composed of an ionic liquid (IL) and an aqueous buffer was used by Schmitzer *et al.*<sup>373</sup> to synthesize chiral biaryl alcohols by combining the chemocatalyzed Suzuki cross-coupling reaction and the enantioselective enzymatic bioreduction. Optimization of the Suzuki step showed that the water-immiscible (1-butyl-3-methylimidazolium bis(trifluoromethylsulfonyl)imide) [bmim][NTf<sub>2</sub>] was optimal for the cross-coupling reaction between 4-iodoacetophenone and boronic acids. Additionally, for the enzymatic step, lyophilized cells of *E. coli* containing an over-expressed organic solvent tolerant ADH were used. In good agreement with the results reported by Gröger *et al.*<sup>374</sup> in aqueous media, it was found that the Pd catalyst did not have a negative impact on the catalytic activity of ADH, while the base and the boronic acid had an important detrimental effect on the

enzymatic activity. By changing the nature of the base (triethylamine instead of K<sub>2</sub>CO<sub>3</sub>) and controlling the equivalents of boronic acid during the first step, the one pot reaction was performed successfully in a sequential mode. Thus, when the Suzuki reaction, performed at 110 °C, was over, the system was cooled at room temperature and the *E. coli* cells, along with the required additives, were added to the reaction media. The cascade sequence proceeded (Scheme 96) successfully with a global conversion higher than 94% and the chiral alcohol was obtained in >99% ee. The main advantage of this one-pot biphasic reaction is that both phases containing the different catalysts can be easily separated and reused (the cells in the aqueous phase and the Pd complex in IL). Additionally, the biphasic system was successfully applied to the synthesis of a variety of biaryl chiral alcohols.

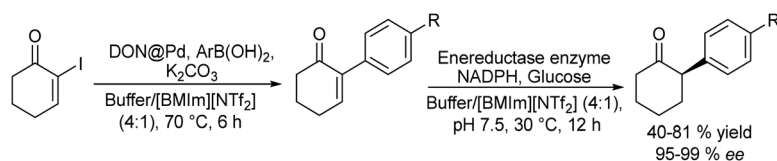
More recently Jiang *et al.*<sup>375</sup> used the same biphasic buffer/[bmim][NTf<sub>2</sub>] media to perform the synthesis of chiral alpha arylcycloketones in a sequential mode. The process involves as the first step the palladium catalyzed Suzuki cross-coupling of 2-iodocyclohexenones with boronic acids, followed by the bioreduction of the alkene group using *E. Coli* whole cells expressing ene-reductase (Scheme 97).

To overcome the inhibitory effect on the enzyme activity of the triphosphine ligands of the Pd homogeneous catalyst, the first step was performed using Pd-immobilized on dendritic organosilica nanoparticles (DON@Pd) as a heterogeneous catalyst. Under optimized reaction conditions of the chemo-enzymatic process, Pd-catalyzed C–C formation took place in the IL phase, and the enzymatic reduction in the buffer phase was satisfactorily achieved and applied efficiently to the synthesis of a variety of chiral alpha arylcycloketones. Moreover, to access enantiocomplementary products site-directed mutation of the ene-reductase was performed.

Cycloalkenes are important products of the petrochemical industry and are employed in several processes like solvents, building blocks for cyclic compounds, *etc.* Ward *et al.* developed a chemo-enzymatic process that allows access to cycloalkenes (C5–C7) from renewable sources.<sup>376</sup> The authors performed a cascade process, where a diacid substrate is bis-decarboxylated *via* a decarboxylase enzyme (UndB), followed by a ring-closing metathesis (RCM) catalyzed by ruthenium Grubbs' catalyst(1) (Scheme 98).

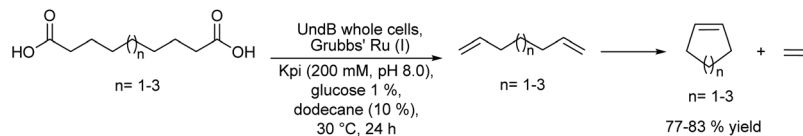


Scheme 96 Synthesis of biaryl chiral alcohols by combining the chemocatalyzed Suzuki cross-coupling reaction with enantioselective enzymatic bioreduction in a sequential mode and in biphasic media.

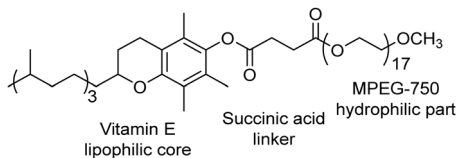


Scheme 97 Synthesis of chiral  $\alpha$ -aryl cycloketones by combining the chemocatalyzed Suzuki cross-coupling with enzymatic bioreduction in biphasic media.





Scheme 98 Chemo-enzymatic conversion of diacids into cycloalkenes in biphasic media and in a concurrent mode.



Scheme 99 Structure of the TPGS-750-M surfactant.

The decarboxylase UndB expressed in *E. Coli* whole cells was identified among different decarboxylases, as the most active, while a biocompatible commercial Grubbs' ruthenium(I) catalyst was selected for the RCM step. The low solubility of the substrate in water limited the yield of the cycloalkene, and therefore to increase substrate solubility different biphasic and micellar systems were studied. Thus, using a biphasic medium composed of water/*n*-dodecane (10%) the chemo-enzymatic process could be successfully performed in sequential and concurrent modes achieving the corresponding cycloalkenes in 87–90% yield. Interestingly, the authors developed engineered *E. coli* cells, to convert oleic acid into diacids, which when combined with engineered *E. coli* cells expressing lipase, the enzyme-optimized decarboxylase and the Ru catalyst were able to transform olive oil into different cycloalkenes in moderate yields (29–33%).

**4.3.2. Compartmentalization using the micellar strategy.** Formation of micelles *via* self-aggregation of surfactant molecules in water provides a useful environment where the hydrophobic region inside the micelle can act as a confined reaction medium for lipophilic substrates and chemical catalysts, while the biocatalyst remains in the hydrophilic aqueous phase. These systems represent a type of spatial compartmentalization where two catalytic processes that co-exist can be separated by the wall-solvent interactions of the micelles, thus overcoming the organic solvent issues encountered in traditional catalysis.

The use of aqueous micellar systems as a new and efficient alternative to traditional organic solvents for metal-catalyzed processes such as Heck, Suzuki, Sonogashira C–C couplings has been recently demonstrated by Lipshutz *et al.*<sup>377</sup> With this idea, micelles formed by a tailor-made TPGS-750-M surfactant

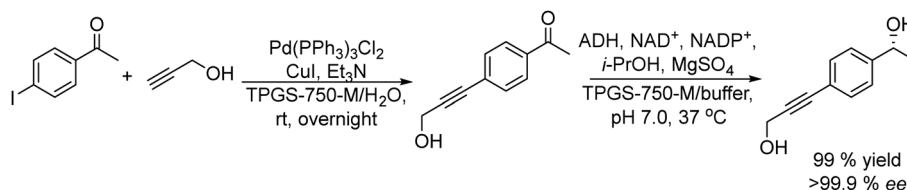
were applied by the authors<sup>378</sup> in some chemo-enzymatic one-pot processes by combining metal-catalyzed reactions with bioreduction using alcohol dehydrogenase (ADH) to produce chiral secondary alcohols. The TPGS-750-M surfactant, containing racemic vitamin E as the hydrophobic tail (Scheme 99), is able to form non-anionic micelles of 50 nm size fully compatible with the ADH. In this system, the metal-catalyzed reaction takes place inside the micelle, while the bioreduction occurs in the aqueous phase. Moreover, the authors showed that micelles are responsible for increasing the enzymatic activity towards highly lipophilic substrates, acting as reservoirs for substrates, catalysts, and products of enzymatic reduction, minimizing enzymatic inhibition and moderating the degree of enzyme saturation.

Different chemo-enzymatic processes involving Pd-catalyzed Sonogashira and Heck couplings, Au-Ag-catalyzed alkyne hydration and asymmetric Rh-catalyzed 1,4-addition were successfully coupled after adjusting substrate concentration and pH with the ADH catalysed reduction in a sequential mode. An example of the combination of Sonogashira cross-coupling with bioreduction in the micellar system is presented in Scheme 100.

The biocompatibility of TPGS-750-M allowed the efficient application of the aqueous micellar approach in a variety of two-step and multistep chemo-enzymatic sequences involving ene-reductases<sup>379</sup> and alcohol dehydrogenases.<sup>380</sup>

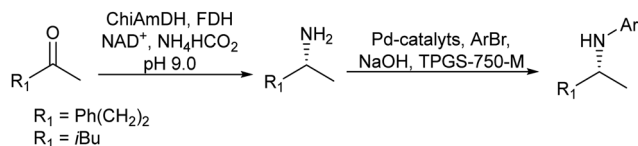
Turner *et al.*<sup>381</sup> also used this surfactant to combine biocatalyzed chiral amine synthesis with the Pd-mediated Buchwald–Hartwig amination to obtain a variety of chiral *N*-aryl amines, which are key scaffolds of many active pharmaceutical components. Amine dehydrogenases (AmDHs) were used in the first step to produce chiral amines from prochiral ketones that were coupled in the second step with aryl bromides in a sequential mode. The addition of the surfactant in the second step allowed retaining the reactants and catalyst inside the micelles, thus preventing the deactivation of the Pd catalyst by the species present in the aqueous media (Scheme 101).

A similar strategy was adopted by Paradisi and Heckman<sup>382</sup> by using  $\omega$ -transaminases in the first step, while in the second step, the coupling of the chiral amine with aryl bromides was performed in a biphasic toluene–buffer medium, instead of micelles, to avoid the deactivation of the Pd catalyst. A variety of



Scheme 100 Combination of Pd-catalyzed Sonogashira cross-coupling with bioreduction in a micellar system.





**Scheme 101** Synthesis of chiral aniline derivatives by combining ketone amination with Buchwald–Hartwig amination in a micellar system.

chiral *N*-arylamines in excellent enantioselectivities (>99.5% ee) and high yields (up to 89%) were obtained.

Hastings *et al.*<sup>383</sup> also used the TPGS-750-M surfactant to combine efficiently two transition metal-catalyzed steps (Heck and metathesis reactions) with enzymatic hydrolysis in a concurrent mode. The reactions proceeded with high yields under mild conditions and at ambient temperature.

Gonzalez-Sabin *et al.*<sup>384</sup> developed a chemo-enzymatic one-pot process in a sequential mode to obtain stilbene derivatives from carboxylic acids. The process combines enzymatic decarboxylation with Pd catalyzed Heck coupling in aqueous media in the presence of different surfactants. Particularly, the Cremophor EL<sup>®</sup> surfactant, a polyethoxylated castor oil classically used in the formulation of low water soluble drugs, resulted in the highly efficient decarboxylation of *p*-hydroxycinnamic acid into 4-vinylphenol using phenolic acid decarboxylase (PAD), which was coupled with the Pd-catalyzed Heck reaction with iodobenzene to obtain (*E*)-4-styrylphenol (Scheme 102).

Interestingly, the micellar compartmentalization avoids the inhibitory effect of the enzyme on the Pd catalyst, allowing superior performances of the chemo-enzymatic process when compared with the process performed using a mixture of water-eutectic solvent (choline chloride/glycerol (1ChCl/2Gly:H<sub>2</sub>O) as the reaction medium with free or immobilized PAD.<sup>385</sup>

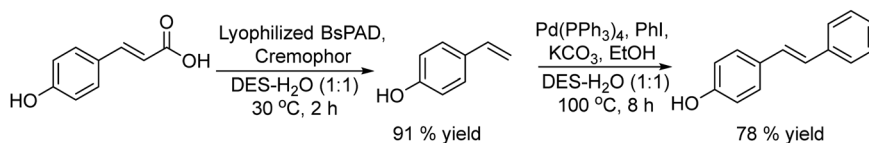
An interesting study recently reported by Kunz *et al.*<sup>386</sup> on the impact of the solvent when combining transition metals, biocatalysts and hydrophobic substrates in one-pot chemo-enzymatic reactions concluded that, while using micellar solutions can improve the process, the formation of micelles protecting the enzyme is not the key factor for the success of the process. In fact, the authors showed that when a chemo-enzymatic process combining Heck cross-coupling and ADH bioreduction of ketone was performed in a binary mixture of water/isopropanol (67/33 (w/w)), the enzyme remained partially undissolved and folded and the transition metal catalyst did not have a negative impact on its activity, while the yield of the target compound increased with respect to the process performed in the presence of a surfactant (TPGS-750-M). Moreover, further improvement in performance was achieved in a surfactant-free microemulsion

composed of water/isopropanol/benzyl alcohol, concluding that the solubility and stability of the components in the reaction media are the key parameters controlling the performance of the cascade process.

The use of particle-assisted emulsions, also referred to as Pickering emulsions, is an alternative to the use of molecular surfactants to confine the catalytic species. Recently, Wu *et al.*<sup>387</sup> reported the Pickering chemo-enzymatic cascade for the one-pot synthesis of chiral esters from ketones (Scheme 103). The authors prepared a silica nanoparticle catalyst containing anchored chiral Ru(II) complexes that act not only as heterogeneous metal catalysts to reduce the ketone into the alcohol, but also as active emulsifiers that form Pickering emulsions to encapsulate the lipase CALB, which catalyzes the subsequent enantioselective esterification of the alcohol. Thus, the first step was performed through an asymmetric transfer hydrogenation promoted by an optimized Ru(II) catalyst using water as a solvent, achieving 100% conversion and ee >90%. Then, the Pickering emulsion was formed by adding hexane directly to the aqueous solution of the first-step reaction by vortex, and then CALB along with the substrate vinyl butyrate was added to the reaction system for the second step, and the reaction proceeded at room temperature for over 12 h, affording 38% of the chiral ester (ee 99%). Interestingly, the particle-stabilized emulsion gave a much better conversion than the classical two-phase systems, which can be attributed to the large-interface area in the Pickering emulsion and the high local concentration of the chiral Ru complex on the particles.

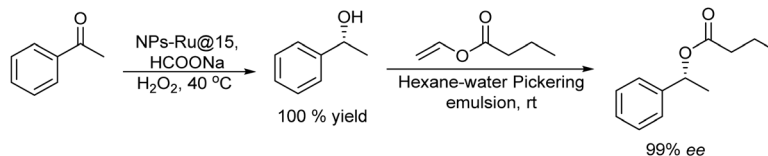
#### 4.3.3. Compartmentalization by encapsulation of catalysts.

The encapsulation of chemo- and biocatalysts is another alternative for the compartmentalization strategy, where the chemo- or the biocatalyst is shielded from external incompatible catalytic species. For instance, Kourist *et al.*<sup>388</sup> developed a chemo-enzymatic new cascade process to obtain biobased antioxidants by combining the decarboxylation of cinnamic acid derivatives catalysed by an encapsulated co-factor-free decarboxylase and the metathesis reaction of the styrene intermediate catalysed by Ru catalysts (see Scheme 104). The study of both steps separately showed that the appropriate ruthenium catalyst for the metathesis step did not show suitable activity under aqueous conditions and required the use of an organic solvent, which in turn, was detrimental for the enzyme stability. The authors designed an elegant approach where the enzyme was entrapped into poly(vinyl alcohol)/poly(ethyleneglycol) (PVA/PEG) cryogels to increase the enzyme stability in organic solvents. Thus, the enzyme remains in an aqueous environment while keeping the conditions hydrophobic for the Ru catalyst, and the substrates

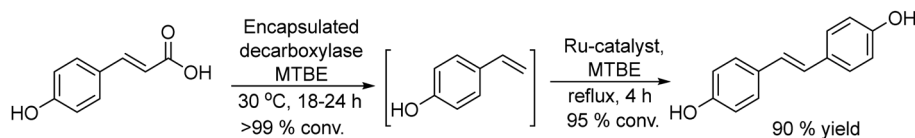


**Scheme 102** Combination of a biocatalyzed decarboxylation step with a Heck reaction in a micellar system to synthesize stilbene derivatives from carboxylic acids.





Scheme 103 Combination of symmetric transfer hydrogenation of ketone with bioesterification in Pickering emulsion.



Scheme 104 Combination of biodecarboxylation with metathesis using the encapsulated enzyme.

and products can freely diffuse through the gel. The chemo-enzymatic process was performed in an optimized organic solvent (methyl *tert*-butyl ether) in a sequential mode, wherein the solution from the enzymatic step was pre-dried with anhydrous  $\text{MgSO}_4$  prior to addition of the Ru catalyst. This synthetic procedure allowed obtaining, for instance, the antioxidant 4,4'-dihydroxystilbene (Scheme 104) in an overall yield of 90%. An interesting advantage is the easy removal of the entrapped enzyme by filtration, which simplifies downstream processing. This approach has high potential to be applied to a wide range of chemo-enzymatic reactions, where enzymes with low tolerance to organic solvents are involved.

Encapsulation of chemical catalysts within protein frameworks, which are known as artificial metallo enzymes,<sup>389</sup> is another strategy to separate biocatalysts from chemo-catalysts in cascade processes. This strategy has been mainly applied to catalysts based on organometallic complexes, where the mutual deactivation of the enzyme and the metal complex is commonly observed. Thus, Ward *et al.*<sup>390</sup> incorporated a biotinylated iridium complex  $[\text{Cp}^*\text{Ir}(\text{Biot-}p\text{-L})\text{Cl}]$  within streptavidin (Sav) creating a novel artificial transfer-hydrogenase (ATHase), where the iridium complex is protected by the protein from other catalytic species outside the Sav shell (Fig. 1).

The authors performed a variety of concurrent cascades by combining the ATHase with several co-factor-dependent redox enzymes using sodium formate as a hydride source. As an example, in Scheme 105 is presented the synthesis of *L*-pipecolic acid from *L*-lysine.

Following a similar strategy, the authors also developed an NAD(P)H-dependent artificial transfer hydrogenase (ATHase), which enabled imine reduction with NADPH as the hydride source and which was concurrently regenerated by a glucose dehydrogenase (GDH) using glucose as the substrate. The integration of this catalytic system with a catalase and a monoamine oxidase enables the production of enantiopure amines in a four-enzyme cascade process under physiological conditions.<sup>391</sup> The benefit of compartmentalizing the Ir complex inside the protein was the improvement of the Ir turnover number (TON) of at least 30 (6% yield) for the free

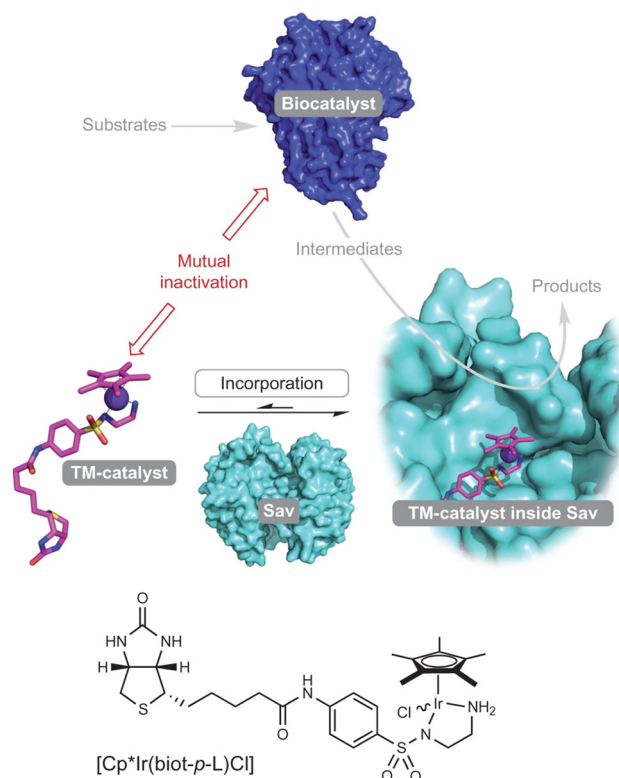
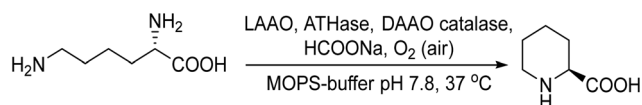


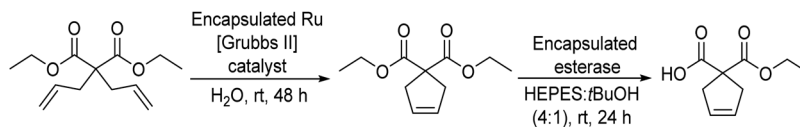
Fig. 1 Reaction cascades resulting from combining an ATHase with a biocatalyst. Reproduced with permission: Copyright 2013, Springer Nature (adapted from ref. 390).



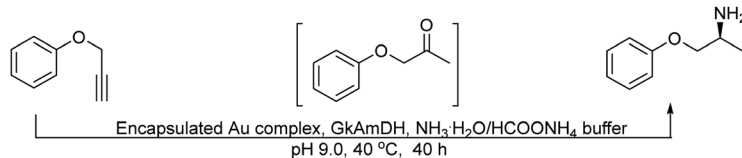
Scheme 105 Combination of ATHase with *L*-amino acid oxidase (LAO) and *D*-amino acid oxidase (DAAO) in a concurrent mode to produce *L*-pipecolic acid from *L*-lysine. MOPS-buffer: 3-morpholinopropane-1-sulfonic acid.







**Scheme 108** A chemo-enzymatic process to obtain cyclic malonic acid monoesters using encapsulated chemo- and biocatalysts.

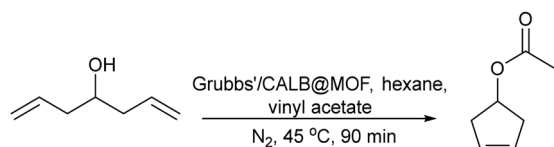


**Scheme 109** Synthesis of chiral amines from propargylethers by combining alkyne hydration with an encapsulated Au complex with bioamination in a concurrent mode.

ketones, can be performed in a concurrent mode, owing to the encapsulation of the gold catalyst preventing enzyme deactivation in the aqueous buffer reaction media. The process provides access to a wide range of chiral amines (25 examples) in 82–97% yield with 96–99% ee. Moreover, the enzyme and chemo-catalyst could also be recovered and reused for five consecutive runs, representing a useful method for the preparation of chiral amines.

Recently, Yang *et al.*<sup>398</sup> have reported the simultaneous encapsulation of a lipase CALB and Grubbs' catalyst, in a multi-compartmental MOF microreactor. The bifunctional catalyst was synthesized through a Pickering double emulsion-directed interfacial synthesis method, by adding both catalysts during the MOF synthesis, specifically MOF-74. The catalytic performance of the prepared Grubbs'/CALB@MOF was tested in the ring-closing metathesis/transesterification cascade process of 1,6-heptadien-4-ol as a model substrate to form cyclopentenyl acetate in a concurrent mode (Scheme 110). After optimization of the lipase/Grubbs' catalyst ratio a conversion of 97.6% and 98% selectivity to the target compound could be achieved.

Interestingly, the activity of the Grubbs'/CALB@MOF catalyst was considerably superior to those exhibited by the homogeneous counterparts (Grubbs'/CALB), a physical mixture of the catalysts (Grubbs'@MOF/CALB@MOF), and traditionally immobilized catalysts on MOF (Grubbs'@MOF/CALB@MOF) and on mesoporous SBA-15 (Grubbs'/CALB@SBA-15). The higher activity exhibited by the Grubbs'/CALB@MOF catalyst is attributed to the restrained mutual inactivation and substrate channeling effects. Thus, the close confinement of the catalytic sites and the dense packing compartments of the MOF facilitate a high local

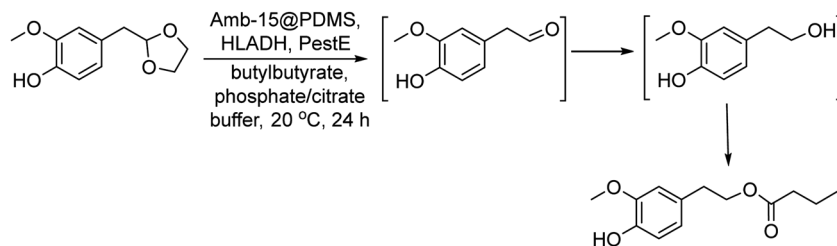


**Scheme 110** One-pot ring-closing metathesis/transesterification cascade reaction of 1,6-heptadien-4-ol to form 3-cyclopentenyl acetate in a concurrent mode.

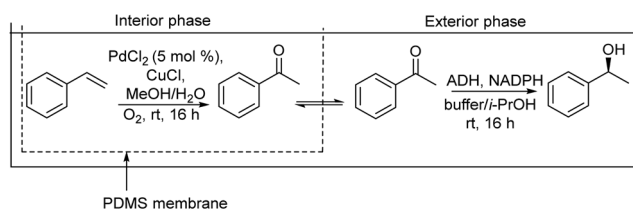
concentration and the efficient transportation of the intermediates to the enzyme sites. Moreover, the catalyst was found to be stable, retaining its activity over five consecutive runs. The combination of encapsulated solid acid catalysts with enzymatic reactions in a one pot linear cascade has been recently reported by Bornscheuer *et al.*<sup>399</sup> The authors performed the synthesis of homovanillyl butyrate (HVB), a derivative of homovanillyl alcohol (HVA) with antioxidant properties,<sup>400</sup> through a chemo-enzymatic cascade in a concurrent mode involving the deacetalization, reduction, and acylation of the lignin depolymerization product G-C2 dioxolane phenol (DOX) (Scheme 111). In this strategy, the acid catalyzed deacetalization of DOX to homovanillin (HV) in aqueous media is achieved by Amberlyst-15 encapsulated in the hydrophobic polydimethylsiloxane (Amberlyst15@PDMS). Then, the HV formed is reduced to HVA by horse liver alcohol dehydrogenase (HLADH) recombinantly produced in *E. coli*, preventing the accumulation and polymerization of HV. Then, through an acyl transferase reaction (using an acyl-transferase/hydrolase variant optimized by the authors (PestE)) the HVA is transformed into butyl ester by transesterification with butyl butyrate, shifting the equilibrium of the HLADH reduction step. The encapsulation of the solid acid catalyst not only prevents the enzyme deactivation by the acid sites, but also allows two incompatible reactions in water media such as deacetalization and transesterification to take place in the same reaction vessel. This example represents an interesting approach to valorize lignin derivatives such as DOX, which is accessible through diol-assisted lignocellulose acid catalyzed depolymerization giving lignin derived acetals.

**4.3.4. Compartmentalization by membrane filtration.** The use of porous membranes to confine chemo- and biocatalysts is another strategy to generate separate compartments where the membrane serves as a filter that allows the passing of products from one compartment to the other. Pioneering work on this strategy was reported by the Gröger group<sup>401</sup> using highly hydrophobic polydimethylsiloxane (PDMS) thimbles for combining Wacker-oxidation of styrenes to acetophenones catalysed by Pd and Cu species with asymmetric bioreduction of the ketone intermediate to chiral alcohols catalysed by an ADH (Scheme 112).





Scheme 111 Synthesis of homovanillyl butyrate by combining acetal hydrolysis with bioreduction followed by bioesterification.



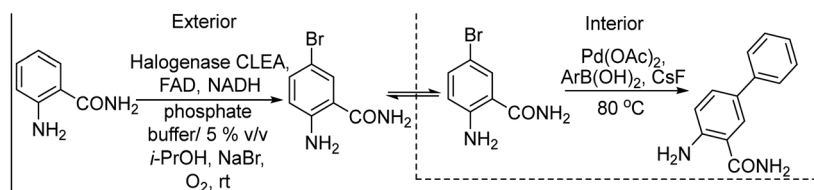
Scheme 112 Combination of Wacker oxidation and enzymatic reduction using a PDMS thimble as the compartmentalization strategy.

Preliminary studies showed that Cu species had a strong negative effect on the enzyme activity. Therefore, to prevent the catalyst deactivation the metals and enzymes were separated using the PDMS thimble. Thus, the Wacker oxidation occurs inside the PDMS membrane, and due to its hydrophobic properties, it allows the intermediate acetophenone formed inside to pass through the membrane to the exterior where the stereoselective enzymatic reduction takes place. Moreover, the membrane retains the metals inside, and the enzyme and co-factor outside, achieving an effective compartmentalization. Following this strategy, the process was performed in a concurrent mode; however, the oxidation in the interior leads to only 20% conversion, as a consequence of the extraction of the methanol (the solvent component required for an efficient Wacker oxidation) into the exterior. To suppress the methanol leaching, the cascade process (Wacker oxidation and enzymatic reduction) was performed in a sequential mode. Thus, ADH and the co-factor were added in a buffer/isopropanol solution to the exterior after completion of the initial Wacker oxidation in the interior. Following this method, the accumulated acetophenone was converted in high yield into the chiral 1-phenylpropanol. The process was successfully extended to a variety of substituted styrenes that were converted into the corresponding chiral 1-phenylpropanol derivatives in high yield and 94–99% ee. Interestingly, the Pd catalyst could be easily recovered and recycled over 15 consecutive cycles and remained active for at least 60 days.

A similar strategy was used for deracemization of achiral 1-phenylethanol derivatives into (*R*)-phenyl ethanol derivatives.<sup>402</sup> The racemic mixture of alcohols is oxidized into acetophenone in the interior chamber of PDMS using  $\text{MnO}_2$  as the oxidant, which is detrimental for the enzyme (ADH). The acetophenone passes through the membrane to the exterior chamber, and after oxidation completion, the ADH is added into the exterior chamber where the ketone is enantioselectively reduced. The process performed in a sequential mode could be applied to the deracemization of a wide range of methyl- and chloro-substituted 1-phenylethanol derivatives achieving up to 93% yield and >99% ee.

Following the PDMS thimble compartmentalization method, Latham *et al.*<sup>403</sup> combined the regioselective flavin-dependent halogenase (Fl-Hal) enzyme with palladium-catalysed Suzuki–Miyaura cross-coupling to perform the regio-controlled arylation of a variety of aromatic compounds. Preliminary optimization studies showed that the enzyme inhibits the metal catalyst due mainly to metal complexation. The PDMS thimble approach overcame this drawback and improved the synthetic efficiency. All reagents were placed in the reaction system from the beginning of the reaction in an aqueous buffer. First, the enzymatic halogenation takes place in the exterior of the thimble at room temperature and after completion, temperature is adjusted to 80 °C to perform the Pd catalysed cross-coupling inside the thimble (see Scheme 113). Moreover, the authors combined the use of halogenase crosslinked aggregates (CLEAs) with membrane compartmentalization, which allowed decreasing the Pd loading from 50 mol % to 2 mol %. The chemo-enzymatic cascade process allowed the regio-controlled arylation of a variety of inactivated aromatic compounds such as benzamides, isoquinolines and indoles, which usually cannot be accomplished through biocatalyzed or chemocatalyzed processes alone.

Rudroff *et al.*<sup>404</sup> performed a chemo-enzymatic cascade reaction in a concurrent mode by combining the Cu/Pd catalyzed C–C cross-coupling of thioesters with boronic acids (Liebeskind and Srogl (L–S) coupling) and the subsequent ADH catalyzed



Scheme 113 Regio-controlled arylation of aromatic compounds in a PDMS thimble system.



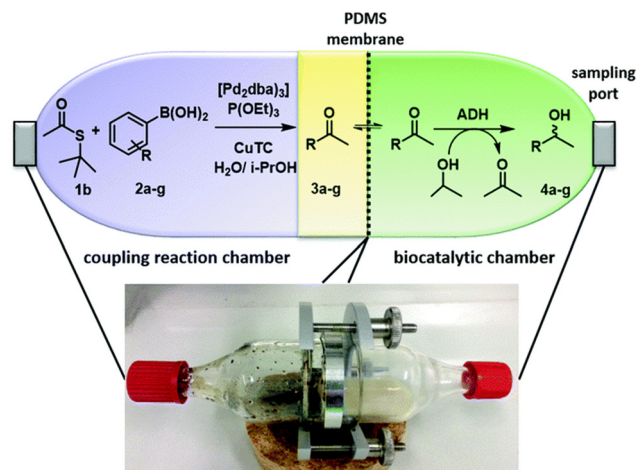


Fig. 3 Reactor device for a chemo-enzymatic reaction sequence in a concurrent fashion.  $\text{Pd}_2(\text{dba})_3$ : tris(dibenzylideneacetone)-dipalladium (0),  $\text{P}(\text{OEt})_3$ : triethyl phosphite,  $\text{CuTC}$ : copper-(*l*)-thiophene-2-carboxylate. Reproduced with permission: Copyright 2018, The Royal Society of Chemistry (adapted from ref. 404).

reduction of the ketone intermediate in a reactor with two compartments separated by a PDMS membrane (see Fig. 3). Although L-S coupling generally works in organic solvents, previous studies showed that *t*-butyl thioester is stable to the hydrolysis when the L-S reaction is performed in aqueous media. Thus, in the cascade process, this substrate could be successfully coupled with boronic acids in a water-isopropanol solvent, yielding the corresponding ketone intermediate, which is transported to the enzymatic compartment where the ADH along with the co-factor ( $\text{NADP}^+$ ) in a buffer solution at pH 8 are retained, giving the chiral secondary alcohol. The control of the pH was key for the enzymatic step since the acidic pH caused mainly by the excess of boronic acid used deactivated the enzyme. The compartmentalized chemo-enzymatic process in a concurrent mode was extended to a variety of halogenated phenylboronic acids and the corresponding chiral secondary alcohols were obtained in up to 99% yield and high enantioselectivity (>99% ee) over two steps.

**4.3.5. Compartmentalization using continuous flow reactors.** Continuous-flow processing is emerging as one of the techniques that can significantly impact the synthesis of organic compounds contributing to the development of green and sustainable industrial processes.<sup>405</sup> In general flow operations are more advantageous than batch processes as they allow the setting up of the reaction parameters and their monitoring more easily, resulting in a more reliable and reproducible process with waste minimization. Therefore, in the last few

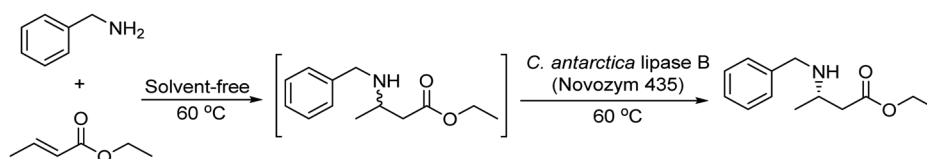
years, the development of the synthesis of fine chemicals in flow for both biocatalyzed<sup>406</sup> and chemocatalyzed processes<sup>407</sup> has been receiving increased attention.

The high versatility of the flow systems towards various reaction conditions allows their combination to perform reaction sequences providing very different reaction conditions for the catalysts, but moreover the flow reactors can be combined with other technologies that can result in the development of entirely automated process with an enlarged throughput.

While immobilized enzymes have been used for a long time in flow systems,<sup>408</sup> the combination of chemo-enzymatic reactions in separate flow reactors has recently emerged as an approach for effective compartmentalization of catalysts and reaction conditions that avoid incompatibility problems. For instance, Gröger *et al.*<sup>409</sup> developed a solvent-free sequential chemo-enzymatic continuous process for the production of chiral  $\beta$ -amino acid esters. Thus, ethyl (*S*)-3-(benzylamino)butanoate (Scheme 114) was obtained by combining the thermal aza-Michael addition of benzylamine to *trans*-ethyl crotonate with a subsequent lipase-catalyzed kinetic resolution *via* enantioselective aminolysis of the racemic intermediate product. The reactor set-up combined a plug-flow reactor for the thermal aza-Michael reaction and a packed-bed reactor for the lipase Novozym 435 (which is commercially available *Candida antarctica* lipase B (CALB)) physically immobilized on a mesoporous poly(methyl methacrylate) support.

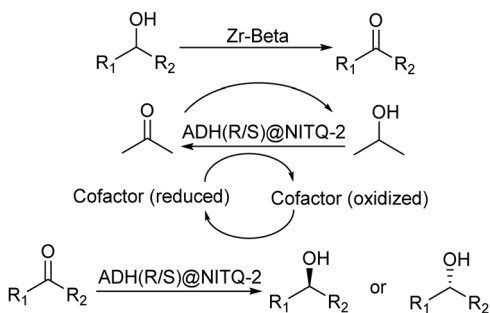
The combined reactors worked continuously for 80 h without significant loss of enzyme activity. The target  $\beta$ -amino ester was obtained with 52% yield and enantiomeric excess of >98%, which is superior to that obtained in a batch mode. The combined flow system allows for higher substrate concentrations, while the productivity of the process is comparable to established industrial processes.

Corma *et al.*<sup>410</sup> developed a continuous flow system to deracemize valuable chiral alcohols through a chemo-enzymatic process by combining two-packed bed reactors (Scheme 115). In a first reactor, the racemic alcohol was oxidized to the corresponding prochiral ketone *via* Oppenauer oxidation using a Zr-beta zeolite as a catalyst at 60 °C and using acetone as the hydrogen acceptor. Then, after removal of the excess of acetone and further dilution with buffer solution, the ketone intermediate was pumped into a second packed-bed reactor where an ADH supported on a 2D zeolite (ITQ-2) performed the stereoselective reduction at 25 °C. A variety of alcohols were deracemized by this procedure in high yields and enantiomeric excess (>99%), independently of the ADH stereo-preference. Moreover, the system could be operated, at least, for 16 days. An interesting feature of this chemo-enzymatic process is that the system meets the principle of



Scheme 114 Solvent-free chemo-enzymatic reaction sequence for the synthesis of  $\beta$ -amino acid ester in flow reactors.

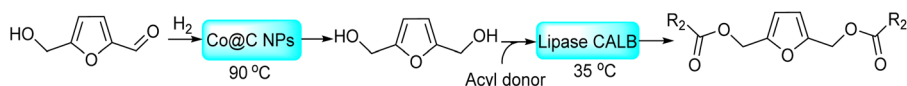




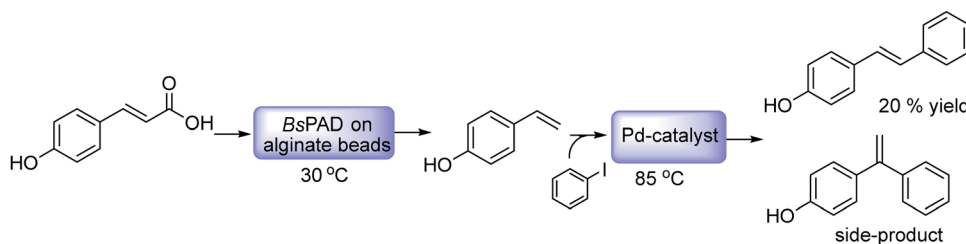
**Scheme 115** Chemo-enzymatic synthesis of chiral alcohol from racemic mixtures using two fixed bed reactors.

100% atom economy because the isopropanol co-produced in the first step acts as a co-factor regenerator in the bioreduction step, while the acetone accompanying the target chiral alcohol is reincorporated at the outset of the process.

The same authors<sup>411</sup> developed a chemo-enzymatic process to prepare diesters of 2,5-bis(hydroxymethyl)furan (BHMF), useful as biobased plasticizers that can be substitutes of phthalates derived from petroleum.<sup>412</sup> Starting from 5-hydroxymethylfurfural (HMF), the process involves as a first step the hydrogenation of HMF into 2,5-bis(hydroxymethyl)furan (BHMF) using monodispersed metallic Co nanoparticles with a thin carbon shell (Co@C) as a catalyst followed by the BHMF bioesterification with vinyl esters using a supported commercial lipase (Novozym 435) (Scheme 116). The process was performed in an integrated two-step continuous flow reactor by combining two fixed bed reactors. In the first reactor the hydrogenation of HMF to BHMF was performed at 90 °C and 10 bar H<sub>2</sub>, using methanol as a solvent. After methanol evaporation, a solution containing the vinyl ester in 2-methyltetrahydrofuran (2-MTHF) was used as the feed for the second fixed bed reactor containing the lipase and heated at 35 °C. The combination of two flow reactors working under optimized reaction conditions (for reduction and subsequent esterification) allowed achieving ~90% overall yield of the diesters of BHMF, while the activity was retained at least for 60 h of operation.



**Scheme 116** Synthesis of diesters of 2,5-bis(hydroxymethyl)furan from HMF by combining reduction with bioesterification in two continuous flow reactors.

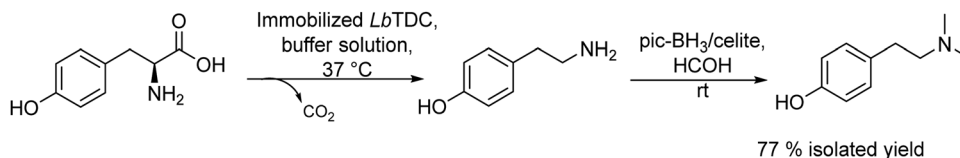


**Scheme 117** Synthesis of (*E*)-4-hydroxy-stilbene from *p*-coumaric acid by combining decarboxylation with Heck reaction in a two-step continuous flow reactor.

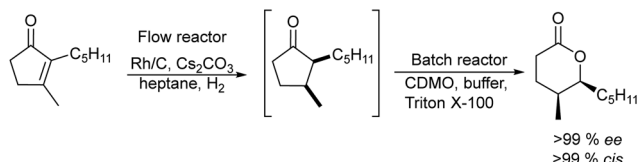
Recently, Kourist *et al.*<sup>8</sup> reported the synthesis of stilbene derivatives of interest in the pharmaceutical industry due to their anti-oxidant and anti-inflammatory activities. For instance, the synthesis of (*E*)-4-hydroxy-stilbene was performed by a two-step continuous flow process involving the enzyme catalyzed decarboxylation of *para*-coumaric acid and subsequent Pd-catalyzed Heck cross-coupling with an aryl halide (Scheme 117). Thus, in the first fixed bed reactor the decarboxylation of *para*-coumaric acid catalyzed by an immobilized phenolic acid decarboxylase (PAD) takes place. The resulting 4-hydroxystyrene is pumped along with the aryl halide into the second reactor where the heterogeneous Pd catalyst (Sn<sub>0.79</sub>Ce<sub>0.2</sub>Pd<sub>0.01</sub>O<sub>2</sub>-d) is placed, giving the target compound. The process was successfully operated for more than 16 h. In this system the use of a choline chloride-based deep eutectic solvent (DES) played a key role to overcome the problem of solvent compatibility while improving substrate concentration (from 5 mM in buffer to 20 mM in DES). Optimization of the reaction conditions allowed broadening the concept for the synthesis of pterostilbene and resveratrol.<sup>413</sup>

Recently, the synthesis of hordenine (4-(2-dimethylamino-ethyl)phenol), a valuable phenolic phytochemical, has been performed through a novel chemo-enzymatic strategy in a fully-automated continuous flow system, starting from the broadly available *L*-tyrosine.<sup>414</sup> The two-step cascade involves as the first step the decarboxylation of *L*-tyrosine into tyramine in a buffer solution catalyzed by an immobilized tyrosine decarboxylase derived from *Lactobacillus brevis* (*LbTDC*). The *N,N*-dimethylation of the resulting tyramine is performed with formaldehyde (reductive amination) in a second reactor where the water insoluble pic-BH<sub>3</sub> (picoline borane) as a reducing agent suspended on Celite is placed. The complete conversion to hordenine is achieved in less than 5 minutes residence time, and the produced hordenine is extracted from the aqueous phase with ethyl acetate in 77% yield (Scheme 118). Compared to the metal-catalyzed *N,N*-dimethylation of tyramine, the chemo-enzymatic strategy reduces the environmental impact of the process and considerably improves its productivity.





Scheme 118 Chemo-enzymatic synthesis of hordenine from L-tyrosine in two-step continuous flow reactors.



Scheme 119 Stereoselective synthesis of natural (*S,S*)-aerangis lactone from dihydrojasnone through a chemo-enzymatic process combining flow and batch reactors.

Besides the above-presented continuous processes performed entirely by combining flow reactors, there are interesting compartmentalized chemo-enzymatic processes that combine flow reactors with batch reactors and with biphasic systems.

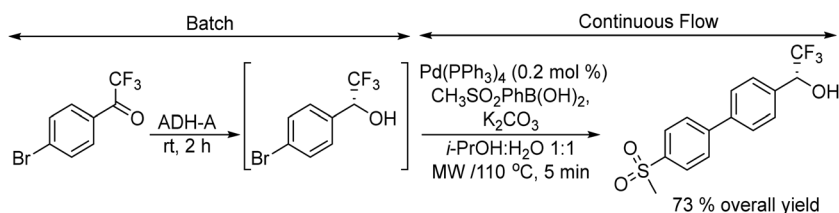
For instance, Mihovilovic *et al.*<sup>415</sup> developed a chemo-enzymatic process for the synthesis of the natural (*S,S*)-aerangis lactone, a compound of interest in the fragrance industry. The process combines the syn-hydrogenation of dihydrojasnone in a flow reactor filled with Rh/C and Cs<sub>2</sub>CO<sub>3</sub>, followed by the Baeyer-Villiger oxidation catalysed by cyclododecanone monooxygenase (CDMO) in a batch reactor (Scheme 119). The hydrogenation in the flow reactor was performed using heptane as a solvent, and the efflux of the flow reactor containing the *cis*-cyclopentanone derivative intermediate was pumped to the batch reactor containing the enzyme and the required additives in an aqueous buffer solution. To facilitate material transfer between the organic and aqueous phases the use of a non-ionic, non-denaturing surfactant (Triton X-100) was required. The *cis*-aerangis lactone was obtained as the sole product (>99% de).

Souza *et al.*<sup>416</sup> developed a chemo-enzymatic continuous flow process for the synthesis of a biaryl intermediate of odanacatib, a drug for the treatment of postmenopausal osteoporosis. The process was performed by combining asymmetric biocatalyzed reduction of 4-bromo-2,2,2-trifluoroacetophenone with ADH in isopropanol as a solvent in a batch mode with a Pd-catalyzed Suzuki–Miyaura cross coupling in a continuous reactor. Thus, the chiral alcohol intermediate obtained in the

first step and the Pd catalyst in an isopropanol solution along with an aqueous solution of the boronic acid and the required base were pumped from separate feeds through a PFA-coil reactor at 110 °C under microwave heating. The desired Odanacatib biaryl intermediate was obtained in 73% overall yield, without isolation of the chiral alcohol intermediate (Scheme 120).

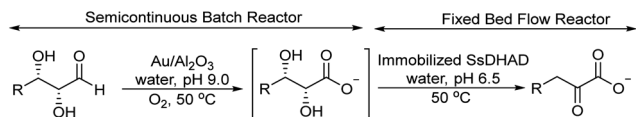
Sieber *et al.*<sup>9</sup> developed a cascade process for the direct synthesis of 2-keto-3-deoxy sugar acids, as important biobased building blocks, starting from the corresponding sugars. The process involves as the first step the chemical oxidation of the sugar, using Au supported on Al<sub>2</sub>O<sub>3</sub>, which is subsequently dehydrated using a dihydroxyacid dehydratase, namely, DHAD derived from *Sulfolobus solfataricus* (SsDHAD) (which has been described as a thermostable enzyme with activity for a broad range of sugar acids) to give the desired 2-keto-3-deoxy sugar acid (Scheme 121). Preliminary studies showed the mutual deactivation of the Au catalyst and the enzyme. To overcome this problem the catalysts were compartmentalized using a fed-batch continuous flow system. So, for instance, in the first step, the L-arabinose was oxidized to L-arabonate in a semicontinuous batch reactor (SCBR) with O<sub>2</sub> flow in the presence of Au/Al<sub>2</sub>O<sub>3</sub> and using water as a solvent yielding L-arabonate (90% yield). Then, the solid catalyst was filtered and a catalase enzyme was added to the mixture to eliminate the H<sub>2</sub>O<sub>2</sub> produced during the oxidation step that deactivates the DHAD enzyme. Subsequently the reaction mixture was introduced in a fixed bed flow reactor, which contains the SsDHAD enzyme immobilized over a Histrap FF crude column. Under these conditions, the desired 2-keto-3-deoxy sugar acid was obtained in good yields (58%). Other aldoses such as xylose, galactose and glucose were transformed into the corresponding keto-deoxy sugar acids in a yield range of 69–91%.

Very recently, Corma *et al.*<sup>417</sup> reported the synthesis of chiral 4-phenyl-2-butanamine derivatives, which are important chiral inductors and building blocks for the synthesis of drugs, starting from prochiral ketones sourced from biomass through a very high atom-economy process. The strategy involves a one-pot aldol condensation-reduction step between benzaldehyde



Scheme 120 Chemo-enzymatic continuous flow process for the synthesis of a biaryl intermediate of odanacatib by combining batch and flow reactors.





**Scheme 121** Chemo-enzymatic synthesis of 2-keto-3-deoxy sugar acids from aldoses by combining a semicontinuous batch reactor with a fixed bed flow reactor.

derivatives and acetone using a bifunctional base/metal catalyst (Pd/MgO) to perform the aldol condensation and C=C hydrogenation respectively. The prochiral 4-phenyl-2-butanone obtained is aminated into the target amine using an electrostatically immobilized transaminase (ATA) on a 2D ITQ-2 zeolite. The first step was performed in a semicontinuous batch reactor (SCBR) at 100 °C, using acetone as the reactant and solvent. After reaction completion, the excess of acetone was eliminated and the obtained 4-phenyl-2-butanone (after adjusting concentration and addition of the required additives) was pumped into a fixed bed reactor where the ATA immobilized NITQ-2 was placed. After the amination step (performed at 37 °C), the corresponding chiral amines were obtained in yields >95% and ~100% ee (Scheme 122).

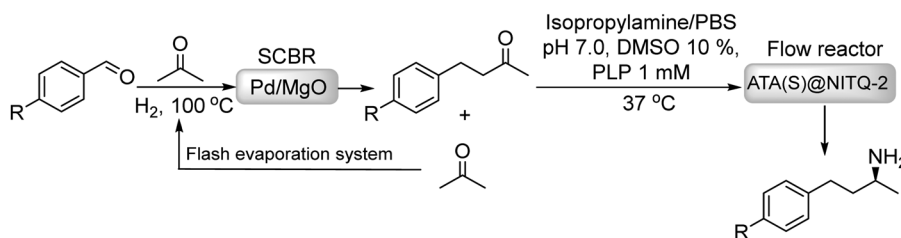
A sophisticated continuous process to produce HMF from glucose was reported by Alipour<sup>418</sup> by combining a packed-bed reactor and a biphasic system as the compartmentalization strategy (Scheme 123). The continuous process has three main steps that are shown in Scheme 123. In the first step, a glucose aqueous solution was isomerized into fructose using an immobilized glucose isomerase in a packed-bed reactor. Then, the resulting glucose/fructose solution was allowed to come into

contact with an immiscible organic phase (octanol) containing a boronic acid derivative (ABA) for preferentially complexing fructose and driving the equilibrium towards more fructose formation. This simultaneous isomerization and reactive extraction (SIRE) are coupled with a second step where the back-extraction of fructose from the organic phase into an immiscible acidic ionic liquid (IL) occurs achieving 90% yield of fructose. Finally, fructose dehydration to HMF is conducted at 50 °C in the biphasic IL/organic solvent reaction medium in the presence of an acid catalyst (HCl) resulting in high HMF yield (>80%).

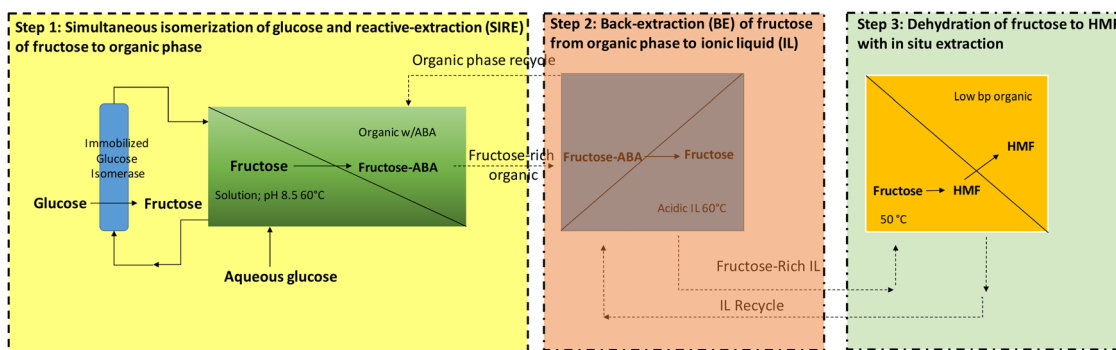
Then, the *in situ* extraction of HMF with a low boiling point organic solvent (such as THF or methyl isobutyl ketone) is performed. Interesting features of this compartmentalized process are the mild reaction conditions under which all steps (at <70 °C and at ambient pressure) are operated along with the possibility to recycle the organic phase, the IL, and THF; furthermore, this process has also been implemented using a hydrolysate from corn stover as the substrate.

## 5. Photo-biocatalytic cascades

In the last few decades, photocatalysis using visible light as the energy source has emerged as an important tool in organic synthesis. The wide substrate scope and mild reaction conditions required for photocatalytic processes provide an interesting opportunity to be combined with biocatalysis in cascade processes. Artificial photosynthesis systems (APSS) that mimic natural photo-synthesis by combining photocatalysts and

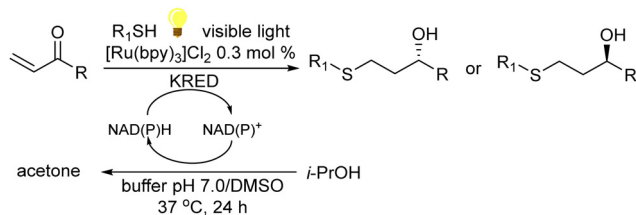


**Scheme 122** Chemo-enzymatic synthesis of 4-phenyl-2-butanamine derivatives by combining a semicontinuous batch reactor with a continuous fixed bed flow reactor.



**Scheme 123** Continuous process for production of HMF from glucose by combining a continuous flow reactor with biphasic systems.



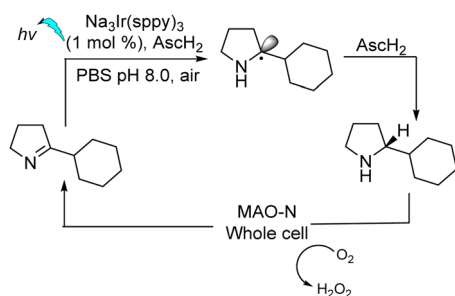


**Scheme 124** Photo-enzymatic synthesis of enantiopure 1,3-mercaptoalkanols in a concurrent mode.

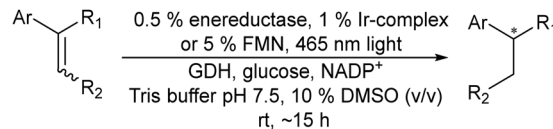
enzymes have been widely described in several reviews<sup>419–424</sup> mainly focused on the design of cascade reaction systems, such as the photoactivation of redox enzymes and photoregeneration of co-factors. In contrast, the combination of photocatalytic and biocatalytic transformations in linear cascades in which both steps contribute to the formation of the final product has been scarcely reported. The main reason may be attributed to the biocatalyst inhibition in the presence of highly reactive oxygen species or radical species generated in the photocatalytic step.<sup>425</sup> The first one-pot sequential cascade example was reported by Lauder *et al.*<sup>426</sup> for the synthesis of enantiopure 1,3-mercaptoalkanols. 1,3-Mercaptoalkanols belong to the volatile sulphur compounds (VSCs), which are responsible for the aroma of a variety of foods and beverages.

In this example the authors coupled in a concurrent mode a photocatalyzed thio-Michael addition between terminal  $\alpha,\beta$ -unsaturated ketones and thiols using  $[\text{Ru}(\text{bpy})_3]\text{Cl}_2$  as a photocatalyst under visible light irradiation with subsequent biocatalytic reduction of the ketone group using two highly selective complementary ketone reductases (KREDs) (Scheme 124). The first step was accomplished in only 5 min, while the bioreduction of the ketone group required 24 h. Following this protocol, a variety of chiral 1,3-mercaptotoalkanols were obtained in moderate to good yields (38–73%) with excellent optical purity (99%).

In another example, Wenger *et al.*<sup>427</sup> developed a photoredox biocatalytic cascade in a concurrent mode for the enantioselective synthesis of amines from imines by a cycling reaction network strategy (Scheme 125). In this approach cyclic imines were reduced into the racemic amines in the first step of the cascade by employing the water soluble  $\text{Na}_3[\text{Ir}(\text{ppy})_3]$  as a photocatalyst, under visible light irradiation. In the enzymatic step, a monoamine oxidase (MAO-N-9) is used to oxidize



**Scheme 125** Photoredox biocatalytic cascade in a concurrent mode for the enantioselective synthesis of amines from imines.

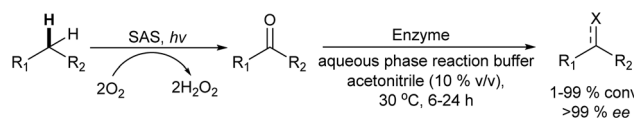


**Scheme 126** Visible-light photocatalyzed isomerization of alkenes and the subsequent double-bond reduction by an ene-reductase in a concurrent mode. GDH/glucose (glucose dehydrogenase/glucose as a co-factor regeneration system).

enantioselectively one of the enantiomers of the amine to the corresponding imine at the expense of molecular oxygen. The cascade required the presence of hydrogen atomic transfer donors such as ascorbic acid ( $\text{AsC}_2\text{H}_2$ ) or thiols that capture the highly reactive  $\alpha$ -amino alkyl intermediates formed in the photocatalyzed step. The continuous cycling of the imine reduction and enantioselective amine oxidation leads to chiral cyclic amines in high yields (95%) and enantiomeric excess (99%).

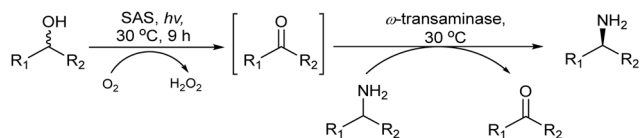
Visible-light photocatalyzed isomerization of alkenes and the subsequent C=C bond stereoselective reduction by ene-reductases were reported by Litman *et al.*<sup>428</sup> In the first step, the photoreduction of *E*- and *Z*-alkenes into a *E/Z* mixture was performed efficiently using flavin mononucleotide (FMN) or a cationic Ir complex as a photocatalyst. In the second step, ene-reductases, which exclusively reduce the *E*- or *Z*-isomer, were employed to obtain the desired chiral compound (Scheme 126). The selection of an adequate photocatalyst for the first step that does not inhibit the reductase or glucose dehydrogenase (used as a co-factor regenerating agent) was a critical point. A variety of 2-phenylbut-2-enedioic acid dimethyl ester derivatives and cyanoacrylates were used as substrates obtaining the target enantiomers with moderate to high yields and high enantioselectivity (99%). Interestingly, the authors showed how the enantio-enriched compounds obtained through the photo-enzymatic cascade could be transformed into a variety of biologically active compounds and valuable synthetic intermediates.

Schmidt *et al.*<sup>425</sup> reported a photo-enzymatic cascade process by combining photooxidation of alkanes (particularly toluene, aryl alkanes or cycloalkane derivatives) with the corresponding aldehydes or ketones followed by an asymmetric biocatalytic transformation (Scheme 127). Thus, from eleven starting alkanes, and using sodium anthraquinone sulfate (SAS) as the photocatalyst combined with 8 different enzymes, 26 products (chiral hydroxynitriles, amines, acyloins and  $\alpha$ -chiral ketones) were obtained with up to 99% ee. The degradation of substrates and inhibition of the biocatalysts due to reactive oxygen species generated in the photocatalytic step as limiting factors affecting the compatibility of both catalytic systems were resolved by using a two-phase system or by temporal and spatial separation of the catalysts.

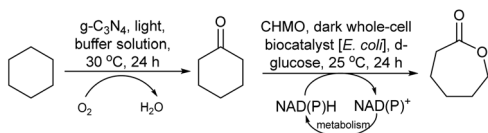


**Scheme 127** SAS-photocatalysed oxyfunctionalisation of alkenes followed by an enzymatic transformation.





Scheme 128 Photo-enzymatic cascade reaction to produce chiral amines from alcohols.



Scheme 129 Photo-biocatalytic cascade oxidation of cyclohexane to  $\epsilon$ -caprolactone.

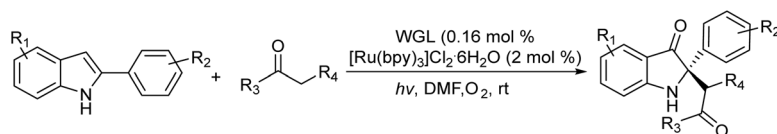
This photo-enzymatic cascade approach was also used to obtain chiral amines from alcohols by coupling the photooxidation of several alcohols followed by the reductive amination of the corresponding carbonyl compound intermediate using a variety of  $\omega$ -transaminases (Scheme 128).<sup>73</sup> The system worked in a concurrent mode; however, the productivity was significantly enhanced when the process was performed in a sequential mode.

Recently, photooxidation of cyclohexane into cyclohexanone has been combined with the Baeyer–Villiger oxidation using cyclohexanone monooxygenase (CHMO) whole-cells to obtain  $\epsilon$ -caprolactone (Scheme 129).<sup>429</sup> Au-doped TiO<sub>2</sub> (Au-TiO<sub>2</sub>) and graphitic carbonitride (g-C<sub>3</sub>N<sub>4</sub>) were evaluated as photocatalysts under visible-light irradiation. The results showed that when the reaction was performed in a concurrent mode no product could be detected, mainly due to the fast photooxidation of the co-factor NADPH. Therefore, the process was performed in a sequential mode, and after the first step, the biocatalyst was added to the reaction mixture and the reaction proceeded for 24 h in the dark. The highest yield of  $\epsilon$ -caprolactone from cyclohexane was achieved using g-C<sub>3</sub>N<sub>4</sub> as the photocatalyst (41%), which was more stable against poisoning than Au-TiO<sub>2</sub>.

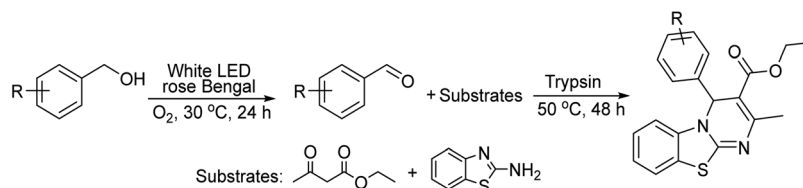
The synthesis of asymmetric 2,2-disubstituted indol-3-ones from 2-arylindoles was reported by He *et al.*<sup>430</sup> by coupling photocatalytic oxidation of 2-arylindoles with the subsequent enantioselective alkylation catalyzed by a lipase in a photo-enzymatic cascade process in a concurrent mode. The photooxidation step was performed using Ru(bpy)<sub>3</sub>Cl<sub>2</sub> as a photocatalyst to obtain the intermediate indolone, which was subsequently asymmetrically alkylated by a wheat germ lipase (WGL) (Scheme 130). A variety of substituted aryl indoles were combined with linear and cyclic ketones as well as dicarbonyl compounds giving the corresponding asymmetric indoles with yields of up to 70% and enantioselectivities of up to 93:7 enantiomeric ratio.

Recently, Yu *et al.*<sup>431</sup> reported for the first time a photo-enzymatic cascade process for the synthesis of 4*H*-pyrimido[2,1-*b*]benzothiazole derivatives from alcohols. In the first step, Rose Bengal (rB) was employed as photocatalyst to oxidize alcohols to aldehydes under visible-light irradiation. Then, the aldehyde intermediate was coupled with ethyl acetoacetate and 2-aminobenzothiazole through the Biginelli reaction biocatalyzed by trypsin to achieve the target product. Intent to do the reaction in a concurrent mode was unsuccessful, probably due to the inactivation of the enzyme by the H<sub>2</sub>O<sub>2</sub> produced in the photocatalytic step. Then, the reaction was optimized in a sequential mode in such a way that after the photocatalytic step, and turning off the light source, the enzyme and substrates (ethyl acetoacetate and 2-aminobenzothiazole) were added and the biocatalyzed multicomponent reaction proceeded (see Scheme 131). Optimization of the solvent showed that a solvent-free procedure was the most favourable approach. Employing a variety of substituted benzyl alcohols fourteen 4*H*-pyrimido[2,1-*b*]benzothiazole derivatives were prepared by a simple operation in high yields (up to 98%) under mild reaction conditions, providing a more efficient and eco-friendly strategy, when compared with conventional methods.

A light-driven Wacker oxidation of allyl (hetero)arene derivatives into ketones was coupled with a biotransamination or bioreduction step to obtain enantioenriched amines and alcohols respectively.<sup>432</sup> The Wacker oxidation was performed in

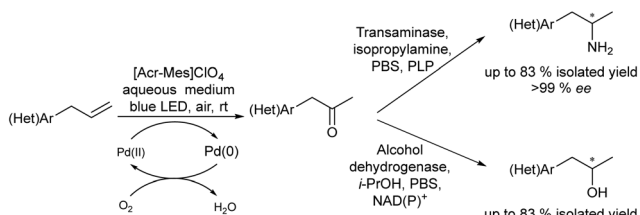


Scheme 130 Photo-enzymatic cascade for the synthesis of asymmetric 2,2-disubstituted indol-3-ones from 2-arylindoles in a concurrent mode.



Scheme 131 A sequential photo-enzymatic cascade process for obtaining 4*H*-pyrimidine [2,1-*b*] benzothiazole derivatives.





Scheme 132 Photo-enzymatic cascade for the synthesis of chiral amines and alcohols.

aqueous media using a Pd(II) complex as a catalyst under aerobic conditions in the presence of 9-mesityl-10-methylacridinium perchlorate ([Acr-Mes]ClO<sub>4</sub>) as a photosensitizer, under blue light irradiation. After oxidation completion, the enzyme (transaminase or alcohol dehydrogenase) and the required reagents and co-factors were added. A wide panel of chiral amines and alcohols were achieved in good isolated yields, up to 83% (99% ee), under mild reaction conditions in aqueous media (Scheme 132).

In a different approach to obtain optically active 1-arylpropan-2-ols, the authors combined the photocatalytic Meerwein arylation between aromatic diazonium salts and isopropenyl acetate under blue LED light irradiation with the bioreduction of the corresponding ketone intermediates.<sup>433</sup> The first step was performed in aqueous medium using [Acr-Mes]ClO<sub>4</sub> as a photocatalyst, and the resulting ketone was reduced to the corresponding chiral alcohol in a sequential step using an alcohol dehydrogenase. Using ADHs of opposite stereopreference a total of 19 pairs of 1-arylpropan-2-ol enantiomers were obtained with global yields of up to 76% and high to excellent stereoselectivity (90 to >99% ee) (Scheme 133). The process allows access to an important chiral scaffold from easily accessible reactants and under mild reaction conditions. Interestingly, the authors also showed that it was possible to obtain both 1-phenylpropan-2-ol antipodes, starting from aniline and generating *in situ* the diazonium salt through a one-pot three-step sequential photobiocatalytic protocol.

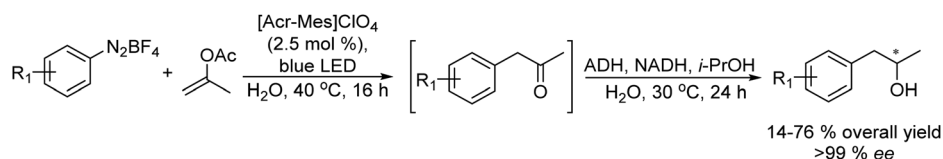
## 6. Conclusions

In this review, we have presented recent examples of the synthesis of valuable organic compounds (including chiral molecules) through linear cascade processes involving the participation of chemocatalysts (homogeneous and heterogeneous) and enzymes.

In the first part of the review, we have shown that one-pot multistep methodologies in a sequential mode, where the

different components are added consecutively and the reaction conditions (pH, temperature, substrate concentration, co-solvent, *etc*) can be adjusted for each reaction step, are the preferred approaches. This is a consequence of the difficulty in finding a compatible operational window where both catalysts can perform efficiently. However, in the last few years the pool of chemo-catalysts (for instance metallic catalysts) able to operate in water has extended enormously, providing new opportunities to combine with biocatalysts, which work in water as their natural world. For instance, the combination of the Wacker oxidation, Suzuki and Heck cross-coupling, and olefin metathesis reactions with enzymatic transformations has been successfully achieved. In addition, while enzyme inhibition by heavy metals is a known phenomenon, catalysts based on transition metals such as Au, Ru, Pd, or Fe have displayed great compatibility with enzymes allowing some cascade processes to proceed in a concurrent manner, as shown by several examples discussed herein. Therefore, searching for compatible catalysts and reaction conditions is one of the main challenges in the future. In this sense, the design of new enzymes based on computational modelling and protein engineering provides enzymes with novel activity, reactivity and stability, which can be substantially improved by the advancements in machine learning and enzyme directed evolution strategies. This fact, along with the development of chemocatalysts able to work efficiently under mild and even physiological reaction conditions, will extend the operational window to combine both catalytic systems, increasing the synthetic applications of chemo-enzymatic cascade reactions.

Furthermore, reaction engineering strategies for solving incompatibility issues in chemo-enzymatic reactions have also been developed, for instance, the use of deep eutectic solvents to solve substrate solubility problems or the spatial separation of catalytic sites through the rational design of enzyme-metal hybrid catalysts to overcome incompatibility problems between catalytic species. However, spatial compartmentalization of the catalytic systems where chemo- and biocatalysts can work effectively without interaction represents a more promising strategy. Thus, the use of biphasic systems and aqueous micellar systems, catalyst encapsulation where the chemo- or the biocatalyst is shielded from external incompatible catalytic species, the use of the porous membranes to confine chemo- and biocatalysts and the use of continuous flow-reactors are reported strategies to generate separate compartments. However, among them, the most promising compartmentalization strategy from the point of view of scalability relies on the continuous flow processes, where incompatible chemo- and biocatalyzed steps can run completely separately under



Scheme 133 Photo-enzymatic cascade for the synthesis of chiral aryl propanols.



optimized reaction conditions. Although the number of examples of chemo-enzymatic cascades in flow reactors is still very limited, their high potential to manufacture specific compounds on a large scale with high productivity will drive their development in the coming years.

## Conflicts of interest

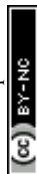
There are no conflicts to declare.

## Acknowledgements

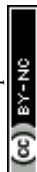
This work has been funded by the Spanish Ministry of Science and Innovation through the “Severo Ochoa Program” (CEX-2021-001230-S) and the PID2021-125897OB-I00 (MCIU/AEI/10.13039/501100011033 by “ERDF A way of making Europe” project. J. M. C. thanks the Margarita Salas grant from the Ministerio de Universidades, Universitat Politècnica de Valencia, Spain, funded by the European Union-Next Generation EU (2021–2023).

## References

- M. C. M. van Oers, F. P. J. T. Rutjes and J. C. M. Van Hest, *Curr. Opin. Biotechnol.*, 2014, **28**, 10–16.
- X. Ma and W. Zhang, *iScience*, 2022, **25**, 105005.
- M. J. Climent, A. Corma, S. Iborra and M. J. Sabater, *ACS Catal.*, 2014, **4**, 870–891.
- M. J. Climent, A. Corma and S. Iborra, *Chem. Rev.*, 2011, **111**, 1072–1133.
- M. Mifsud, S. Gargiulo, S. Iborra, I. W. C. E. Arends, F. Hollmann and A. Corma, *Nat. Commun.*, 2014, **5**, 1–6.
- F. Dumeignil, M. Guehl, A. Gimbernat, M. Capron, N. L. Ferreira, R. Froidevaux, J. S. Girardon, R. Wojcieszak, P. Dhulster and D. Delcroix, *Catal. Sci. Technol.*, 2018, **8**, 5708–5734.
- J. H. Schrittwieser, S. Velikogne, M. Hall and W. Kroutil, *Chem. Rev.*, 2018, **118**, 270–348.
- B. Grabner, A. K. Schweiger, K. Gavric, R. Kourist and H. Gruber-Woelfler, *React. Chem. Eng.*, 2020, **5**, 263–269.
- J. M. Sperl, J. M. Carsten, J. K. Guterl, P. Lommes and V. Sieber, *ACS Catal.*, 2016, **6**, 6329–6334.
- J. Enoki, J. Meisborn, A. C. Müller and R. Kourist, *Front. Microbiol.*, 2016, **7**, 1–8.
- D. Kracher and R. Kourist, *Curr. Opin. Green Sustainable Chem.*, 2021, **32**, 100538.
- Y. Liu, P. Liu, S. Gao, Z. Wang, P. Luan, J. González-Sabín and Y. Jiang, *Chem. Eng. J.*, 2021, **420**, 127659.
- M. Makkee, A. P. G. Kieboom, H. Van Bekkum and J. A. Roels, *J. Chem. Soc., Chem. Commun.*, 1980, **19**, 930–931.
- J. F. Ruddlesden and A. Stewart, *J. Chem. Res.*, 1981, **13**, 378–379.
- M. Makkee, A. P. G. Kieboom and H. van Bekkum, *Carbohydr. Res.*, 1985, **138**, 237–245.
- J. V. Allen and J. M. J. Williams, *Tetrahedron Lett.*, 1996, **37**, 1859–1862.
- P. M. Dinh, J. A. Howarth, A. R. Hudnott, J. M. J. Williams and W. Harris, *Tetrahedron Lett.*, 1996, **37**, 7623–7626.
- S. T. Chen, W. H. Huang and K. T. Wang, *J. Org. Chem.*, 1994, **59**, 7580–7581.
- T. Riermeier, U. Dingerdissen, P. Groß, W. Holla, M. Beller and D. A. Schichl, DE19955283, 2001.
- A. L. E. Larsson, B. A. Person and J. Backvall, *Angew. Chem., Int. Ed. Engl.*, 1997, **36**, 1211–1212.
- J. H. Choi, Y. H. Kim, S. H. Nam, S. T. Shin, M. J. Kim and J. Park, *Angew. Chem., Int. Ed.*, 2002, **41**, 2373–2376.
- O. Pàmies and J. E. Bäckvall, *Chem. Rev.*, 2003, **103**, 3247–3261.
- A. Berkessel, M. L. Sebastian-Ibarz and T. N. Müller, *Angew. Chem., Int. Ed.*, 2006, **45**, 6567–6570.
- V. Köhler and N. J. Turner, *Chem. Commun.*, 2014, **51**, 450–464.
- H. Gröger, in *Cooperative Catalysis: Designing Efficient Catalysts for Synthesis*, ed. R. Peters, Wiley, 2015, pp. 325–350.
- P. Hoyos, V. Pace and A. R. Alcántara, *Adv. Synth. Catal.*, 2012, **354**, 2585–2611.
- O. Verho and J. E. Bäckvall, *J. Am. Chem. Soc.*, 2015, **137**, 3996–4009.
- J. C. Wasilke, S. J. Obrey, R. T. Baker and G. C. Bazan, *Chem. Rev.*, 2005, **105**, 1001–1020.
- P. Hoyos, V. Pace, M. J. Hernáiz and A. R. Alcántara, in *Dynamic Kinetic Resolution via Hydrolase-Metal Combo Catalysis*, ed. R. N. Patel, John Wiley & Sons, 2016, pp. 373–396.
- B. Martin-Matute and J.-E. Bäckvall, in *Asymmetric Organic Synthesis with Enzymes*, ed. V. Gotor, I. Alfonso and E. García-Urdiales, Wiley, 2008, pp. 89–113.
- C. Ascaso-Alegre and J. Mangas-Sanchez, *Eur. J. Org. Chem.*, 2022, e202200093.
- S. González-Granda, L. Escot, I. Lavandera and V. Gotor-Fernández, *Angew. Chem., Int. Ed.*, 2023, **62**, e202217713.
- S. González-Granda, J. Albarrán-Velo, I. Lavandera and V. Gotor-Fernández, *Chem. Rev.*, 2023, **123**, 5297–5346.
- H. Gröger and W. Hummel, *Curr. Opin. Chem. Biol.*, 2014, **19**, 171–179.
- F. Rudroff, M. D. Mihovilovic, H. Gröger, R. Snajdrova, H. Iding and U. T. Bornscheuer, *Nat. Catal.*, 2018, **1**, 12–22.
- D. Kracher and R. Kourist, *Curr. Opin. Green Sustainable Chem.*, 2021, **32**, 100538.
- H. U. Blaser, C. Malan, B. Pugin, F. Spindler, H. Steiner and M. Studer, *Adv. Synth. Catal.*, 2003, **345**, 103–151.
- F. D. Klingler, *Acc. Chem. Res.*, 2007, **40**, 1367–1376.
- R. Noyori and T. Ohkuma, *Angew. Chem., Int. Ed.*, 2001, **40**, 40–73.
- D. J. Newman and G. M. Cragg, *J. Nat. Prod.*, 2016, **79**, 629–661.
- S. K. Talapatra, B. Talapatra and K. C. Nicolaou, *Chemistry of plant natural products: Stereochemistry, conformation, synthesis, biology, and medicine*, Springer, Berlin Heidelberg, 2015.
- T. Wright, *Pharmaceuticals: classes, therapeutic agents, areas of application.*, Wiley-VCH, Weinheim, 2001.



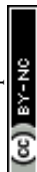
- 43 J. H. Lee, K. Han, M. J. Kim and J. Park, *Eur. J. Org. Chem.*, 2010, 999–1015.
- 44 A. Parvulescu, J. Janssens, J. Vanderleyden and D. De Vos, *Top. Catal.*, 2010, 53, 931–941.
- 45 C. C. Gruber, I. Lavandera, K. Faber and W. Kroutil, *Adv. Synth. Catal.*, 2006, 348, 1789–1805.
- 46 C. V. Voss, C. C. Gruber, K. Faber, T. Knaus, P. Macheroux and W. Kroutil, *J. Am. Chem. Soc.*, 2008, 130, 13969–13972.
- 47 A. Díaz-Rodríguez, N. Ríos-Lombardía, J. H. Sattler, I. Lavandera, V. Gotor-Fernández, W. Kroutil and V. Gotor, *Catal. Sci. Technol.*, 2015, 5, 1443–1446.
- 48 D. Ghislieri and N. J. Turner, *Top. Catal.*, 2014, 57, 284–300.
- 49 W. Hussain, D. J. Pollard, M. Truppo and G. J. Lye, *J. Mol. Catal. B: Enzym.*, 2008, 55, 19–29.
- 50 H. Kohls, M. Anderson, J. Dickerhoff, K. Weisz, A. Córdova, P. Berglund, H. Brundiek, U. T. Bornscheuer and M. Höhne, *Adv. Synth. Catal.*, 2015, 357, 1808–1814.
- 51 E. Keinan, K. K. Seth and R. Lamed, *Ann. N. Y. Acad. Sci.*, 1987, 501, 130–149.
- 52 W. Hummel, *Appl. Microbiol. Biotechnol.*, 1990, 34, 15–19.
- 53 D. Metrangolo-Ruiz de Temiño, W. Hartmeier and M. B. Ansorge-Schumacher, *Enzyme Microb. Technol.*, 2005, 36, 3–9.
- 54 R. C. Simon, N. Richter, E. Busto and W. Kroutil, *ACS Catal.*, 2014, 4, 129–143.
- 55 C. K. Savile, J. M. Janey, E. C. Mundorff, J. C. Moore, S. Tam, W. R. Jarvis, J. C. Colbeck, A. Krebber, F. J. Fleitz, J. Brands, P. N. Devine, G. W. Huisman and G. J. Hughes, *Science*, 2010, 329, 305–309.
- 56 D. Méndez-Sánchez, J. Mangas-Sánchez, I. Lavandera, V. Gotor and V. Gotor-Fernández, *ChemCatChem*, 2015, 7, 4016–4020.
- 57 E. Liardo, N. Ríos-Lombardía, F. Morís, J. González-Sabín and F. Rebolledo, *Eur. J. Org. Chem.*, 2018, 3031–3035.
- 58 E. Liardo, N. Ríos-Lombardía, F. Morís, F. Rebolledo and J. González-Sabín, *ACS Catal.*, 2017, 7, 4768–4774.
- 59 X. Li, L. Xu, G. Wang, H. Zhang and Y. Yan, *Process Biochem.*, 2013, 48, 1905–1913.
- 60 R. A. Sheldon, *Chirotechnology: Industrial synthesis of optically active compounds*, Marcel Dekker, Inc., New York, 1993.
- 61 L. Hintermann, *Top. Organomet. Chem.*, 2010, 31, 123–155.
- 62 I. Schnapperelle, W. Hummel and H. Gröger, *Chem. – Eur. J.*, 2012, 18, 1073–1076.
- 63 F. Uthoff and H. Gröger, *J. Org. Chem.*, 2018, 83, 9517–9521.
- 64 F. Thoff, H. Sato and H. Röger, *ChemCatChem*, 2017, 9, 555–558.
- 65 D. González-Martínez, V. Gotor and V. Gotor-Fernández, *Adv. Synth. Catal.*, 2019, 361, 2582–2593.
- 66 L. Hintermann and A. Labonne, *Synthesis*, 2007, 1121–1150.
- 67 G. A. Olah and D. Meidar, *Synthesis*, 1978, 671–672.
- 68 P. Schaaf, V. Gojic, T. Bayer, F. Rudroff, M. Schnürch and M. D. Mihovilovic, *ChemCatChem*, 2018, 10, 920–924.
- 69 M. J. Rodríguez-Álvarez, N. Ríos-Lombardía, S. Schumacher, D. Pérez-Iglesias, F. Morís, V. Cadierno, J. García-Álvarez and J. González-Sabín, *ACS Catal.*, 2017, 7, 7753–7759.
- 70 S. Mathew, A. Sagadevan, D. Renn and M. Rueping, *ACS Catal.*, 2021, 11, 12565–12569.
- 71 S. González-Granda, G. Steinkellner, K. Gruber, I. Lavandera and V. Gotor-Fernández, *Adv. Synth. Catal.*, 2023, 365, 1036–1047.
- 72 T. Sehl, H. C. Hailes, J. M. Ward, R. Wardenga, E. Von Lieres, H. Offermann, R. Westphal, M. Pohl and D. Rother, *Angew. Chem., Int. Ed.*, 2013, 52, 6772–6775.
- 73 J. Gacs, W. Zhang, T. Knaus, F. G. Mutti, I. W. C. E. Arends and F. Hollmann, *Catalysts*, 2019, 9, 305.
- 74 M. L. Corrado, T. Knaus and F. G. Mutti, *ChemBioChem*, 2021, 22, 2345–2350.
- 75 N. Ahlsten, A. Bartoszewicz and B. Martín-Matute, *Dalton Trans.*, 2012, 41, 1660–1670.
- 76 P. Lorenzo-Luis, A. Romerosa and M. Serrano-Ruiz, *ACS Catal.*, 2012, 2, 1079–1086.
- 77 N. Ríos-Lombardía, C. Vidal, M. Cocina, F. Morís, J. García-Álvarez and J. González-Sabín, *Chem. Commun.*, 2015, 51, 10937–10940.
- 78 N. Ríos-Lombardía, C. Vidal, E. Liardo, F. Morís, J. García-Álvarez and J. González-Sabín, *Angew. Chem., Int. Ed.*, 2016, 55, 8691–8695.
- 79 S. González-Granda, I. Lavandera and V. Gotor-Fernández, *Angew. Chem.*, 2021, 133, 14064–14070.
- 80 A. Abate, E. Brenna, G. Fronza, C. Fuganti, F. G. Gatti, S. Serra and E. Zardonì, *Helv. Chim. Acta*, 2004, 87, 765–780.
- 81 S. González-Granda, N. V. Tzouras, S. P. Nolan, I. Lavandera and V. Gotor-Fernández, *Adv. Synth. Catal.*, 2022, 364, 3856–3866.
- 82 S. J. Freakley, S. Kochius, J. van Marwijk, C. Fenner, R. J. Lewis, K. Baldenius, S. S. Marais, D. J. Opperman, S. T. L. Harrison, M. Alcalde, M. S. Smit and G. J. Hutchings, *Nat. Commun.*, 2019, 10, 4178.
- 83 J. Bach, R. Berenguer, J. Garcia and J. Vilarrasa, *Tetrahedron Lett.*, 1995, 36, 3425–3428.
- 84 J. Aleu, B. Bergamo, E. Brenna, C. Fuganti and S. Serra, *Eur. J. Org. Chem.*, 2000, 3031–3038.
- 85 E. Brenna, C. Fuganti, P. Grasselli and S. Serra, *Eur. J. Org. Chem.*, 2001, 1349–1357.
- 86 K. Burgess and L. D. Jennings, *J. Am. Chem. Soc.*, 1991, 113, 6129–6139.
- 87 T. Itoh, E. Akasaki and Y. Nishimura, *Chem. Lett.*, 2002, 154–155.
- 88 A. Ghanem and V. Schurig, *Tetrahedron: Asymmetry*, 2003, 14, 57–62.
- 89 E. Lindner, A. Ghanem, I. Warad, K. Eichele, H. A. Mayer and V. Schurig, *Tetrahedron: Asymmetry*, 2003, 14, 1045–1053.
- 90 A. Kamal, M. Sandbhor, A. A. Shaik and V. Sravanthi, *Tetrahedron: Asymmetry*, 2003, 14, 2839–2844.
- 91 S. Sgalla, G. Fabrizi, R. Cirilli, A. Maccone, A. Bonamore, A. Boffi and S. Cacchi, *Tetrahedron: Asymmetry*, 2007, 18, 2791–2796.
- 92 D. Lee, E. A. Huh, M. J. Kim, H. M. Jung, J. H. Koh and J. Park, *Org. Lett.*, 2000, 2, 2377–2379.



- 93 Y. K. Choi, J. H. Suh, D. Lee, I. T. Lim, J. Y. Jung and M. J. Kim, *J. Org. Chem.*, 1999, **64**, 8423–8424.
- 94 A. Boffi, S. Cacchi, P. Ceci, R. Cirilli, G. Fabrizi, A. Prastaro, S. Niembro, A. Shafir and A. Vallribera, *ChemCatChem*, 2011, **3**, 347–353.
- 95 S. Fushiya, Y. Kabe, Y. Ikegaya and F. Takano, *Planta Med.*, 1998, **64**, 598–602.
- 96 I. Gill and R. Valivety, *Angew. Chem.*, 2000, **39**, 3804–3808.
- 97 G. Sabitha, B. Thirupathaiah and J. S. Yadav, *Synth. Commun.*, 2007, **37**, 1683–1688.
- 98 S. Barradas, M. C. Carreño, M. González-López, A. Latorre and A. Urbano, *Org. Lett.*, 2007, **9**, 5019–5022.
- 99 S. Barradas, A. Urbano and M. C. Carreño, *Chem. – Eur. J.*, 2009, **15**, 9286–9289.
- 100 J. M. Longmire, Z. Guoxin and X. Zhang, *Tetrahedron Lett.*, 1997, **38**, 375–378.
- 101 E. Burda, W. Hummel and H. Gröger, *Angew. Chem., Int. Ed.*, 2008, **47**, 9551–9554.
- 102 A. Prastaro, P. Ceci, E. Chiancone, A. Boffi, R. Cirilli, M. Colone, G. Fabrizi, A. Stringaro and S. Cacchi, *Green Chem.*, 2009, **11**, 1929–1932.
- 103 E. Burda, W. Bauer, W. Hummel and H. Gröger, *ChemCatChem*, 2010, **2**, 67–72.
- 104 S. Itsuno, *Prog. Polym. Sci.*, 2005, **30**, 540–558.
- 105 D. González-Martínez, V. Gotor and V. Gotor-Fernández, *ChemCatChem*, 2019, **11**, 5800–5807.
- 106 J. M. Longmire, G. Zhu and X. Zhang, *Tetrahedron Lett.*, 1997, **38**, 375–378.
- 107 P. V. Ramachandran, G. M. Chen, Z. H. Lu and H. C. Brown, *Tetrahedron Lett.*, 1996, **37**, 3795–3798.
- 108 A. W. H. Dawood, J. Bassut, R. O. M. A. de Souza and U. T. Bornscheuer, *Chem. – Eur. J.*, 2018, **24**, 16009–16013.
- 109 C. A. Fleckenstein and H. Plenio, *Chem. – Eur. J.*, 2008, **14**, 4267–4279.
- 110 J. E. Dander, M. Giroud, S. Racine, E. R. Darzi, O. Alvizo, D. Entwistle and N. K. Garg, *Commun. Chem.*, 2019, **2**, 82.
- 111 A. Berkessel and H. Gröger, *Asymmetric Organocatalysis*, Wiley-VCH, Weinheim, 2005.
- 112 B. List and J. W. Yang, *Science*, 2006, **313**, 1584–1586.
- 113 P. Melchiorre, M. Marigo, A. Carlone and G. Bartoli, *Angew. Chem., Int. Ed.*, 2008, **47**, 6138–6171.
- 114 K. Baer, M. Krauß, E. Burda, W. Hummel, A. Berkessel and H. Gröger, *Angew. Chem., Int. Ed.*, 2009, **48**, 9355–9358.
- 115 G. Rulli, N. Duangdee, K. Baer, W. Hummel, A. Berkessel and H. Gröger, *Angew. Chem., Int. Ed.*, 2011, **50**, 7944–7947.
- 116 S. Sonoike, T. Itakura, M. Kitamura and S. Aoki, *Chem. – Asian J.*, 2012, **7**, 64–74.
- 117 M. Heidlindemann, G. Rulli, A. Berkessel, W. Hummel and H. Gröger, *ACS Catal.*, 2014, **4**, 1099–1103.
- 118 G. Rulli, N. Duangdee, W. Hummel, A. Berkessel and H. Gröger, *Eur. J. Org. Chem.*, 2017, 812–817.
- 119 L. Schober, F. Tonin, U. Hanefeld and H. Gröger, *Eur. J. Org. Chem.*, 2022, e202101035.
- 120 C. Ascaso-Alegre, R. P. Herrera and J. Mangas-Sánchez, *Angew. Chem., Int. Ed.*, 2022, **61**, e202209159.
- 121 J. Tian, J. Zhong, Y. Li and D. Ma, *Angew. Chem., Int. Ed.*, 2014, **53**, 13885–13888.
- 122 A. Erkkilä, I. Majander and P. M. Pihko, *Chem. Rev.*, 2007, **107**, 5416–5470.
- 123 D. Roca-Lopez, D. Sadaba, I. Delso, R. P. Herrera, T. Tejero and P. Merino, *Tetrahedron: Asymmetry*, 2010, **21**, 2561–2601.
- 124 L. F. Tietze, F. Stecker, J. Zinngrebe and K. M. Sommer, *Chem. – Eur. J.*, 2006, **12**, 8770–8776.
- 125 L. F. Tietze, K. M. Sommer, J. Zinngrebe and F. Stecker, *Angew. Chem., Int. Ed.*, 2004, **44**, 257–259.
- 126 C. J. Li and T. H. Chan, *Organometallics*, 1991, **10**, 2548–2549.
- 127 B. Zhao, X. Peng, S. Cui and Y. Shi, *J. Am. Chem. Soc.*, 2010, **132**, 11009–11011.
- 128 M. Fuchs, M. Schober, J. Pfeffer, W. Kroutil, R. Birner-Gruenberger and K. Faber, *Adv. Synth. Catal.*, 2011, **353**, 2354–2358.
- 129 C. J. Li, *Chem. Rev.*, 2005, **105**, 3095–3165.
- 130 T. Ishiyama, T. A. Ahiko and N. Miyaura, *J. Am. Chem. Soc.*, 2002, **124**, 12414–12415.
- 131 N. Schweigert, A. J. B. Zehnder and R. I. L. Eggen, *Environ. Microbiol.*, 2001, **3**, 81–91.
- 132 T. V. Hansen and L. Skattebøl, *Tetrahedron Lett.*, 2005, **46**, 3357–3358.
- 133 V. Berberian, C. C. R. Allen, N. D. Sharma, D. R. Boyd and C. Hardacre, *Adv. Synth. Catal.*, 2007, **349**, 727–739.
- 134 Y. X. Li, W. J. Zuo, W. L. Mei, H. Q. Chen and H. F. Dai, *Chin. J. Nat. Med.*, 2014, **12**, 297–299.
- 135 S. P. B. Ovenden, M. Cobbe, R. Kissell, G. W. Birrell, M. Chavchich and M. D. Edstein, *J. Nat. Prod.*, 2011, **74**, 74–78.
- 136 J. M. Berry, T. D. Bradshaw, I. Fichtner, R. Ren, C. H. Schwalbe, G. Wells, E. H. Chew, M. F. G. Stevens and A. D. Westwell, *J. Med. Chem.*, 2005, **48**, 639–644.
- 137 D. Mal and S. Ray, *Eur. J. Org. Chem.*, 2008, 3014–3020.
- 138 D. Pan, S. K. Mal, G. K. Kar and J. K. Ray, *Tetrahedron*, 2002, **58**, 2847–2852.
- 139 T. Rammial, S. A. Taylor, J. A. C. Clyburne and C. J. Walsby, *Chem. Commun.*, 2007, 2066–2068.
- 140 M. Ghandi and M. Shahidzadeh, *J. Organomet. Chem.*, 2006, **691**, 4918–4925.
- 141 D. Koszelewski, D. Paprocki, A. Brodzka, A. Kęciak, M. Wilk and R. Ostaszewski, *Sustainable Chem. Pharm.*, 2022, **25**, 100576.
- 142 J. Samsonowicz-Górski, A. Hrunyk, A. Brodzka, R. Ostaszewski and D. Koszelewski, *Green Chem.*, 2023, **25**, 6306–6314.
- 143 R. Kourist, *Biocatalysis in Organic Synthesis. Science of Synthesis*, Thieme, Stuttgart, 2015, vol. 1–3.
- 144 C. Palumbo, E. E. Ferrandi, C. Marchesi, D. Monti, S. Riva, R. Psaro and M. Guidotti, *ChemistrySelect*, 2016, **1**, 1795–1798.
- 145 C. Cativiela, J. M. Fraile, J. I. García and J. A. Mayoral, *J. Mol. Catal. A: Chem.*, 1996, **112**, 259–267.
- 146 J. Magano and J. R. Dunetz, *Org. Process Res. Dev.*, 2012, **16**, 1156–1184.



- 147 J. I. Song and D. K. An, *Chem. Lett.*, 2007, **36**, 886–887.
- 148 H. Sand and R. Weberskirch, *RSC Adv.*, 2017, **7**, 33614–33626.
- 149 J. M. Hoover and S. S. Stahl, *J. Am. Chem. Soc.*, 2011, **133**, 16901–16910.
- 150 D. Schwendenwein, A. K. Ressmann, M. Entner, V. Savic, M. Winkler and F. Rudroff, *Catalysts*, 2021, **11**, 932.
- 151 D. Schwendenwein, A. K. Ressmann, M. Doerr, M. Höhne, U. T. Bornscheuer, M. D. Mihovilovic, F. Rudroff and M. Winkler, *Adv. Synth. Catal.*, 2019, **361**, 2544–2549.
- 152 S. Giparakis, M. Winkler and F. Rudroff, *Green Chem.*, 2023, **26**, 1338–1344.
- 153 A. Rapeyko, M. J. Climent, A. Corma, P. Concepción and S. Iborra, *ChemSusChem*, 2015, **8**, 3270–3282.
- 154 P. Zambelli, A. Pinto, D. Romano, E. Crotti, P. Conti, L. Tamborini, R. Villa and F. Molinari, *Green Chem.*, 2012, **14**, 2158–2161.
- 155 R. A. Reck, *J. Am. Oil Chem. Soc.*, 1985, **62**, 355–365.
- 156 T. V. RajanBabu and A. L. Casalnuovo, in *Comprehensive asymmetric catalysis I–III*, ed. E. N. Jacobsen, A. Pfaltz, H. Yamamoto, Springer, Berlin, 1999, p. 367.
- 157 M. A. and N. V. Kalevaru, in *Industrial Catalysis and Separations Innovations for Process Intensification*, ed. K. V. Raghavan and B. M. Reddy, Apple Academic Press, 2014, pp. 61–103.
- 158 C. Plass, A. Hinzmann, M. Terhorst, W. Brauer, K. Oike, H. Yavuzer, Y. Asano, A. J. Vorholt, T. Betke and H. Gröger, *ACS Catal.*, 2019, **9**, 5198–5203.
- 159 A. Hinzmann, M. Stricker and H. Gröger, *ACS Sustainable Chem. Eng.*, 2020, **8**, 17088–17096.
- 160 E. J. Craven, J. Latham, S. A. Shepherd, I. Khan, A. Diaz-Rodriguez, M. F. Greaney and J. Micklefield, *Nat. Catal.*, 2021, **4**, 385–394.
- 161 L. Bering, E. J. Craven, S. A. Sowerby Thomas, S. A. Shepherd and J. Micklefield, *Nat. Commun.*, 2022, **13**, 380.
- 162 J. Gorzynski Smith, *Synthesis*, 1984, 629–656.
- 163 W. J. Choi and C.-Y. Choi, *Biotechnol. Bioprocess Eng.*, 2005, **10**, 167–179.
- 164 A. Archelas and R. Furstoss, *Top. Curr. Chem.*, 1999, 159–191.
- 165 C. A. Denard, M. J. Bartlett, Y. Wang, L. Lu, J. F. Hartwig and H. Zhao, *ACS Catal.*, 2015, **5**, 3817–3822.
- 166 K. Wu, L. Chen, H. Fan, Z. Zhao, H. Wang and D. Wei, *Tetrahedron Lett.*, 2016, **57**, 899–904.
- 167 S. González-Granda, L. Escot, I. Lavandera and V. Gotor-Fernández, *ACS Catal.*, 2022, **12**, 2552–2560.
- 168 R. J. Cherney, P. Carter, J. V. Duncia, D. S. Gardner and J. B. Santella, WO2004071460A2, 2004.
- 169 P. H. Carter, R. J. Cherney, D. G. Batt, J. V. Duncia, D. S. Gardner, S. Ko, A. S. Srivastava and M. G. Yang, WO2005021500A1, 2005.
- 170 P. Süß, S. Borchert, J. Hinze, S. Illner, J. Von Langermann, U. Kragl, U. T. Bornscheuer and R. Wardenga, *Org. Process Res. Dev.*, 2015, **19**, 2034–2038.
- 171 R. Kourist, P. Domínguez de María and K. Miyamoto, *Green Chem.*, 2011, **13**, 2607–2618.
- 172 S. Barth and F. Effenberger, *Tetrahedron: Asymmetry*, 1993, **4**, 823–833.
- 173 J. Enoki, C. Mügge, D. Tischler, K. Miyamoto and R. Kourist, *Chem. – Eur. J.*, 2019, **25**, 5071–5076.
- 174 Y. S. Lin, P. Y. Wang, A. C. Wu and S. W. Tsai, *J. Mol. Catal. B: Enzym.*, 2011, **68**, 245–249.
- 175 T. Uemura, X. Zhang, K. Matsumura, N. Sayo, H. Kumobayashi, T. Ohta, K. Nozaki and H. Takaya, *J. Org. Chem.*, 1996, **61**, 5510–5516.
- 176 K. Tenbrink, M. Seßler, J. Schatz and H. Gröger, *Adv. Synth. Catal.*, 2011, **353**, 2363–2367.
- 177 M. Scholl, S. Ding, C. W. Lee and R. H. Grubbs, *Org. Lett.*, 1999, **1**, 953–956.
- 178 G. Moroy, C. Denhez, H. El Mourabit, A. Toribio, A. Dassonville, M. Decarme, J. H. Renault, C. Mirand, G. Bellon, J. Sapi, A. J. P. Alix, W. Hornebeck and E. Bourguet, *Bioorg. Med. Chem.*, 2007, **15**, 4753–4766.
- 179 J. J. Chen, Y. Zhang, S. Hammond, N. Dewdney, T. Ho, X. Lin, M. F. Browner and A. L. Castelhana, *Bioorg. Med. Chem. Lett.*, 1996, **6**, 1601–1606.
- 180 P. Galatsis, B. Caprathe, J. Gilmore, A. Thomas, K. Linn, S. Sheehan, W. Harter, C. Kostlan, E. Lunney, C. Stankovic, J. Rubin, K. Brady, H. Allen and R. Talanian, *Bioorg. Med. Chem. Lett.*, 2010, **20**, 5184–5190.
- 181 J. Liu, Y. Yang and R. Ji, *Helv. Chim. Acta*, 2004, **87**, 1935–1939.
- 182 M. Korpak and J. Pietruszka, *Adv. Synth. Catal.*, 2011, **353**, 1420–1424.
- 183 M. T. Barros, C. D. Maycock and M. R. Ventura, *Org. Lett.*, 2003, **5**, 4097–4099.
- 184 Y. Wang, M. J. Bartlett, C. A. Denard, J. F. Hartwig and H. Zhao, *ACS Catal.*, 2017, **7**, 2548–2552.
- 185 J. H. Hansen, B. T. Parr, P. Pelphrey, Q. Jin, J. Autschbach and H. M. L. Davies, *Angew. Chem.*, 2011, **123**, 2592–2596.
- 186 H. S. Toogood, J. M. Gardiner and N. S. Scrutton, *ChemCatChem*, 2010, **2**, 892–914.
- 187 Y. C. Chung, D. Janmanchi and H. L. Wu, *Org. Lett.*, 2012, **14**, 2766–2769.
- 188 M. H. Wang, D. T. Cohen, C. B. Schwamb, R. K. Mishra and K. A. Scheidt, *J. Am. Chem. Soc.*, 2015, **137**, 5891–5894.
- 189 M. Kashiwagi, K. I. Fuhshuku and T. Sugai, *J. Mol. Catal. B: Enzym.*, 2004, **29**, 249–258.
- 190 S. Talukdar, J. L. Hsu, T. C. Chou and J. M. Fang, *Tetrahedron Lett.*, 2001, **42**, 1103–1105.
- 191 M. M. Meloni and M. Taddei, *Org. Lett.*, 2001, **3**, 337–340.
- 192 E. Liardo, R. González-Fernández, N. Ríos-Lombardía, F. Morís, J. García-Álvarez, V. Cadierno, P. Crochet, F. Rebolledo and J. González-Sabín, *ChemCatChem*, 2018, **10**, 4676–4682.
- 193 E. Liardo, N. Ríos-Lombardía, F. Morís, J. González-Sabín and F. Rebolledo, *Org. Lett.*, 2016, **18**, 3366–3369.
- 194 C. Palo-Nieto, S. Afewerki, M. Anderson, C. W. Tai, P. Berglund and A. Córdova, *ACS Catal.*, 2016, **6**, 3932–3940.
- 195 A. Caiazzo, P. M. L. Garcia, R. Wever, J. C. M. Van Hest, A. E. Rowan and J. N. H. Reek, *Org. Biomol. Chem.*, 2009, **7**, 2926–2932.



- 196 H. Salminen, H. Jaakkola and M. Heinonen, *J. Agric. Food Chem.*, 2008, **56**, 11178–11186.
- 197 M. C. Bohin, J. P. Vincken, H. T. W. M. Van Der Hijden and H. Gruppen, *J. Agric. Food Chem.*, 2012, **60**, 4136–4143.
- 198 C. Simons, U. Hanefeld, I. W. C. E. Arends, T. Maschmeyer and R. A. Sheldon, *Top. Catal.*, 2006, **40**, 35–44.
- 199 J. A. Karlowsky, N. M. Laing, T. Baudry, N. Kaplan, D. Vaughan, D. J. Hoban and G. G. Zhanel, *Antimicrob. Agents Chemother.*, 2007, **51**, 1580–1581.
- 200 L. De Luca, G. Nieddu, A. Porcheddu and G. Giacomelli, *Curr. Med. Chem.*, 2008, **16**, 1–20.
- 201 M. A. S. Mertens, F. Thomas, M. Nöth, J. Moegling, I. El-Awaad, D. F. Sauer, G. V. Dhoke, W. Xu, A. Pich, S. Herres-Pawlis and U. Schwaneberg, *Eur. J. Org. Chem.*, 2019, 6341–6346.
- 202 C. Broca, M. Manteghetti, R. Gross, Y. Baissac, M. Jacob, P. Petit, Y. Sauvaire and G. Ribes, *Eur. J. Pharmacol.*, 2000, **390**, 339–345.
- 203 G. Ribes, C. Broca, P. Petit, M. Jacob, Y. Baissac, M. Manteghetti, M. Roye and Y. Sauvaire, *Diabetologia*, 1996, **39**, A234.
- 204 M. Seitz and O. Reiser, *Curr. Opin. Chem. Biol.*, 2005, **9**, 285–292.
- 205 M. Sendzik, W. Guarnieri and D. Hoppe, *Synthesis*, 1998, 1287–1297.
- 206 M. D. Swift and A. Sutherland, *Org. Biomol. Chem.*, 2006, **4**, 3889–3891.
- 207 R. C. Simon, E. Busto, J. H. Schrittwieser, J. H. Sattler, J. Pietruszka, K. Faber and W. Kroutil, *Chem. Commun.*, 2014, **50**, 15669–15672.
- 208 J. B. Routien, *J. Bacteriol.*, 1966, **91**, 1663.
- 209 R. G. Werner, L. F. Thorpe, W. Reuter and K. H. Nierhaus, *Eur. J. Biochem.*, 1976, **68**, 1–3.
- 210 N. Tabata, H. Tomoda, Y. Takahashi, K. Haneda, Y. Iwai, H. B. Woodruff and S. Omura, *J. Antibiot.*, 1993, **46**, 756–761.
- 211 K. Akagawa, R. Umezawa and K. Kudo, *Beilstein J. Org. Chem.*, 2012, **8**, 1333–1337.
- 212 V. V. Rostovtsev, L. G. Green, V. V. Fokin and K. B. Sharpless, *Angew. Chem., Int. Ed.*, 2002, **41**, 2596–2599.
- 213 C. W. Tornøe, C. Christensen and M. Meldal, *J. Org. Chem.*, 2002, **67**, 3057–3064.
- 214 R. Breinbauer and M. Köhn, *ChemBioChem*, 2003, **4**, 1147–1149.
- 215 V. D. Bock, H. Hiemstra and J. H. Van Maarseveen, *Eur. J. Org. Chem.*, 2006, 51–68.
- 216 K. B. Sharpless and R. Manetsch, *Expert Opin. Drug Discovery*, 2006, **1**, 525–538.
- 217 J. E. Moses and A. D. Moorhouse, *Chem. Soc. Rev.*, 2007, **36**, 1249–1262.
- 218 K. C. Hartmuth and K. B. Sharpless, *Drug Discovery Today*, 2003, **8**, 1128–1137.
- 219 M. Meldal and C. W. Tomøe, *Chem. Rev.*, 2008, **108**, 2952–3015.
- 220 R. Huisgen, *1,3-Dipolar cycloaddition chemistry*, Wiley, New York, 1984.
- 221 S. Su, J. R. Giguere, S. E. Schaus and J. A. Porco, *Tetrahedron*, 2004, **60**, 8645–8657.
- 222 L. S. Campbell-Verduyn, W. Szymański, C. P. Postema, R. A. Dierckx, P. H. Elsinga, D. B. Janssen and B. L. Feringa, *Chem. Commun.*, 2010, **46**, 898–900.
- 223 J. E. T. Van Hylckama Vlieg, L. Tang, J. H. Lutje Spelberg, T. Smilda, G. J. Poelarends, T. Bosma, A. E. J. Van Merode, M. W. Fraaije and D. B. Janssen, *J. Bacteriol.*, 2001, **183**, 5058–5066.
- 224 C. Aguirre-Pranzoni, R. D. Tosso, F. R. Bisogno, M. Kurina-Sanz and A. A. Orden, *Process Biochem.*, 2019, **79**, 114–117.
- 225 C. De Souza De Oliveira, K. T. De Andrade and A. T. Omori, *J. Mol. Catal. B: Enzym.*, 2013, **91**, 93–97.
- 226 N. Asano, *Glycobiology*, 2003, **13**, 93–104.
- 227 R. A. Dwek, T. D. Butters, F. M. Platt and N. Zitzmann, *Nat. Rev. Drug Discovery*, 2002, **1**, 65–75.
- 228 G. S. Jacob, *Curr. Opin. Struct. Biol.*, 1995, **5**, 605–611.
- 229 R. M. Moriarty, C. I. Mitan, N. Branză-Nichita, K. R. Phares and D. Parrish, *Org. Lett.*, 2006, **8**, 3465–3467.
- 230 A. K. Samland and G. A. Sprenger, *Appl. Microbiol. Biotechnol.*, 2006, **71**, 253–264.
- 231 L. J. Whalen and C.-H. Wong, *Aldrichimica Acta*, 2006, **39**, 63–71.
- 232 M. Sugiyama, Z. Hong, P. H. Liang, S. M. Dean, L. J. Whalen, W. A. Greenberg and C. H. Wong, *J. Am. Chem. Soc.*, 2007, **129**, 14811–14817.
- 233 E. Sverrisdóttir, T. M. Lund, A. E. Olesen, A. M. Drewes, L. L. Christrup and M. Kreilgaard, *Eur. J. Pharm. Sci.*, 2015, **74**, 45–62.
- 234 M. A. Rashid, K. R. Gustafson, Y. Kashman, J. H. Cardellina II, J. B. Mc Mohan and M. R. Boyd, *Nat. Prod. Lett.*, 1995, **6**, 153–156.
- 235 J. D. Guzman, T. Pesnot, D. A. Barrera, H. M. Davies, E. McMahan, D. Evangelopoulos, P. N. Mortazavi, T. Munshi, A. Maitra, E. D. Lamming, R. Angell, M. C. Gershater, J. M. Redmond, D. Needham, J. M. Ward, L. E. Cuca, H. C. Hailes and S. Bhakta, *J. Antimicrob. Chemother.*, 2014, **70**, 1691–1703.
- 236 L. Moreno, J. Párraga, A. Galán, N. Cabedo, J. Primo and D. Cortes, *Bioorg. Med. Chem.*, 2012, **20**, 6589–6597.
- 237 W. Lin and S. Ma, *Org. Chem. Front.*, 2017, **4**, 958–966.
- 238 T. Pesnot, M. C. Gershater, J. M. Ward and H. C. Hailes, *Adv. Synth. Catal.*, 2012, **354**, 2997–3008.
- 239 A. Bonamore, L. Calisti, A. Calcaterra, O. H. Ismail, M. Gargano, I. D'Acquarica, B. Botta, A. Boffi and A. Maccone, *ChemistrySelect*, 2016, **1**, 1525–1528.
- 240 J. Zhao, B. R. Lichman, J. M. Ward and H. C. Hailes, *Chem. Commun.*, 2018, **54**, 1323–1326.
- 241 V. Erdmann, B. R. Lichman, J. Zhao, R. C. Simon, W. Kroutil, J. M. Ward, H. C. Hailes and D. Rother, *Angew. Chem., Int. Ed.*, 2017, **56**, 12503–12507.
- 242 K. Ye, Y. Ke, N. Keshava, J. Shanks, J. A. Kapp, R. R. Tekmal, J. Petros and H. C. Joshi, *Proc. Natl. Acad. Sci. U. S. A.*, 1998, **95**, 1601–1606.
- 243 G. François, G. Timperman, W. Eling, L. Ake, J. Holenz and G. Bringmann, *Antimicrob. Agents Chemother.*, 2000, **41**, 2533–2539.



- 244 C. R. Chapple, L. Cardozo, W. D. Steers and F. E. Govier, *Int. J. Clin. Pract.*, 2006, **60**, 959–966.
- 245 M. Odachowski, M. F. Greaney and N. J. Turner, *ACS Catal.*, 2018, **8**, 10032–10035.
- 246 T. Kanemitsu, Y. Yamashita, K. Nagata and T. Itoh, *Heterocycles*, 2007, **74**, 199–203.
- 247 W. Liu, S. Liu, R. Jin, H. Guo and J. Zhao, *Org. Chem. Front.*, 2015, **2**, 288–299.
- 248 Y. Jin, L. Ou, H. Yang and H. Fu, *J. Am. Chem. Soc.*, 2017, **139**, 14237–14243.
- 249 H. Xiang, S. Ferla, C. Varricchio, A. Brancale, N. L. Brown, G. W. Black, N. J. Turner and D. Castagnolo, *ACS Catal.*, 2023, **13**, 3370–3378.
- 250 A. Corma, S. Iborra and A. Velty, *Chem. Rev.*, 2007, **107**, 2411–2502.
- 251 A. A. Rosatella, S. P. Simeonov, R. F. M. Frade and C. A. M. Afonso, *Green Chem.*, 2011, **13**, 754–793.
- 252 F. Chacón-Huete, C. Messina, B. Cigana and P. Forgione, *ChemSusChem*, 2022, **15**, e202200328.
- 253 A. Velty, S. Iborra and A. Corma, *ChemSusChem*, 2022, **15**, e202200181.
- 254 H. Son Le, Z. Said, M. Tuan Pham, T. Hieu Le, I. Veza, V. Nhanh Nguyen, B. Deepanraj and L. Huong Nguyen, *Fuel*, 2022, **324**, 124474.
- 255 B. Hurtado, K. S. Arias, M. J. Climent, P. Concepción, A. Corma and S. Iborra, *ChemSusChem*, 2022, **15**, e202200194.
- 256 K. S. Arias, A. Garcia-Ortiz, M. J. Climent, A. Corma and S. Iborra, *ACS Sustainable Chem. Eng.*, 2018, **6**, 4239–4245.
- 257 R. van den Berg, J. A. Peters and H. van Bekkum, *Carbohydr. Res.*, 1994, **253**, 1–12.
- 258 R. Huang, W. Qi, R. Su and Z. He, *Chem. Commun.*, 2010, **46**, 1115–1117.
- 259 H. Huang, C. A. Denard, R. Alamillo, A. J. Crisci, Y. Miao, J. A. Dumesic, S. L. Scott and H. Zhao, *ACS Catal.*, 2014, **4**, 2165–2168.
- 260 C. Megías-Sayago, S. Navarro-Jaén, F. Drault and S. Ivanova, *Catalysts*, 2021, **11**, 1395.
- 261 E. Nikolla, Y. Román-Leshkov, M. Moliner and M. E. Davis, *ACS Catal.*, 2011, **1**, 408–410.
- 262 X. Chen, L. Zhang, B. Zhang, X. Guo and X. Mu, *Sci. Rep.*, 2016, **6**, 1–13.
- 263 X. Li, P. Jia and T. Wang, *ACS Catal.*, 2016, **6**, 7621–7640.
- 264 M. J. Taylor, L. J. Durndell, M. A. Isaacs, C. M. A. Parlett, K. Wilson, A. F. Lee and G. Kyriakou, *Appl. Catal., B*, 2016, **180**, 580–585.
- 265 K. Yan, J. Liao, X. Wu and X. Xie, *RSC Adv.*, 2013, **3**, 3853–3856.
- 266 M. Audemar, C. Ciotonea, K. De Oliveira Vigier, S. Royer, A. Ungureanu, B. Dragoi, E. Dumitriu and F. Jérôme, *ChemSusChem*, 2015, **8**, 1885–1891.
- 267 T. Ema, S. Ide, N. Okita and T. Sakai, *Adv. Synth. Catal.*, 2008, **350**, 2039–2044.
- 268 Y. Ni, Y. Su, H. Li, J. Zhou and Z. Sun, *J. Biotechnol.*, 2013, **168**, 493–498.
- 269 Y. C. He, Z. C. Tao, X. Zhang, Z. X. Yang and J. H. Xu, *Bioresour. Technol.*, 2014, **161**, 461–464.
- 270 M. Chatterjee, T. Ishizaka and H. Kawanami, *Green Chem.*, 2016, **18**, 487–496.
- 271 Z.-Y. Yang, Y.-C. Hao, S.-Q. Hu, M.-H. Zong, Q. Chen and N. Li, *Adv. Synth. Catal.*, 2021, **363**, 1033–1037.
- 272 A. Dunbabin, F. Subrizi, J. M. Ward, T. D. Sheppard and H. C. Hailes, *Green Chem.*, 2017, **19**, 397–404.
- 273 P. Zhang, X. Liao, C. Ma, Q. Li, A. Li and Y. He, *ACS Sustainable Chem. Eng.*, 2019, **7**, 17636–17642.
- 274 X.-L. Liao, Q. Li, D. Yang, C.-L. Ma, Z.-B. Jiang and Y.-C. He, *Appl. Biochem. Biotechnol.*, 2020, **192**, 794–811.
- 275 M. Jin, L. Da Costa Sousa, C. Schwartz, Y. He, C. Sarks, C. Gunawan, V. Balan and B. E. Dale, *Green Chem.*, 2016, **18**, 957–966.
- 276 X. Liu, Y. Wang, S. Jin, X. Li and Z. Zhang, *Arab. J. Chem.*, 2020, **13**, 4916–4925.
- 277 Q. Yang, Z. Tang, J. Xiong and Y. He, *Catalysts*, 2023, **13**, 37.
- 278 Y. C. He, C. X. Jiang, J. W. Jiang, J. H. Di, F. Liu, Y. Ding, Q. Qing and C. L. Ma, *Bioresour. Technol.*, 2017, **238**, 698–705.
- 279 X. X. Xue, C. L. Ma, J. H. Di, X. Y. Huo and Y. C. He, *Bioresour. Technol.*, 2018, **268**, 292–299.
- 280 Y. He, Y. Ding, C. Ma, J. Di, C. Jiang and A. Li, *Green Chem.*, 2017, **19**, 3844–3850.
- 281 X. Q. Feng, Y. Y. Li, C. L. Ma, Y. Xia and Y. C. He, *RSC Adv.*, 2020, **10**, 40365–40372.
- 282 Y. Y. Li, Q. Li, P. Q. Zhang, C. L. Ma, J. H. Xu and Y. C. He, *Bioresour. Technol.*, 2021, **320**, 124267.
- 283 R. M. Williams, *Aldrichimica Acta*, 1992, **25**, 11–25.
- 284 S. Servi, D. Tessaro and G. Pedrocchi-Fantoni, *Coord. Chem. Rev.*, 2008, **252**, 715–726.
- 285 L. Gong, Y. Xiu, J. Dong, R. Han, G. Xu and Y. Ni, *Bioresour. Technol.*, 2021, **337**, 125344.
- 286 T. K. Chakraborty, S. Tapadar and S. Kiran Kumar, *Tetrahedron Lett.*, 2002, **43**, 1317–1320.
- 287 C. P. Ferraz, M. Zieliński, M. Pietrowski, S. Heyte, F. Dumeignil, L. M. Rossi and R. Wojcieszak, *ACS Sustainable Chem. Eng.*, 2018, **6**, 16332–16340.
- 288 C. P. Ferraz, N. J. S. Costa, E. Teixeira-Neto, Â. A. Teixeira-Neto, C. W. Liria, J. Thuriot-Roukos, M. T. Machini, R. Froidevaux, F. Dumeignil, L. M. Rossi and R. Wojcieszak, *Catalysts*, 2020, **10**, 75.
- 289 L. Hu, A. He, X. Liu, J. Xia, J. Xu, S. Zhou and J. Xu, *ACS Sustainable Chem. Eng.*, 2018, **6**, 15915–15935.
- 290 M. M. Cajnko, U. Novak, M. Grilc and B. Likozar, *Biotechnol. Biofuels*, 2020, **13**, 1–11.
- 291 A. Lancien, R. Wojcieszak, E. Cuvelier, M. Duban, P. Dhulster, S. Paul, F. Dumeignil, R. Froidevaux and E. Heuson, *ChemCatChem*, 2021, **13**, 247–259.
- 292 M. J. Hülsey, H. Yang and N. Yan, *ACS Sustainable Chem. Eng.*, 2018, **6**, 5694–5707.
- 293 A. D. Sadiq, X. Chen, N. Yan and J. Sperry, *ChemSusChem*, 2018, **11**, 532–535.
- 294 J. Dai, F. Li and X. Fu, *ChemSusChem*, 2020, **13**, 6498–6508.
- 295 T. T. Pham, X. Chen, T. Söhnle, N. Yan and J. Sperry, *Green Chem.*, 2020, **22**, 1978–1984.



- 296 Y. C. Hao, M. H. Zong, Z. L. Wang and N. Li, *Bioresour. Bioprocess.*, 2021, **8**, 1–9.
- 297 F. van Rantwijk and R. A. Sheldon, *Chem. Rev.*, 2007, **107**, 2757–2785.
- 298 T. Itoh, *Chem. Rev.*, 2017, **117**, 10567–10607.
- 299 M. Moniruzzaman, K. Nakashima, N. Kamiya and M. Goto, *Biochem. Eng. J.*, 2010, **48**, 295–314.
- 300 A. A. M. Elgharbawy, M. Moniruzzaman and M. Goto, *Biochem. Eng. J.*, 2020, **154**, 107426.
- 301 P. Xu, S. Liang, M.-H. Zong and W.-Y. Lou, *Biotechnol. Adv.*, 2021, **51**, 107702.
- 302 A. Schindl, M. L. Hagen, S. Muzammal, H. A. D. Gunasekera and A. K. Croft, *Front. Chem.*, 2019, **7**, 347.
- 303 H. T. Imam, V. Krasňan, M. Rebroš and A. C. Marr, *Molecules*, 2021, **26**, 4791.
- 304 M. K. Potdar, G. F. Kelso, L. Schwarz, C. Zhang and M. T. W. Hearn, *Molecules*, 2015, **20**, 16788–16816.
- 305 Y. Dai, J. van Spronsen, G.-J. Witkamp, R. Verpoorte and Y. H. Choi, *Anal. Chim. Acta*, 2013, **766**, 61–68.
- 306 A. Paiva, R. Craveiro, I. Aroso, M. Martins, R. L. Reis and A. R. C. Duarte, *ACS Sustainable Chem. Eng.*, 2014, **2**, 1063–1071.
- 307 O. S. Hammond, D. T. Bowron and K. J. Edler, *Angew. Chem., Int. Ed.*, 2017, **56**, 9782–9785.
- 308 M. Shaibuna, L. V. Theresa and K. Sreekumar, *Soft Matter*, 2022, **18**, 2695–2721.
- 309 B. Nian and X. Li, *Int. J. Biol. Macromol.*, 2022, **217**, 255–269.
- 310 M. Pätzold, S. Siebenhaller, S. Kara, A. Liese, C. Sylдатk and D. Holtmann, *Trends Biotechnol.*, 2019, **37**, 943–959.
- 311 P. Xu, G.-W. Zheng, M.-H. Zong, N. Li and W.-Y. Lou, *Bioresour. Bioprocess.*, 2017, **4**, 34.
- 312 L. Cicco, G. Dilauro, F. M. Perna, P. Vitale and V. Capriati, *Org. Biomol. Chem.*, 2021, **19**, 2558–2577.
- 313 V. Gotor-Fernández and C. E. Paul, *J. Biotechnol.*, 2019, **293**, 24–35.
- 314 Z. Maugeri and P. Domínguez de María, *ChemCatChem*, 2014, **6**, 1535–1537.
- 315 P. Vitale, V. M. Abbinante, F. M. Perna, A. Salomone, C. Cardellicchio and V. Capriati, *Adv. Synth. Catal.*, 2017, **359**, 1049–1057.
- 316 L. Cicco, N. Ríos-Lombardía, M. J. Rodríguez-Álvarez, F. Morís, F. M. Perna, V. Capriati, J. García-Álvarez and J. González-Sabín, *Green Chem.*, 2018, **20**, 3468–3475.
- 317 E. Liardo, N. Ríos-Lombardía, F. Morís, J. González-Sabín and F. Rebolledo, *Org. Lett.*, 2016, **18**, 3366–3369.
- 318 N. Ríos-Lombardía, C. Vidal, E. Liardo, F. Morís, J. García-Álvarez and J. González-Sabín, *Angew. Chem. Int. Ed.*, 2016, **55**, 8691–8695.
- 319 J. Paris, N. Ríos-Lombardía, F. Morís, H. Gröger and J. González-Sabín, *ChemCatChem*, 2018, **10**, 4417–4423.
- 320 J. Paris, A. Telzerow, N. Ríos-Lombardía, K. Steiner, H. Schwab, F. Morís, H. Gröger and J. González-Sabín, *ACS Sustainable Chem. Eng.*, 2019, **7**, 5486–5493.
- 321 A. Telzerow, J. Paris, M. Håkansson, J. González-Sabín, N. Ríos-Lombardía, M. Schürmann, H. Gröger, F. Morís, R. Kourist, H. Schwab and K. Steiner, *ACS Catal.*, 2019, **9**, 1140–1148.
- 322 D. Xu, W. Tang, Z. Tang and Y. He, *Catalysts*, 2023, **13**, 467.
- 323 Q. Li, J. Di, X. Liao, J. Ni, Q. Li, Y. C. He and C. Ma, *Green Chem.*, 2021, **23**, 8154–8168.
- 324 W. He, Y. C. He and J. Ye, *Front. Bioeng. Biotechnol.*, 2023, **11**, 1–10.
- 325 L. Li, Q. Li, J. Di, Y. He and C. Ma, *ACS Sustainable Chem. Eng.*, 2023, **11**, 7515–7525.
- 326 Y. Liu, L. Li, C. Ma and Y. C. He, *Bioresour. Technol.*, 2023, **387**, 129638.
- 327 J. Di, Q. Li, C. Ma and Y. C. He, *Bioresour. Technol.*, 2023, **369**, 128425.
- 328 J. Ni, Q. Li, L. Gong, X. L. Liao, Z. J. Zhang, C. Ma and Y. He, *ACS Sustainable Chem. Eng.*, 2021, **9**, 13084–13095.
- 329 W. He, J. Ni, Y. C. He and J. Ye, *Int. J. Biol. Macromol.*, 2022, **222**, 1201–1210.
- 330 Y. Liu, Y. Wu, Y. C. He and C. Ma, *Ind. Crops Prod.*, 2023, **202**, 117033.
- 331 S. Zhang, C. Ma, Q. Li, Q. Li and Y. C. He, *Bioresour. Technol.*, 2022, **344**, 126299.
- 332 S. Zhang, C. Wu, C. Ma, L. Li and Y. C. He, *Bioresour. Technol.*, 2023, **371**, 128579.
- 333 C. Wu, Q. Li, J. Di, Y. C. He and C. Ma, *Fuel*, 2023, **343**, 127830.
- 334 R. Gao, Q. Li, J. Di, Q. Li, Y. C. He and C. Ma, *Ind. Crops Prod.*, 2023, **193**, 116199.
- 335 C. Wu, C. Ma, Q. Li, H. Chai and Y. C. He, *Bioresour. Technol.*, 2023, **385**, 129454.
- 336 Q. Li, C. L. Ma and Y. C. He, *Bioresour. Technol.*, 2023, **378**, 128965.
- 337 X. Li, X. Cao, J. Xiong and J. Ge, *Small*, 2020, **16**, 1902751.
- 338 K. E. Metzger, M. M. Moyer and B. G. Trewyn, *ACS Catal.*, 2021, **11**, 110–122.
- 339 K. Engström, E. V. Johnston, O. Verho, K. P. J. Gustafson, M. Shakeri, C.-W. Tai and J.-E. Bäckvall, *Angew. Chem., Int. Ed.*, 2013, **52**, 14006–14010.
- 340 N. Zhang, R. Hübner, Y. Wang, E. Zhang, Y. Zhou, S. Dong and C. Wu, *ACS Appl. Nano Mater.*, 2018, **1**, 6378–6386.
- 341 A. K. Ganai, P. Shinde, B. B. Dhar, S. Sen Gupta and B. L. V. Prasad, *RSC Adv.*, 2013, **3**, 2186–2191.
- 342 L. Gao, Z. Wang, Y. Liu, P. Liu, S. Gao, J. Gao and Y. Jiang, *Chem. Commun.*, 2020, **56**, 13547–13550.
- 343 M. Kalantari, Y. Liu, E. Strounina, Y. Yang, H. Song and C. Yu, *J. Mater. Chem. A*, 2018, **6**, 17579–17586.
- 344 Y. Liu, N. Guo, W. Kong, S. Gao, G. Liu, L. Zhou, J. Gao and Y. Jiang, *Green Synth. Catal.*, 2023, In press.
- 345 M. Budhiraja, A. Ali and V. Tyagi, *Eur. J. Org. Chem.*, 2023, e202201426.
- 346 A. Corma, H. García and F. X. Llabrés i Xamena, *Chem. Rev.*, 2010, **110**, 4606–4655.
- 347 P. García-García, M. Müller and A. Corma, *Chem. Sci.*, 2014, **5**, 2979–3007.
- 348 M. Viciano-Chumillas, M. Mon, J. Ferrando-Soria, A. Corma, A. Leyva-Pérez, D. Armentano and E. Pardo, *Acc. Chem. Res.*, 2020, **53**, 520–531.



- 349 Y. Chen, S. Han, X. Li, Z. Zhang and S. Ma, *Inorg. Chem.*, 2014, **53**, 10006–10008.
- 350 S. Dutta, N. Kumari, S. Dubbu, S. W. Jang, A. Kumar, H. Ohtsu, J. Kim, S. H. Cho, M. Kawano and I. S. Lee, *Angew. Chem., Int. Ed.*, 2020, **59**, 3416–3422.
- 351 Y. Wang, N. Zhang, E. Zhang, Y. Han, Z. Qi, M. B. Ansorge-Schumacher, Y. Ge and C. Wu, *Chem. – Eur. J.*, 2019, **25**, 1716–1721.
- 352 Y. Wu, J. Shi, S. Mei, H. A. Katimba, Y. Sun, X. Wang, K. Liang and Z. Jiang, *ACS Catal.*, 2020, **10**, 9664–9673.
- 353 Z. Wang, Y. Liu, X. Dong and Y. Sun, *ACS Appl. Mater. Interfaces*, 2021, **13**, 49974–49981.
- 354 H. Hu, Y. Chang, Z. Wang, J. Cui, S. Jia and Y. Du, *J. Colloid Interface Sci.*, 2023, **650**, 1833–1841.
- 355 J. Gao, Z. Wang, R. Guo, Y. Hu, X. Dong, Q. Shi and Y. Sun, *Catal. Sci. Technol.*, 2022, **13**, 991–999.
- 356 Y. Wang, N. Zhang, R. Hübner, D. Tan, M. Löffler, S. Facsko, E. Zhang, Y. Ge, Z. Qi and C. Wu, *Adv. Mater. Interfaces*, 2019, **6**, 1801664.
- 357 J. M. Palomo, *Chem. Commun.*, 2019, **55**, 9583–9589.
- 358 M. Filice, M. Marciello, M. D. P. Morales and J. M. Palomo, *Chem. Commun.*, 2013, **49**, 6876–6878.
- 359 M. Filice, N. Losada-Garcia, C. Perez-Rizquez, M. Marciello, M. D. Morales and J. M. Palomo, *Appl. Nano*, 2021, **2**, 1–13.
- 360 X. Wu, S. Liu, J. Xiong, B. Chen, M.-H. Zong, J.-G. Yang and W.-Y. Lou, *Appl. Catal., A*, 2020, **608**, 117899.
- 361 J. M. Naapuri, N. Losada-Garcia, J. Deska and J. M. Palomo, *Nanoscale*, 2022, **14**, 5701–5715.
- 362 J. M. Naapuri, N. Losada-Garcia, R. A. Rothemann, M. C. Pichardo, M. H. G. Pechtl, J. M. Palomo and J. Deska, *ChemCatChem*, 2022, **14**, e202200362.
- 363 R. Benavente, D. Lopez-Tejedor, M. del Puerto Morales, C. Perez-Rizquez and J. M. Palomo, *Nanoscale*, 2020, **12**, 12917–12927.
- 364 T. Görbe, K. P. J. Gustafson, O. Verho, G. Kervefors, H. Zheng, X. Zou, E. V. Johnston and J.-E. Bäckvall, *ACS Catal.*, 2017, **7**, 1601–1605.
- 365 X. Li, X. Hu, Y. Qiao, T. Lu, Y. Bai, J. Xiong, X. Li, Q. Gou and J. Ge, *Chem. Eng. J.*, 2023, **452**, 139356.
- 366 C. A. Denard, H. Huang, M. J. Bartlett, L. Lu, Y. Tan, H. Zhao and J. F. Hartwig, *Angew. Chem.*, 2014, **126**, 475–479.
- 367 N. Scalacci, G. W. Black, G. Mattedi, N. L. Brown, N. J. Turner and D. Castagnolo, *ACS Catal.*, 2017, **7**, 1295–1300.
- 368 C. Risi, F. Zhao and D. Castagnolo, *ACS Catal.*, 2019, **9**, 7264–7269.
- 369 A. Gimbernat, M. Guehl, M. Capron, N. Lopes Ferreira, R. Froidevaux, J. S. Girardon, P. Dhulster, D. Delcroix and F. Dumeignil, *ChemCatChem*, 2017, **9**, 2080–2084.
- 370 R. Q. Zhang, C. L. Ma, Y. F. Shen, J. F. Sun, K. Jiang, Z. B. Jiang, Y. J. Dai and Y. C. He, *Catal. Lett.*, 2020, **150**, 2220–2227.
- 371 L. Zhu, J. Di, Q. Li, Y. C. He and C. Ma, *J. Mol. Liq.*, 2023, **380**, 121741.
- 372 M. Horvat, V. Welch, R. Rädisch, S. Hecko, A. Schiefer, F. Rudroff, B. Wilding, N. Klempier, M. Pátek, L. Martinková and M. Winkler, *Catal. Sci. Technol.*, 2022, **12**, 62–66.
- 373 V. Gauchot, W. Kroutil and A. R. Schmitzer, *Chem. – Eur. J.*, 2010, **16**, 6748–6751.
- 374 E. Burda, W. Hummel and H. Gröger, *Angew. Chem., Int. Ed.*, 2008, **47**, 9551–9554.
- 375 P. Luan, Y. Liu, Y. Li, R. Chen, C. Huang, J. Gao, F. Hollmann and Y. Jiang, *Green Chem.*, 2021, **23**, 1960–1964.
- 376 S. Wu, Y. Zhou, D. Gerngross, M. Jeschek and T. R. Ward, *Nat. Commun.*, 2019, **10**, 5060.
- 377 B. H. Lipshutz, S. Ghorai and M. Cortes-Clerget, *Chem. – Eur. J.*, 2018, **24**, 6672–6695.
- 378 M. Cortes-Clerget, N. Akporji, J. Zhou, F. Gao, P. Guo, M. Parmentier, F. Gallou, J. Y. Berthon and B. H. Lipshutz, *Nat. Commun.*, 2019, **10**, 1–10.
- 379 N. Akporji, V. Singhania, J. Dussart-Gautheret, F. Gallou and B. H. Lipshutz, *Chem. Commun.*, 2021, **57**, 11847–11850.
- 380 A. B. Wood, J. R. A. Kincaid and B. H. Lipshutz, *Green Chem.*, 2022, **24**, 2853–2858.
- 381 S. C. Cosgrove, M. P. Thompson, S. T. Ahmed, F. Parmeggiani and N. J. Turner, *Angew. Chem., Int. Ed.*, 2020, **59**, 18156–18160.
- 382 C. M. Heckmann and F. Paradisi, *Chem. – Eur. J.*, 2021, **27**, 16616–16620.
- 383 C. J. Hastings, N. P. Adams, J. Bushi and S. J. Kolb, *Green Chem.*, 2020, **22**, 6187–6193.
- 384 N. Ríos-Lombardía, M. J. Rodríguez-Álvarez, F. Morís, R. Kourist, N. Comino, F. López-Gallego, J. González-Sabín and J. García-Álvarez, *Front. Chem.*, 2020, **8**, 1–11.
- 385 N. Ríos-Lombardía, M. J. Rodríguez-Álvarez, F. Morís, R. Kourist, N. Comino, F. López-Gallego, J. González-Sabín and J. García-Álvarez, *Front. Chem.*, 2020, **8**, 139.
- 386 E. Hofmann, L. Schmauser, J. Neugebauer, D. Touraud, F. Gallou and W. Kunz, *Chem. Eng. J.*, 2023, **472**, 144599.
- 387 S. Wang, L. Scandurra, R. Hübner, U. G. Nielsen and C. Wu, *ChemCatChem*, 2023, **15**, e202201229.
- 388 Á. Gómez Baraibar, D. Reichert, C. Mügge, S. Seger, H. Gröger and R. Kourist, *Angew. Chem., Int. Ed.*, 2016, **55**, 14823–14827.
- 389 Y. Lu, N. Yeung, N. Sieracki and N. M. Marshall, *Nature*, 2009, **460**, 855–862.
- 390 V. Köhler, Y. M. Wilson, M. Dürrenberger, D. Ghislieri, E. Churakova, T. Quinto, L. Knörr, D. Häussinger, F. Hollmann, N. J. Turner and T. R. Ward, *Nat. Chem.*, 2012, **5**, 93–99.
- 391 Y. Okamoto, V. Köhler and T. R. Ward, *J. Am. Chem. Soc.*, 2016, **138**, 5781–5784.
- 392 Y. Okamoto, V. Köhler, C. E. Paul, F. Hollmann and T. R. Ward, *ACS Catal.*, 2016, **6**, 3553–3557.
- 393 M. A. S. Mertens, D. F. Sauer, U. Markel, J. Schiffels, J. Okuda and U. Schwaneberg, *Catal. Sci. Technol.*, 2019, **9**, 5572–5576.
- 394 Z. J. Wang, K. N. Clary, R. G. Bergman, K. N. Raymond and F. D. Toste, *Nat. Chem.*, 2013, **5**, 100–103.



- 395 J. Pauly, H. Gröger and A. V. Patel, *ChemCatChem*, 2019, **11**, 1503–1509.
- 396 J. Pauly, H. Gröger and A. V. Patel, *Catalysts*, 2019, **9**, 547.
- 397 F. Chang, C. Wang, Q. Chen, Y. Zhang and G. Liu, *Angew. Chem. Int. Ed.*, 2022, **61**, e202114809.
- 398 D. Tian, R. Hao, X. Zhang, H. Shi, Y. Wang, L. Liang, H. Liu and H. Yang, *Nat. Commun.*, 2023, **14**, 1–14.
- 399 H. Terholsen, J. R. H. Meyer, Z. Zhang, P. J. Deuss and U. T. Bornscheuer, *ChemSusChem*, 2023, **16**, e202300168.
- 400 S. Grasso, L. Siracusa, C. Spatafora, M. Renis and C. Tringali, *Bioorg. Chem.*, 2007, **35**, 137–152.
- 401 H. Sato, W. Hummel and H. Gröger, *Angew. Chem., Int. Ed.*, 2015, **54**, 4488–4492.
- 402 H. Sato, R. Yamada, Y. Watanabe, T. Kiryu, S. Kawano, M. Shizuma and H. Kawasaki, *RSC Adv.*, 2022, **12**, 10619–10624.
- 403 J. Latham, J. M. Henry, H. H. Sharif, B. R. K. Menon, S. A. Shepherd, M. F. Greaney and J. Micklefield, *Nat. Commun.*, 2016, **7**, 1–8.
- 404 P. Schaaf, T. Bayer, M. Koley, M. Schnürch, U. T. Bornscheuer, F. Rudroff and M. D. Mihovilovic, *Chem. Commun.*, 2018, **54**, 12978–12981.
- 405 M. B. Plutschack, B. Pieber, K. Gilmore and P. H. Seeberger, *Chem. Rev.*, 2017, **117**, 11796–11893.
- 406 P. De Santis, L.-E. Meyer and S. Kara, *React. Chem. Eng.*, 2020, **5**, 2155–2184.
- 407 C. Yang, R. Li, K. A. I. Zhang, W. Lin, K. Landfester and X. Wang, *Nat. Commun.*, 2020, **11**, 1239.
- 408 R. A. Messing and A. M. Filbert, *J. Agric. Food Chem.*, 1975, **23**, 920–923.
- 409 S. Strompen, M. Weiß, H. Gröger, L. Hilterhaus and A. Liese, *Adv. Synth. Catal.*, 2013, **355**, 2391–2399.
- 410 J. M. Carceller, M. Mifsud, M. J. Climent, S. Iborra and A. Corma, *Green Chem.*, 2020, **22**, 2767–2777.
- 411 K. S. Arias, J. M. Carceller, M. J. Climent, A. Corma and S. Iborra, *ChemSusChem*, 2020, **13**, 1864–1875.
- 412 L. Hu, L. Lin, Z. Wu, S. Zhou and S. Liu, *Renew. Sustainable Energy Rev.*, 2017, **74**, 230–257.
- 413 F. Lackner, K. Hiebler, B. Grabner and H. Gruber-Woelfler, *Catalysts*, 2020, **10**, 1–13.
- 414 S. Gianolio, D. Roura Padrosa and F. Paradisi, *Green Chem.*, 2022, **24**, 8434–8440.
- 415 M. J. Fink, M. Schön, F. Rudroff, M. Schnürch and M. D. Mihovilovic, *ChemCatChem*, 2013, **5**, 724–727.
- 416 R. de Oliveira Lopes, A. S. de Miranda, B. Reichart, T. Glasnov, C. O. Kappe, R. C. Simon, W. Kroutil, L. S. M. Miranda, I. C. R. Leal and R. O. M. A. de Souza, *J. Mol. Catal. B: Enzym.*, 2014, **104**, 101–107.
- 417 J. M. Carceller, K. S. Arias, M. J. Climent, S. Iborra and A. Corma, *Natl. Sci. Rev.*, 2022, **9**, nwac135.
- 418 S. Alipour, *Green Chem.*, 2016, **18**, 4990–4998.
- 419 S. H. Lee, D. S. Choi, S. K. Kuk and C. B. Park, *Angew. Chem., Int. Ed.*, 2018, **57**, 7958–7985.
- 420 J. A. Maciá-Agulló, A. Corma and H. Garcia, *Chem. – Eur. J.*, 2015, **21**, 10940–10959.
- 421 J. Kim and C. B. Park, *Curr. Opin. Chem. Biol.*, 2019, **49**, 122–129.
- 422 L. Schmermund, V. Jurkaš, F. F. Özgen, G. D. Barone, H. C. Büchenschütz, C. K. Winkler, S. Schmidt, R. Kourist and W. Kroutil, *ACS Catal.*, 2019, **9**, 4115–4144.
- 423 F. F. Özgen, M. E. Runda and S. Schmidt, *ChemBioChem*, 2021, **22**, 790–806.
- 424 M. A. Emmanuel, S. G. Bender, C. Bilodeau, J. M. Carceller, J. S. DeHovitz, H. Fu, Y. Liu, B. T. Nicholls, Y. Ouyang, C. G. Page, T. Qiao, F. C. Raps, D. R. Sorigué, S. Z. Sun, J. Turek-Herman, Y. Ye, A. Rivas-Souchet, J. Cao and T. K. Hyster, *Chem. Rev.*, 2023, **123**, 5459–5520.
- 425 W. Zhang, E. F. Fuego, F. Hollmann, L. L. Martin, M. Pesic, R. Wardenga, M. Höhne and S. Schmidt, *Eur. J. Org. Chem.*, 2019, 80–84.
- 426 K. Lauder, A. Toscani, Y. Qi, J. Lim, S. J. Charnock, K. Korah and D. Castagnolo, *Angew. Chem., Int. Ed.*, 2018, **57**, 5803–5807.
- 427 X. Guo, Y. Okamoto, M. R. Schreier, T. R. Ward and O. S. Wenger, *Chem. Sci.*, 2018, **9**, 5052–5056.
- 428 Z. C. Litman, Y. Wang, H. Zhao and J. F. Hartwig, *Nature*, 2018, **560**, 355–359.
- 429 P. Li, Y. Ma, Y. Li, X. Zhang and Y. Wang, *ChemBioChem*, 2020, **21**, 1852–1855.
- 430 X. Ding, C.-L. Dong, Z. Guan and Y.-H. He, *Angew. Chem., Int. Ed.*, 2019, **58**, 118–124.
- 431 Y. Yu, W.-F. Lu, Z.-J. Yang, N. Wang and X.-Q. Yu, *Bioorg. Chem.*, 2021, **107**, 104534.
- 432 J. Albarrán-Velo, V. Gotor-Fernández and I. Lavandera, *Adv. Synth. Catal.*, 2021, **363**, 4096–4108.
- 433 L. Rodríguez-Fernández, J. Albarrán-Velo, I. Lavandera and V. Gotor-Fernández, *Adv. Synth. Catal.*, 2023, **365**, 1883–1892.

